M o n o g r a p h

urn:lsid:zoobank.org:pub:98563124-EFCC-4542-B5AB-E14C0C3978DD

Antarctic Kinorhyncha:
Seven new species from the Antarctic Peninsula

Martin V. SØRENSEN [1,*], Lara MACHERIOTOU [2], Ulrike BRAECKMAN [3],
Craig R. SMITH [4] & Jeroen INGELS [5]

[1] Natural History Museum of Denmark, University of Copenhagen, 2100 Copenhagen, Denmark.
[2,3] Marine Biology Research Group, Department of Biology, Ghent University, 9000 Ghent, Belgium.
[4] Department of Oceanography, University of Hawai'i at Mānoa, Honolulu HI 96822, Hawaii, USA.
[5] Coastal and Marine Laboratory, Florida State University, St. Teresa FL 32346, Florida, USA.
[5] National Institute for Water and Atmospheric Research, Wellington 6021, New Zealand.

[*] Corresponding author: mvsorensen@snm.ku.dk
[2] Email: lara.macheriotou@ugent.be
[3] Email: Ulrike.Braeckman@ugent.be
[4] Email: craigsmi@hawaii.edu
[5] Email: jeroen.ingels@niwa.co.nz

[1] urn:lsid:zoobank.org:author:4143D650-12FC-4914-93F5-2C39339A7156
[2] urn:lsid:zoobank.org:author:1037C143-8562-41A3-8149-BC3DE4323845
[3] urn:lsid:zoobank.org:author:6C48F169-ECC8-4F98-A9CF-9B2A664DA903
[4] urn:lsid:zoobank.org:author:F004E0AC-049A-48D6-9369-EBE18ECEF53C
[5] urn:lsid:zoobank.org:author:F6107F36-C67F-4CB8-A6C0-DFBF66D3C464

Abstract. With only three named species, Antarctica is the continent with the least explored kinorhynch biodiversity. The present contribution provides the most comprehensive study of Antarctic kinorhynchs collected along the coast of the West Antarctic Peninsula. Quantitative samples were collected in three regions along the Peninsula: in Andvord Bay Fjord at the Danco Coast, in the Gerlache Strait, and on the open continental shelf west of the Peninsula. Comparison of the sampling areas suggests that the highest kinorhynch abundance was in the Gerlache Strait, where kinorhynchs were over six times more abundant than in Andvord Bay. Lowest abundance was on the open shelf, where the abundance was four times lower than in Andvord Bay. Among all examined specimens 98% were found in the top 4 cm of the sediment. All adult kinorhynchs were identified, and the study revealed the presence of the known Antarctic species *Polacanthoderes shiraseae* and at least seven species new to science: *Condyloderes notios* sp. nov., *Polacanthoderes grzelakae* sp. nov., *Echinoderes ahlfeldae* sp. nov., *E. nataliae* sp. nov., *E. kathleenhannae* sp. nov., *E. antarcticus* sp. nov., and *E. crux* sp. nov. In addition to the five new species of *Echinoderes*, two potentially known species are reported. *Echinoderes* aff. *angustus* shows close resemblance to the Arctic *E. angustus*, and the specimens only differed by their lack of a midventral fissure in segment 2, present in Arctic specimens of *E. angustus* only. A detailed examination of the *E. angustus* type material revealed new diagnostic details for the species, i.e., a complete mapping of sensory spots, presence of a middorsal protuberance between segments 10 and 11, and a tergal division of segment 11. Another unidentified species, *Echinoderes* aff. *beringiensis/romanoi/xalkutaat*,

showed such close resemblance to three congeners that further studies are needed to identify clear diagnostic characters for the species, or alternatively clarify whether they should be synonymised. The comparisons prompted by the two unidentified species led to the suggestion of a new species group, the *Echinoderes remanei* species group, including *E. remanei*, *E. angustus*, *E. beringiensis*, *E. cernunnos*, *E. drogoni*, *E. galadrielae*, *E. obtuspinosus*, *E. quasae*, *E. pennaki*, *E. romanoi*, and *E. xalkutaat*. In addition, the *Echinoderes aragorni* species group is proposed, including the New Zealand species *E. aragorni* and the new species *E. crux*.

Keywords. Antarctica, *Condyloderes*, *Echinoderes*, kinorhynchs, meiofauna, *Polacanthoderes*, Scalido-phora, taxonomy.

Introduction

Kinorhynchs have been collected and described from marine localities throughout the world, and the phylum as a whole has a global distribution (Neuhaus 2013). However, as is the case with several other meiofaunal groups, there is a strong sampling bias towards the Northern Hemisphere, which leaves great gaps in our knowledge about the Southern Hemisphere kinorhynch biodiversity (Garraffoni *et al.* 2021). In the Southern Hemisphere the kinorhynch biodiversity in Indonesian and Oceanian regions is the best explored, especially thanks to research efforts around New Zealand. No less than 28 species are described from Indonesia and Oceania, and two additional species described from the Northeast Pacific and Subantarctica, respectively, have been reported (Higgins 1967; Brown & Higgins 1983; Brown 1985; Adrianov & Malakhov 1999; Sørensen *et al.* 2000; Lemburg 2002; Neuhaus & Blasche 2006; Sørensen & Thormar 2010; Ostmann *et al.* 2012; Grzelak & Sørensen 2022, 2024; Sørensen 2023; Sørensen & Grzelak 2024). In contrast to this, only 16 species (13 from south of the equator) have been described from South America, including Galapagos and the Falkland Islands. Four additional species with type localities elsewhere have been reported, which sums up to 20 kinorhynch species known from South America (Lang 1949, 1953; Gerlach 1956; Kirsteuer 1964; Higgins 1968; Schmidt 1974; Martorelli & Higgins 2004; Neuhaus 2004; Dal Zotto *et al.* 2013; Sørensen 2014; Grzelak *et al.* 2021; Cepeda *et al.* 2022a; Rucci *et al.* 2022). Slightly fewer species are known from the Southern Hemisphere part of Africa, and our available knowledge is mostly thanks to sampling efforts northeast of Madagascar. A total of nine species have been described from the south equatorial part of Africa, and five additional species described from elsewhere have been reported (Zelinka 1913; Omer-Cooper 1957; Higgins 1969a; Randsø *et al.* 2019; Cepeda *et al.* 2020, 2022b, 2022c).

The remaining Southern Hemisphere continent, Antarctica, is by far the least explored in terms of kinorhynch diversity. If we restrict the marine habitats of Antarctica to the actual shelf of the continent, only three species are known. The first species described from Antarctica was *Campyloderes vanhoeffeni* Zelinka, 1913. It was collected during the German Gauß Expedition (1901–1903), which focused on the Subantarctic Kerguelen Islands and the part of Antarctica closest to the islands. Ten years after the expedition, Zelinka (1913) described the species, based on specimens from the Kerguelen Islands and Wilhelm II Land in Antarctica. Subsequently, *C. vanhoeffeni* has been recorded from most parts of the world and has been known either as the first known example of a cosmopolitan kinorhynch species or, perhaps more likely, a representative of a cryptic species complex (Neuhaus 2004; Neuhaus & Sørensen 2013).

After the description of *C. vanhoeffeni*, nearly 100 years would pass before Antarctic kinorhynchs were addressed again through taxonomic looking glasses. Based on material from the German ANDEEP-1

cruise, Sørensen (2008a) described *Polacanthoderes martinezi* Sørensen, 2008a from the South Shetland Islands, which surface the Scotia Sea from an extension of the Antarctic Peninsula shelf. The species was also type species for the new genus *Polacanthoderes* Sørensen, 2008a. The third and most recently described species from Antarctica was *Polacanthoderes shiraseae* Yamasaki *et al.*, 2022. The description by Yamasaki *et al.* (2022) was extraordinary in several ways. First of all, their sampling area covered an immense range of the Antarctic coast line, from Lützow-Holm Bay (closest to Africa) to Totten Glacier (closest to Australia), which enabled them to demonstrate a great distributional range for *P. shiraseae*. But in addition, they invested considerable effort in examining the high level of intraspecific variation in tube and spine patterns of both *P. martinezi* and *P. shiraseae*, and corroborated the observations on the latter with molecular barcoding. Further details and implications of this study will be discussed below under the discussion of *Polacanthoderes* spp.

Thus, with only three named and known species, Antarctica represents the least explored continent when it comes to kinorhynch biodiversity. Even if we extend the geographic range to include the Subantarctic islands, our knowledge is still rather limited. As mentioned above, *C. vanhoeffeni* is known from the Kerguelen Islands, but this record also represents the only known kinorhynch species for the Subantarctic part of the Indian Ocean. Except for this single record, most of our knowledge about Subantarctic Kinorhyncha is concentrated around the minute islands between, or near, the tip of South America and the Antarctic Peninsula. From South Georgia and the South Sandwich Islands, which are situated right at the border between the Antarctic Ocean and the South Atlantic, Lang (1949) described three species: *Echinoderes pilosus* Lang, 1949, *Cristaphyes odhneri* (Lang, 1949), and *Leiocanthus sculptus* (Lang, 1949). Much more recently, Sánchez *et al.* (2024) described *Echinoderes australis* Sánchez *et al.*, 2024 from the South Orkney Trench, even closer to the Antarctic Peninsula, and reported the presence of a congener that showed very close resemblance to the Arctic species *Echinoderes angustus* Higgins & Kristensen, 1988.

The purpose of the present contribution is to expand our knowledge about the Antarctic kinorhynch fauna, and seven new species are described based on comprehensive sampling along the east coast of the Antarctic Peninsula.

Material and methods

The study area is located along the west coast of the Antarctic Peninsula and includes three study sites at depths of ~542–560 m (Inner Basin B, IBB at 64°52′ S, 62°26′ W; Middle Basin A, MBA at 64°52′ S, 62°34′ W; Outer Basin A, OBA at 64°47′ S, 62°44′ W) in Andvord Bay fjord on the Danco Coast, one site at ~690 m in the Gerlache Strait (Gerl) between the Peninsula mainland and coastal islands (64°39′ S, 62°55′ W), and one site (Station B) at ~590 m on the open shelf (64°48′ S, 65°21′ W) (Fig. 1). Sampling was conducted during two cruises of the FjordEco project (https://fjordeco.wordpress.com/), LMG15-10 (Nov.–Dec. 2015) and NBP16-03 (Mar.–Apr. 2016), which aimed at evaluating the drivers of productivity and biodiversity, and their sensitivity to climate warming, along a transect from inner Andvord Bay fjord, a West Antarctic Peninsula fjord, out onto the open continental shelf. See Lundesgaard *et al.* (2020) for a description of the oceanographical setting of the present study. A megacorer with tubes of 9.52 cm internal diameter was used to retrieve essentially undisturbed bottom sediment from a total of 30 locations. Twenty of the sampled locations had kinorhynchs, and 18 these yielded adult specimens (Table 1): three within ~1 km of IBB, seven within ~1 km of MBA, one within ~1 km of OBA, three within ~1 km of Gerl, and four within ~1 km of Station B (Fig. 1). Sample depths ranged from 499 to 708 m. Cores with the samples for ecological and taxonomic studies were split into three vertical layers, 0–1 cm, 1–3 cm, and 3–5 cm, and each layer was fixed separately in 10% buffered formalin.

Subsequently, the samples were washed in a 32 µm sieve, the meiofauna was extracted from the sieved sediment by LUDOX flotation (Somerfield & Warwick 1996), sorted to main groups, and stored in tubes with 96% ethanol. All tubes with kinorhynchs were dispatched to the Natural History Museum of Denmark (NHMD) for further preparation, examination, and description or identification.

Before further preparation, the unmounted kinorhynchs were visually inspected under an Olympus SZX10 dissecting microscope and divided into juveniles and adults. The juvenile specimens were transferred back to the tubes, while approximately half of the adults were processed for light microscopy (LM) and the other half for scanning electron microscopical (SEM). Specimens for LM were re-hydrated through a graded ethanol-water series, dehydrated through a graded water-glycerine series, left overnight in 100% glycerine, and finally mounted between two cover slips attached to an HS plastic slide. The specimens were examined with an Olympus BX51 microscope with differential interference contrast and photographed with an Olympus DP27 camera. Examined specimens were deposited in the collections of NHMD and Smithsonian Institution, National Museum of Natural History (USNM) (see Table 1 for catalogue numbers). Specimens for SEM were transferred to 100% ethanol and subsequently to 100% acetone through an ethanol-acetone series, critical point dried, mounted on aluminium stubs, sputter coated with gold, and examined with a Zeiss Sigma 360VP scanning electron microscope.

An attempt was made to identify all adult specimens with the interactive identification keys for Echinoderidae (Yamasaki *et al*. 2020b) and for other Kinorhyncha (Sørensen & Yamasaki 2024).
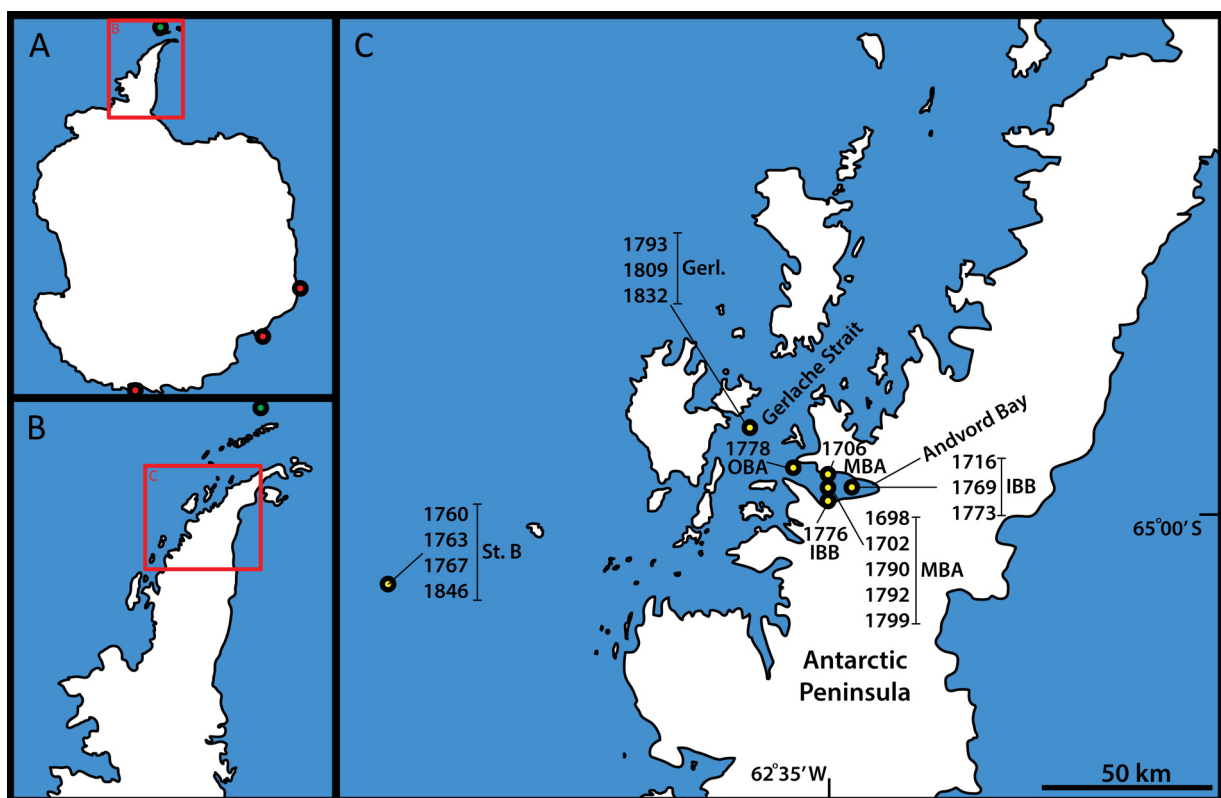
Fig. 1. Map showing the sampling stations. **A**. Overview of Antarctica, with the Antarctic Peninsula framed. Previous records of *Polacanthoderes martinezi* Sørensen, 2008 (green dots) and *P. shiraseae* Yamasaki *et al*., 2022 (red dots) are marked. **B**. Antarctic Peninsula with sampling area framed. **C**. Sampling area with station numbers and stations indicated as yellow dots. Study sites in Andvord Bay refer to OBA – Outer Basin A; MBA – Middle Basin A; IBB – Inner Basin B. Only stations yielding adult kinorhynch specimens are included.

Table 1 (continued on next page). Coordinates and basic data on sampling stations, species identities of *Condyloderes* Higgins, 1969, *Echinoderes* Claparède, 1863, and *Polacanthoderes* Sørensen, 2008, type status, and catalogue numbers. The list only includes stations with adult specimens, and juveniles of Echinoderidae are not listed. Study sites in Andvord Bay refer to: IBB = Inner Basin B; MBA = Middle Basin A; and OBA = Outer Basin A.

CRS stn	Depth (m)	Date	Area	Position	Species	Mount	Type status and catalogue number
1698	541	Nov. 28, 2015	Andvord Bay, MBA	64°51.60′ S 62°33.80′ W	*E. ahlfeldae* sp. nov.	LM	7♂♂, paratypes (NHMD-1784762 to 1784766, USNM-1740029 to 1740030), 1 juvenile, non-type (NHMD-001784767)
						SEM	2♂♂, 1♀, non-types
					E. aff. *angustus*	LM	1♂, non-type (NHMD-1790691)
					E. nataliae sp. nov.	SEM	1♀, non-type
1702	502	Nov. 30, 2015	Andvord Bay, MBA	64°51.15′ S 62°34.44′ W	*C. notios* sp. nov.	LM	1♂, holotype (NHMD-1784659)
					E. aff. *angustus*	SEM	1♀, non-type
					E. nataliae sp. nov.	SEM	2♂♂, 1♀, non-types
1706	499	Dec. 1, 2015	Andvord Bay, MBA	64° 50.47′ S 62°35.12′ W	*C. notios* sp. nov.	LM	juvenile, non-type (NHMD-1784660)
					E. nataliae sp. nov.	LM	1♂, paratype (NHMD-1786672)
					P. grzelakae sp. nov.	LM	♂, holotype (NHMD-1784249)
						SEM	1♀, non-type
1716	551	Dec. 6, 2015	Andvord Bay, IBB	64°52.36′ S 62°25.49′ W	*E. nataliae* sp. nov.	LM	1♂, paratype (NHMD-1786673)
1760	596	Dec. 21, 2015	Stn B, open continental shelf	64°47.86′ S 65°21.09′ W	*E. crux* sp. nov.	SEM	1♀, holotype (NHMD-1790632), 1♀, paratype (NHMD-1790633)
1763	593	Apr. 3, 2016	Stn B, open continental shelf	64°48.41′ S 65°21.82′ W	*P. shiraseae*	LM	1♂, 1♀, non-types (NHMD-1784624 to 1784625)
1767	590	Apr. 4, 2016	Stn B, open continental shelf	64°47.99′ S 65°20.55′ W	*Polacanthoderes* sp. 1	SEM	1♂, non-type
1769	547	Apr. 5, 2016	Andvord Bay, IBB	64°52.37′ S 62°25.27′ W	*E. ahlfeldae* sp. nov.	LM	1♂, paratype (NHMD-1784768)
					E. grzelakae sp. nov.	LM	1♀, paratype (NHMD-1740027)
1773	553	Apr. 6, 2016	Andvord Bay, IBB	64°52.35′ S 62°25.88′ W	*E. ahlfeldae* sp. nov.	SEM	1♂, non-type
					E. aff. *angustus*	SEM	1♂, non-type
					E. nataliae sp. nov.	LM	1♀, paratype (NHMD-1786674)
						SEM	1♂, 2♀♀, non-types
					P. grzelakae sp. nov.	LM	1♂, paratype (NHMD-1784250)
1776	551	Apr. 7, 2016	Andvord Bay, IBB	64°52.53′ S 62°33.90′ W	*E.* aff. *angustus*	SEM	1♂, non-type
					P. grzelakae sp. nov.	LM	1♂, paratype (USNM-1740028)
						SEM	1♂, non-type
					Polacanthoderes sp. 1	SEM	1♂, non-type
					Polacanthoderes sp. 2	SEM	1♂, non-type
1778	567	Apr. 8, 2016	Andvord Bay, OBA	64°47.01′ S 62°43.90′ W	*E. ahlfeldae* sp. nov.	LM	1♀/♂, non-type (NHMD-1784769)
					E. nataliae sp. nov.	LM	1♂, holotype (NHMD-1786668), 3♂♂, 2♀♀, paratypes (NHMD-1786669 to 1786671, USNM-1740037 to 1740038)
						SEM	2♂♂, non-types
					E. antarcticus sp. nov.	LM	♀, holotype (NHMD-1786932)
1790	532	Apr. 10, 2016	Andvord Bay, MBA	64°51.49′ S 62°34.01′ W	*E. ahlfeldae* sp. nov.	LM	4♂♂, 2♀♀, paratypes (NHMD-1784770 to 1784773, USNM-1740031 to 1740032)
					E. nataliae sp. nov.	LM	2♂♂, 1♀, 1 juvenile, paratypes (NHMD-1786675 to 1786676, NHMD-1786678, USNM-1740039)
						SEM	4♂♂, 1♀, non-types

Table 1 (continued). Coordinates and basic data on sampling stations, species identities of *Condyloderes* Higgins, 1969, *Echinoderes* Claparède, 1863, and *Polacanthoderes* Sørensen, 2008, type status, and catalogue numbers. (For further details, see legend on preceding page.)

CRS stn	Depth (m)	Date	Area	Position	Species	Mount	Type status and catalogue number
1792	525	Apr. 11, 2016	Andvord Bay, MBA	64°51.40′ S 62°34.01′ W	*E. ahlfeldae* sp. nov.	LM	♀, holotype (NHMD-1784759), 1♂, 2♀♀, paratypes (NHMD-1784760 to 1784761, USNM-1740033)
						SEM	4♂♂, 2♀♀, non-types
					E. aff. *angustus*	LM	1♀, non-type (NHMD-1790692)
					E. nataliae sp. nov.	LM	1♂, paratype (NHMD- 1786679)
						SEM	1♂, 3♀♀, non-types
1793	701	Apr. 11, 2016	Gerlache Strait	64°39.53′ S 62°55.03′ W	*C. notios* sp. nov.	SEM	juvenile, non-type
					E. ahlfeldae sp. nov.	LM	1♂, paratype (NHMD-1784774)
						SEM	12♂♂, 7♀♀, non-types
					E. aff. *angustus*	SEM	1♂, 1♀, non-types
					Echinoderes aff. *beringiensis/romanoi/xalkutaat*	LM	1♀, non-type (NHMD- 1790694)
						SEM	1♂, non-type
					E. nataliae sp. nov.	SEM	5♂♂, 1♀, non-types
					E. kathleenhannae sp. nov.	LM	♂, holotype (NHMD-1786779)
						SEM	1♀, non-type
					P. grzelakae sp. nov.	LM	3♀♀, paratypes (NHMD-1784251, 1784284, 1784303)
						SEM	4♂♂, 1♀, non-types
1799	541	Apr. 13, 2016	Andvord Bay, MBA	64°51.51′ S 62°33.83′ W	*E. ahlfeldae* sp. nov.	SEM	4♂♂, 1♀, non-types
					E. nataliae sp. nov.	LM	1♂, paratype (NHMD- 1786680)
						SEM	1♀, non-type
1809	694	Apr. 15, 2016	Gerlache Strait	64°39.59′ S 62°55.09′ W	*E. ahlfeldae* sp. nov.	LM	6♂♂, 5♀♀, paratypes (NHMD-1784775 to 1784782, USNM-1740034 to 1740036)
						SEM	11♂♂, 6♀♀, non-types
					E. aff. *angustus*	LM	1♂, non-types (NHMD-1790693)
						SEM	2♂♂, non-types
					Echinoderes aff. *beringiensis/romanoi/xalkutaat*	LM	1♂, 3♀♀, non-types (NHMD-1790695 to 1790698)
						SEM	2♂♂, 3♀♀, non-types
					E. nataliae sp. nov.	SEM	5♂♂, 1♀, non-types
					E. antarcticus sp. nov.	LM	1♀, paratype (USNM-1740040)
					P. grzelakae sp. nov.	LM	2♂♂, 1♀, paratypes (NHMD-1784304 to 1784306)
						SEM	3♂♂, 1♀, non-types
					Polacanthoderes sp. 1	SEM	1♂, non-type
1832	631	Apr. 21, 2016	Gerlache Strait	64°39.30′ S 62°55.98′ W	*C. notios* sp. nov.	SEM	3♂♂, 2 juvenile, non-types
					E. ahlfeldae sp. nov.	SEM	1♂, 7♀♀, non-types
					Echinoderes aff. *beringiensis/romanoi/xalkutaat*	SEM	2♀♀, non-types
					E. kathleenhannae sp. nov.	SEM	3♂♂, 1♀, non-types
					E. antarcticus sp. nov.	SEM	1♀, non-type
					P. grzelakae sp. nov.	SEM	4♂♂, 5♀, non-types
					Pycnophyidae sp.	SEM	juvenile, non-type
1846	572	Apr. 25, 2016	St. B, open continental shelf	64°47.93′ S 65°21.23′ W	*P. shiraseae*	LM	2♀♀, non-types (NHMD-1784626 to 1784627)

Species with uncertain identities, i.e., *Echinoderes* aff. *angustus* Higgins & Kristensen, 1988 and *Echinoderes* aff. *beringiensis/romanoi/xalkutaat*, were compared with relevant specimens from museum collections and personal reference collections. Comparative material for *E. angustus* included: LM images of the male holotype (USNM 233200), one female paratype and three male paratypes (both USNM 233202), kindly provided by Maria Herranz, and LM slides with one female (NHMD 99368) and one male (NHMD 99369) paratype; additional non-type specimens mounted for SEM included one female specimen collected in August 2023 (see Zalewska *et al.* 2024) in Disko Fjord, Greenland, close to the type locality of this species, and two females and two males collected in fjords of Spitsbergen, Svalbard in July and August 2013 (see Grzelak & Sørensen 2018). Comparative material for *E. romanoi* Landers & Sørensen, 2016 included LM slides with the holotype and four paratypes (NHMD 100307 to 100311), re-examination of four SEM specimens stored in the personal references collection of Martin V. Sørensen, and unpublished SEM images by S.L. Landers. Comparative material for *E. obtuspinosus* Sørensen *et al.*, 2012 included an LM slide of a female paratype (NHMD 99894). Comparative material for *E. pennaki* Higgins, 1960 included: LM images of the female holotype (USNM 29746) and SEM of three non-type females, kindly provided by Maria Herranz. Specimens of *E. beringiensis* Adrianov & Maiorova, 2022 and *E. xalkutaat* Cepeda *et al.*, 2019a were not available, and the comparisons were exclusively based on information from their original descriptions (Cepeda *et al.* 2019a; Adrianov & Maiorova 2022).

All measurements were made with Cell^D software. Line art illustrations were made with Adobe Illustrator CS6 based on LM images of holo- and paratypes, supplemented with information from SEM; whenever morphological variation occurred among the examined specimens, the line art follows the holotype morphology. Images for figure plates were edited with Adobe Photoshop CS6, and the final figure plates were composed with Adobe Illustrator CS6.

Abbreviations

The following abbreviations are used for collections and museums:

MVS = Personal reference collection of Martin V. Sørensen
NHMD = Natural History Museum of Denmark, Denmark
USNM = United States National Museum of Natural History/Smithsonian Institution, National Museum of Natural History

The following abbreviations are used in the tables:

ac = acicular spine
cu = cuspidate spine
gco1/2 = glandular cell outlet type 1/2
LA = lateral accessory
LD = laterodorsal
ltas = lateral terminal accessory spine
lts = lateral terminal spine
LV = lateroventral
MD = middorsal
ML = midlateral
MSW-X = maximum sternal width, with X indicating segment with greatest sternal width
MTS = midterminal spine
ne = nephridiopore
pa = female papilla
PD = paradorsal
pe = penile spines
PE1 = penile spine pair 1, dorsal

PE2	=	penile spine pair 2, median
PE3	=	penile spine pair 3, ventral
pr	=	protuberance
pr*	=	protuberance not present in all specimens
S	=	segment length
sac	=	short acicular spine (unique for *Polacanthoderes* spp.)
SD	=	subdorsal
si	=	sieve plate
SL	=	sublateral
ss	=	sensory spot
ss*	=	sensory spot not present in all specimens
ss3	=	sensory spots type 3 (the projecting kind)
ss6	=	sensory spots type 6 (unique for *Condyloderes* spp.)
SW-10	=	standard width, always measured on segment 10
TL	=	trunk length
TL (CUM)	=	cumulative trunk length from sum of segment lengths
tu	=	tube
VL	=	ventrolateral
VM	=	ventromedial
–	=	missing data
(♀)	=	female condition of sexually dimorphic character
(♂)	=	male condition of sexually dimorphic character

The following abbreviations are used in the figures:

fl	=	flare-like extensions from secondary fringe
fpa	=	female papilla
lac	=	lateral accessory cuspidate spine
lagco2	=	lateral accessory glandular cell outlet type 2
lasac	=	lateral accessory short acicular spine
lat	=	lateral accessory tube
ldgco2	=	laterodorsal glandular cell outlet type 2
lds	=	laterodorsal acicular spine
ldsac	=	laterodorsal short acicular spine
ldso	=	laterodorsal slit-like opening
ldss	=	laterodorsal sensory spot
ldt	=	laterodorsal tube
ltas	=	lateral terminal accessory spine
lts	=	lateral terminal spine
lvc	=	lateroventral cuspidate spine
lvgco2	=	lateroventral glandular cell outlet type 2
lvs	=	lateroventral acicular spine
lvt	=	lateroventral tube
mdgco1	=	middorsal glandular cell outlet type 1
mdf	=	middorsal fissure
mds	=	middorsal acicular spine
mdss	=	middorsal sensory spot
mlgco2	=	midlateral glandular cell outlet type 2
mlsac	=	midlateral short acicular spine
mlss	=	midlateral sensory spot

mlt	=	midlateral tube
mts	=	midterminal spine
mvf	=	midventral fissure
mvp	=	midventral placid
ne	=	nephridiopore
pdgco1/2	=	paradorsal glandular cell outlet type 1/2
pdss	=	paradorsal sensory spot
pe1	=	penile spine pair 1, dorsal
pe2	=	penile spine pair 2, median
pe3	=	penile spine pair 3, ventral
pr	=	protuberance
psp	=	primary spinoscalid
sdgco2	=	subdorsal glandular cell outlet type 2
sdsac	=	subdorsal short acicular spine
sdso	=	subdorsal slit-like opening
sdss	=	subdorsal sensory spot
sdt	=	subdorsal tube
se	=	sternal extension
sec	=	introvert sector followed by sector number
set	=	setae
si	=	sieve plate
slgco2	=	sublateral glandular cell outlet type 2
slsac	=	sublateral short acicular spine
slso	=	sublateral slit-like opening
slss	=	sublateral sensory spot
slt	=	sublateral tube
sp	=	spinoscalid, follow by introvert ring number
spe	=	spermatozoa
te	=	tergal extensions
tr	=	trichoscalid
trs	=	trichoscalid-like scalid
vlc	=	ventrolateral cuspidate spine
vlgco1	=	ventrolateral glandular cell outlet type 1
vlss	=	ventrolateral sensory spot
vlt	=	ventrolateral tube
vmgco1	=	ventromedial glandular cell outlet type 1
vmsac	=	ventromedial short acicular spine
vmso	=	ventromedial slit-like opening
vmss	=	ventromedial glandular sensory spot

Results

Distribution and abundance

All kinorhynch specimens were counted during the initial sorting process, and the number of individuals summed up to 621 specimens. After mounting and identification, this number was reduced, either because the number of specimens found in a tube did not match the initial count, because the specimens were too damaged/dirty to be processed, or because the specimens got lost during processing. Thus, after this stage, the operational number of specimens summed up to 211 identified adult individuals and 345 juvenile individuals, of which only an insignificant number could be identified to species level (Table 2).

Table 2. Overview of kinorhynch abundance per station and vertical layer at each station. Original counts are numbers of specimens indicated after the original extraction and sorting. Observed values are actual numbers of specimens recorded during the subsequent mounting and identification. All observed adults have been identified to species level. Study sites include: Gerl. = Gerlache Strait; IBB = Inner Basin B, Andvord Bay; MBA = Middle Basin A, Andvord Bay; OBA = Outer Basin A, Andvord Bay; St. B. = Open continental shelf.

CRS station, layer (cm), and study site	Original count per layer	Sum of original counts per station	Observed adults per layer	Observed juveniles per layer	Sum of observed specimens per layer	Sum of observed specimens per station
1698 0–1 MBA	11	51	1	5	6	39
1698 1–3	40		11	22	33	
1702 1–3 MBA	14	14	5	5	10	10
1706 0–1 MBA	16	17	2	7	9	10
1706 1–3	1		1	0	1	
1716 0–1 IBB	7	7	1	6	7	7
1756 0–1 St. B	1	1	0	1	1	1
1760 0–1 St. B	7	7	2	5	7	7
1763 0–1 St. B	1	3	0	1	1	5
1763 3–5	2		2	2	4	
1767 0–1 St. B	2	8	1	2	3	4
1767 1–3	6		0	1	1	
1769 0–1 IBB	9	10	2	2	4	5
1769 1–3	1		0	1	1	
1773 0–1 IBB	10	13	5	6	11	14
1773 1–3	3		2	1	3	
1776 0–1 ICC	10	11	5	4	9	10
1776 3–5	1		0	1	1	
1778 0–1 OBA	35	38	10	18	28	30
1778 1–3	3		0	2	2	
1781 1–3 OBA	5	5	0	4	4	4
1790 0–1 MBA	29	37	14	18	32	40
1790 1–3	8		0	8	8	
1792 0–1 MBA	5	26	0	3	3	22
1792 1–3	21		16	3	19	
1793 0–1 Gerl.	62	108	14	37	51	101
1793 1–3	45		26	23	49	
1793 3–5	1		0	1	1	
1799 0–1 MBA	7	9	6	3	9	10
1799 1–3	2		1	0	1	
1809 0–1 Gerl.	111	124	47	59	106	119
1809 1–3	10		7	3	10	
1809 3–5	3		1	2	3	
1832 0–1 Gerl.	40	129	5	25	30	115
1832 1–3	87		22	61	83	
1832 3–5	2		0	2	2	
1846 0–1 St. B	2	3	2	0	2	3
1846 1–3	1		0	1	1	
Total	621	621	211	345	556	556

The sampling was roughly concentrated to three separate areas along the distal part of the Antarctic Peninsula west coast: in Andvord Bay fjord on the Danco Coast, in the Gerlache Strait that separates a string of islands from the Peninsula, and on the open continental shelf west of the islands (Fig. 1). The

Table 3. Overview of kinorhynch abundance per vertical layer and sampling region across all stations. Since the number of stations differed between the regions, the average number of specimens per station in each region is indicated. Original counts are numbers of specimens indicated after the original extraction and sorting. Observed values are actual numbers of specimens recorded during the subsequent processing and identification.

Layer (cm)	Original count	Observed adults	Observed juveniles	Sum of observed specimens
0–1	365	117	202	319
1–3	247	91	135	226
3–5	9	3	8	11

Region	Original count	Original average/station	Observed count	Observed average/station
Andvord Bay	238	19.8	202	16.8
Gerlache Strait	361	120.3	335	111.7
Open continental shelf	22	4.4	20	4.0

three areas yielded considerably different amounts of kinorhynchs, i.e., 335 (observed) specimens from the Gerlache Strait vs 202 from Andvord Bay and 20 from the open continental shelf (Table 3). This clearly shows that kinorhynch abundance was lowest at the open shelf locations, but it also leaves the impression that the kinorhynch abundance is about 1.5 times higher in the Gerlache Strait compared to Andvord Bay. However, it also has to be taken into consideration that the Andvord Bay material was obtained from 12 stations, whereas the Gerlache Strait sampling only included three stations. If this sampling bias is taken into account, the average number of specimens per station in the Gerlache Strait is 111.7 (SD = 9.45) vs 16.8 (SD = 12.88) in the Andvord Bay, which suggests that the abundance is more than six times higher in the strait. On the contrary, the average station in the open continental shelf area yielded an average of 4.0 (SD = 2.24) specimens per station, thus only 25% of the specimens found in Andvord Bay.

If the vertical distribution of specimens in the sediment is compared across all stations, it is clear that the highest abundance (319 specimens observed in total) is found in the top 0–1 cm layer (Table 3). However, the following 1–3 cm layer also yielded a considerable number of specimens, i.e., 226 in total. The observed vertical distribution suggests that 98% of all kinorhynch specimens can be found in the top 4 cm fraction of the sediment. There were no obvious differences in the distribution of adults and juveniles in the different layers.

Based on the identification of 211 adult specimens, the study revealed the presence of 10, potentially 12, species of Kinorhyncha. Seven species are new to science and are described herein. One species, *Polacanthoderes shiraseae*, is a known Antarctic species; two morphotypes of *Polacanthoderes* are either undescribed species, hybrids, or morphological variations of known *Polacanthoderes* species, and two species had a morphology so close to Arctic congeners that it is uncertain whether they should be seen as undescribed species or known species with a bi-polar distribution.

Among the 10 (potentially 12) species observed, seven belong to the specious genus *Echinoderes* Claparède, 1863 (family Echinoderidae Carus, 1885), and additional two (potentially four) to *Polacanthoderes* (family Echinoderidae). Among the adult specimens, only a single non-Echinoderidae species was recorded, i.e., an undescribed species of *Condyloderes* Higgins, 1969b. Interestingly, among the 319 observed specimens (adults and juveniles), only a single juvenile specimen of Pycnophyidae Zelinka, 1896 was recorded.

The abundance and frequency of the different species differed considerably (Table 4). The most abundant species was *Echinoderes ahlfeldae* sp. nov.; a total of 90 specimens was detected, which is exactly twice as many as found for the second most abundant species, *Echinoderes nataliae* sp. nov. In terms of frequency though, *E. nataliae* was slightly more common, as it appeared on 61% of the stations vs 55% for *E. ahlfeldae*. The third species with a notable occurrence was *Polacanthoderes grzelakae* sp. nov., which had an abundance of 30 specimens and a frequency of 39%. All remaining species occurred with 13 specimens or less, and only *Echinoderes* aff. *angustus* had a frequency reaching 39%, as for *P. grzelakae*. The rarest identified species was *Echinoderes crux* sp. nov., which occurred with two specimens at a single station.

Species descriptions

Class Cyclorhagida (Zelinka, 1896) Herranz *et al*. 2022
Order Kentrorhagata Sørensen *et al.*, 2015
Family Centroderidae Zelinka, 1896
Genus *Condyloderes* Higgins, 1969b

Condyloderes notios sp. nov
urn:lsid:zoobank.org:act:3F5ACC7E-5173-4871-8465-642D9E7F473C
Figs 2–4, Tables 5–6

Diagnosis

Condyloderes with acicular spines in middorsal positions on segments 1 to 10, and in lateroventral positions on segments 1 to 9; laterodorsal acicular spines present on segment 10, at least in males. Unpaired cuspidate spines present in paradorsal position on segments 1, 5, and 7. Paired cuspidate spines present in lateral accessory positions on segment 1, in ventrolateral positions on segment 5, in lateroventral positions on segment 8, and in ventrolateral positions on segment 9. Female morphology unknown.

Etymology

The species name *notios* is from the Greek νότιος = 'southern', with reference to the species being the southernmost representative of *Condyloderes* and only the second member of the genus recorded from the Southern Hemisphere.

Material examined

Holotype
ANTARCTICA • ♂ (mounted for LM in Fluoromount G on HS slide); Antarctic Peninsula, CRS 1702; 64°51.15′ S, 62°34.44′ W; 502 m b.s.l.; 30 Nov. 2015; FjordEco1; soft sediment; NHMD 1784659.

Additional material
ANTARCTICA – **Antarctic Peninsula** • 1 juv. (mounted for LM in Fluoromount G on HS slide); CRS 1706; 64°50.47′ S, 62°35.12′ W; 499 m b.s.l.; 1 Dec. 2015; FjordEco1; soft sediment; NHMD 1784660 • 1 juv. (mounted for SEM); CRS 1793; 64°39.53′ S, 62°55.03′ W; 701 m b.s.l.; 11 Apr. 2016; FjordEco2; soft sediment; MVS • 3 ♂♂, 2 juv. (mounted for SEM); CRS 1832; 64°39.30′ S, 62°55.98′ W; 631 m b.s.l.; 21 Apr. 2016; FjordEco2; soft sediment; MVS.

Description

General. Adults with head, neck and eleven trunk segments (Figs 2, 3A, 4A–D). An overview of measurements and dimensions is given in Table 5. Distributions of cuticular structures, i.e., sensory

Table 4. Number of identified adult specimens per species and station.

CRS station	*C. notios* sp. nov.	*P. grzelakae* sp. nov.	*P. shiraseae*	*Polacanthoderes* sp. 1	*Polacanthoderes* sp. 2	*E. ahlfeldae* sp. nov.	*E. antarcticus* sp. nov.	*E. crux* sp. nov.	*E. kathleenhannae* sp. nov.	*E. nataliae* sp. nov.	*E. aff. angustus*	*E. aff. beringiensis/ romanoi/xalkutaat*	Species richness
Andvord Bay													
1698	–	–	–	–	–	10	–	–	–	1	1	–	3
1702	1	–	–	–	–	–	–	–	–	3	1	–	3
1706	–	2	–	–	–	–	–	–	–	1	–	–	2
1716	–	–	–	–	–	–	–	–	–	1	–	–	1
1769	–	1	–	–	–	1	–	–	–	–	–	–	2
1773	–	1	–	–	–	1	–	–	–	4	1	–	4
1776	–	2	–	1	1	–	–	–	–	–	1	–	4
1778	–	–	–	–	–	1	1	–	–	8	–	–	3
1790	–	–	–	–	–	6	–	–	–	8	–	–	2
1792	–	–	–	–	–	10	–	–	–	5	1	–	3
1799	–	–	–	–	–	5	–	–	–	2	–	–	2
Gerlache Strait													
1793	–	8	–	–	–	20	–	–	2	6	2	2	6
1809	–	7	–	1	–	28	1	–	–	6	3	9	7
1832	3	9	–	–	–	8	1	–	4	–	–	2	6
Open continental shelf													
1760	–	–	–	–	–	–	–	2	–	–	–	–	1
1763	–	–	2	–	–	–	–	–	–	–	–	–	1
1767	–	–	–	1	–	–	–	–	–	–	–	–	1
1846	–	–	2	–	–	–	–	–	–	–	–	–	1
Total	4	30	4	3	1	90	3	2	6	45	10	13	

spots and spines, are summarized in Table 6. Only males and juveniles were available for examination, so female dimorphism remains unknown for this species.

HEAD. Consists of a retractable mouth cone and an introvert (Fig. 4C). Only one specimen had its head partially protruded and thus information on head morphology is limited. Outer oral styles are composed of two units, with the proximal unit being considerably thicker than the distal.

INTROVERT. Primary spinoscalids are composed of a single unit, with a basal, transverse fringe and a row of fine hairs extending about ¼ down along the proximal part of the scalid; the distal ¾ are smooth, with a few transverse, partial wrinkles, giving the distal part a finger-like appearance. Remaining scalids appear to be located in introvert rings 2 to 5; they are composed of a basal sheath with a median fringe and a pointed end-piece. Scalids of Ring 4 (located centrally in each introvert sector) are flanked by a pair of thin, thread-like appendages, covered with minute hairs; the hair-covering makes them resemble thin trichoscalids. Trichoscalids are well-developed and located in the posteriormost ring.

NECK. Consists of 16 placids with condyles (Fig. 4D). All placids are about 12 μm in length, but differ in width. The midventral placid is the broadest, 15 μm wide. It is flanked by two pairs of narrow placids, each measuring 7 μm in width. From the two pairs of narrow, ventromedial placids, the placids alternate

Table 5. Measurements from light microscopy of *Condyloderes notios* sp. nov. (in µm).

Character	NHMD-1784659 (♂)		
TL	271	PD1 (cu)	18
TL (CUM)	335	PD5 (cu)	18
MSW-6	80	PD7 (cu)	18
MSW-6/TL	29.5%	–	
SW-10	63	LA1 (cu)	18
SW-10/TL	23.2%	LV5 (cu)	18
S1	23	LV8 (cu)	27
S2	28	LV9 (cu)	21
S3	28	–	
S4	28	LV1 (ac)	38
S5	28	LV2 (ac)	35
S6	30	LV3 (ac)	32
S7	39	LV4 (ac)	39
S8	39	LV5 (ac)	41
S9	39	LV6 (ac)	41
S10	28	LV7 (ac)	41
S11	25	LV8 (ac)	42
–		LV9 (ac)	50
MD1 (ac)	34	LD10 (ac)	34
MD2 (ac)	32	–	
MD3 (ac)	36	LTAS	193
MD4 (ac)	36	MTS	117
MD5 (ac)	35	MTS/TL	43.2%
MD6 (ac)	36		
MD7 (ac)	41		
MD8 (ac)	48		
MD9 (ac)	56		
MD10 (ac)	37		

between broad (width: 13 µm) and narrow (width: 7 µm) ones towards the narrow middorsal placid. All condyles form structures with a narrow posterior part that broadens anteriorly, which makes them resemble small mushrooms. The midventral placid has three condyles, whereas other broad placids have two condyles, and narrow ones have a single.

Segment 1. Consists of a complete cuticular ring. Acicular spines are present in middorsal and lateroventral positions, and cuspidate spines are present as an unpaired paradorsal spine and as paired lateral accessory spines; direction (left or right) of lateral shift in position of the unpaired paradorsal cuspidate spine differs between specimens. Sensory spots are present as two pair in subdorsal positions, two pairs in laterodorsal positions, and one pair in ventromedial positions. Sensory spots on this and following eight segments are slightly protruding and composed of numerous micropapillae around a central pore, i.e., corresponding to sensory spot type 6 sensu Neuhaus *et al.* (2019). The surface of the tergal plate is reticulated at its anterior half and has a narrow zone with minute triangular hairs, in between the reticulated part and the relatively broad free flap; sternal plate surfaces are reticulated throughout, from anterior margin to posterior free flaps; dense coverings of thin cuticular hairs are present in areas anterior to the middorsal and lateroventral acicular spines. The free flaps, marking the posterior segment margins, have longitudinal lines that extend beyond the margins of the free flaps and form minute, pointed tips. The posterior margin is mostly straight, with notches at the attachment sites of the lateroventral spines, and with a small and rather narrow midventral indentation, only expanding over the paraventral areas (Figs 2A–B, 3B–C, 4D–G).

Table 6. Summary of nature and location of sensory spots, tubes, and spines arranged by series in *Condyloderes notios* sp. nov. * marks unpaired structures in otherwise paired positions. $^{-x}$ indicates number of specimens (out of 4 examined adults) in which the character trait is missing.

Segment	Position							
	MD	PD	SD	LD	LA	LV	VL	VM
1	ac	cu*	ss6,ss6	ss6,ss6	cu	ac	–	ss6
2	ac	ss6	ss6	ss6,ss6	–	ac	–	ss6
3	ac	ss6	ss6	ss6	–	ac	–	ss6
4	ac	ss6	ss6^{-1}	–	–	ac	–	ss6
5	ac	cu*,ss6	ss6	ss6	–	ac	cu	ss6
6	ac	ss6	ss6	ss6	–	ac	–	ss6
7	ac	cu*,ss6	ss6	ss6	–	ac	–	ss6
8	ac	ss6	ss6	ss6	–	ac, cu	–	ss6
9	ac	ss6	–	ne,ss6	–	ac	cu	ss6
10	ac	–	ss3^{-1}	ac	–	ss6	–	–
11	mts	–	ss3	–	ltas	–	ss3	ss6

SEGMENT 2. As the following eight segments, consists of a tergal and two sternal plates. Acicular spines are present in middorsal and lateroventral positions. Sensory spots are present in paradorsal, subdorsal, laterodorsal (two pairs), and ventromedial positions. Tergal plate and lateral halves of sternal plates are covered with minute, triangular hairs; ventralmost halves of sternal plates with reticulated surfaces. Free flaps as on preceding segment and posterior segment margin mostly straight, but with notches at the attachment sites of the lateroventral spines (Figs 2A–B, 3B–C, 4E–G).

SEGMENT 3. As preceding segment, but only with one pair of laterodorsal sensory spots (Figs 2A–B, 3B–C, 4E).

SEGMENT 4. As preceding segment, but without laterodorsal sensory spots. Subdorsal sensory spots usually present, but were missing in one specimen (Figs 2A–B, 3B–C, 4E, H).

SEGMENT 5. With acicular spines in middorsal and lateroventral positions, and cuspidate spines present as an unpaired paradorsal spine and as paired ventrolateral spines; direction of lateral shift in position of the unpaired paradorsal cuspidate spine differs between specimens and irrespective of position of paradorsal cuspidate spine on segment 1. Sensory spots present in paradorsal, subdorsal, laterodorsal, and ventromedial positions. Cuticular ornamentation, free flap, and posterior segment margin as on preceding segment (Figs 2A–B, 3B–C, 4H–J).

SEGMENT 6. With same arrangement of cuticular structures as on segment 3 (Figs 2A–B, 3B–E, 4H–J).

SEGMENT 7. With acicular spines in middorsal and lateroventral positions, and an unpaired, cuspidate spine in paradorsal position; direction of lateral shift in position of the unpaired paradorsal cuspidate spine differs between specimens and irrespective of position of paradorsal cuspidate spines on preceding segments. Sensory spots present in paradorsal, subdorsal, laterodorsal, and ventromedial positions. Cuticular ornamentation, free flap, and posterior segment margin as on preceding segment (Figs 2A–B, 3D–E, 4K–M).

SEGMENT 8. With acicular spines in middorsal and lateroventral positions, and cuspidate spines also in lateroventral positions, attaching posterior to acicular spines. Sensory spots present in paradorsal, subdorsal, laterodorsal, and ventromedial positions. Cuticular ornamentation, free flap, and posterior segment margin as on preceding segment (Figs 2A–B, 3D–E, G–H, 4L–M).
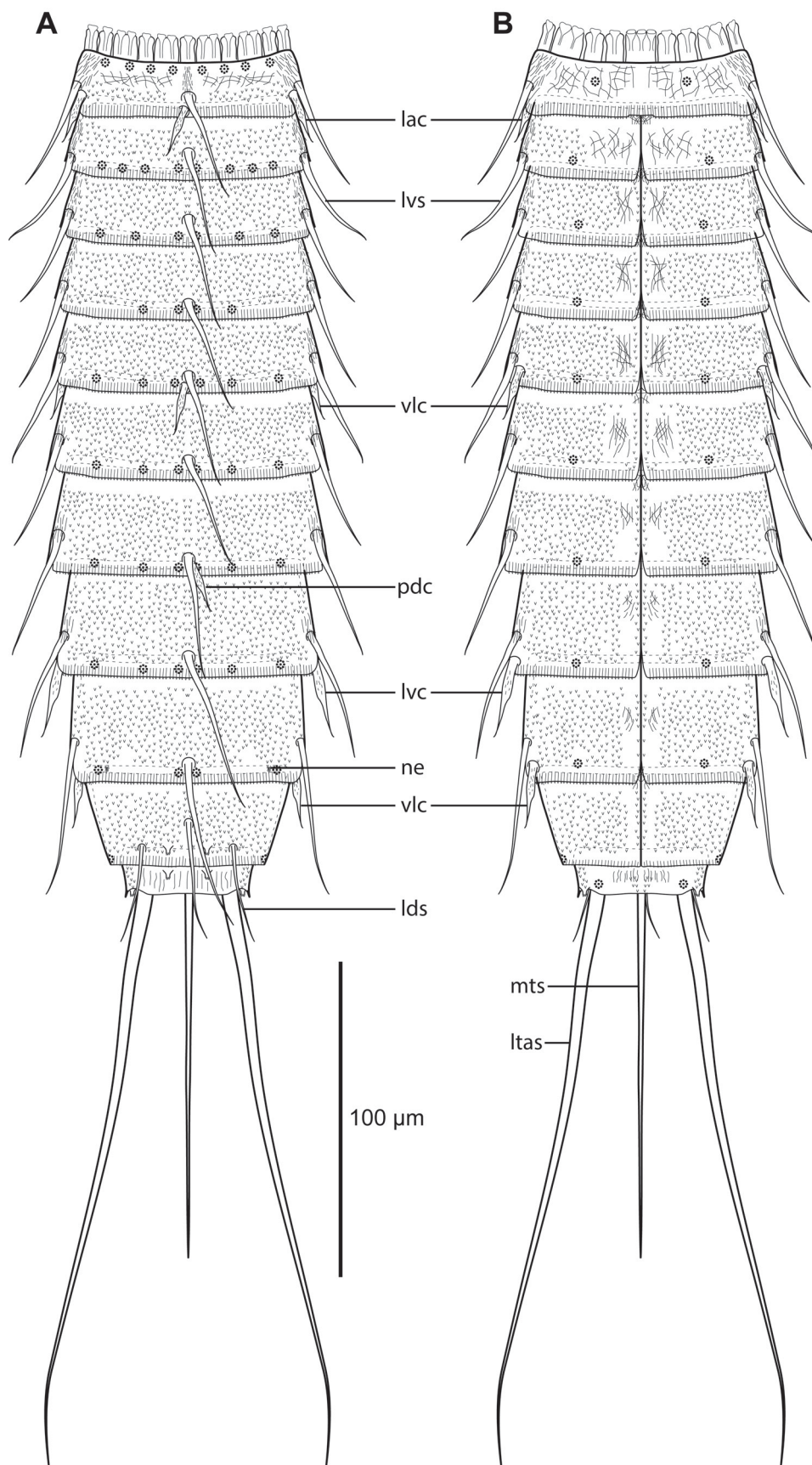
Fig. 2. Line art illustrations of *Condyloderes notios* sp. nov. **A**. Male, dorsal view. **B**. Male, ventral view.

Fig. 3. Light micrographs showing overviews and details in male holotype (NHMD 1784659) of *Condyloderes notios* sp. nov. **A**. Ventral overview. **B**. Segments 1 to 6, dorsal view. **C**. Segments 1 to 6, ventral view. **D**. Segments 6 to 10, dorsal view. **E**. Segments 6 to 10, ventral view. **F**. Segments 9 to 11, dorsal view. **G**. Segments 8 to 11, focused inside specimen. **H**. Segments 8 to 11, ventral view. Scale bars: A = 100 µm; B–H = 25 µm.

Segment 9. With acicular spines in middorsal and lateroventral positions, and cuspidate spines in ventrolateral positions. Sensory spots present in paradorsal, laterodorsal, and ventromedial positions. A pair of minute nephridiopores, appearing as a tuft of short micropapillae, is located next to, but more dorsal than, the laterodorsal sensory spots (Fig. 4O). Cuticular ornamentation, free flap, and posterior segment margin as on preceding segment (Figs 2A–B, 3D–H, 4N–P).

Segment 10. With acicular spines in middorsal and laterodorsal positions. Sensory spots type 3, i.e., stalked sensory spots, present in subdorsal positions (but missing in one specimen); sensory spots type 6 present in lateroventral positions, at the posterior segment margin. Cuticular ornamentation, free flap, and posterior segment margin otherwise as on preceding segment (Figs 2A–B, 3D–H, 4N–P).

Segment 11. Consists of a tergal and a sternal plate. Lateral terminal accessory spines and midterminal spine are present; lateral terminal accessory spines are about 70% longer than the midterminal. Stalked sensory spots type 3 are present in subdorsal and ventrolateral positions, and sensory spots type 6 in ventromedial positions. The tergal plate is covered with minute, triangular hairs, whereas the sternal plate is mostly smooth and ornamented with fine, longitudinal lines. A free flap with irregular longitudinal lines is present at the tergal plate only; the sternal plate terminates in a finely serrated edge (Figs 2A–B, 3G–H, 4N–P).

Distribution

Antarctic Peninsula: Gerlache Strait and Andvord Bay MBA, 499 to 701 m. See Fig. 1 for geographic overview of stations and Table 1 for station and specimen information.

Diagnostic remarks

The placids with condyles, and the segment composition, with segment 1 composed of a closed cuticular ring, segments 2 to 10 composed of one tergal and two sternal plates, and segment 11 of one tergal and one sternal plate, easily assigns the new species to *Condyloderes*. The genus currently accommodates eleven species, including *Condyloderes notios* sp. now.

The new species is most easily distinguished from its congeners by its unique cuspidate spine pattern. The presence of cuspidate spines in mid- or paradorsal positions is only shared with three other species, i.e., *Condyloderes agnetis* Dal Zotto *et al.*, 2019, *C. shirleyi* Neuhaus *et al.*, 2019, and *C. storchi* Higgins in Martorelli & Higgins, 2004. However, none of the three species have paradorsal cuspidate spines on segment 1, which in itself makes *C. notios* sp. nov. differ from all other congeners. Of the three species, the Mediterranean *C. agnetis* differs the most, by having paired paradorsal cuspidate spines on segments 3 and 7 (Dal Zotto *et al.* 2019), opposite to the unpaired ones on segments 1, 5, and 7 in *C. notios*. In both species the cuspidate spines are reported as paradorsal, but in *C. agnetis* the cuspidate spines are clearly more laterally displaced, and thus very close to being subdorsal. In contrast, the unpaired paradorsal cuspidate spines in *C. notios* are so close to the middorsal line that they almost could be interpreted as middorsal.

Condyloderes shirleyi and *C. storchi* show more similarity to the new species, as they both have unpaired middorsal or paradorsal cuspidate spines on segments 5 and 7, but besides lacking a paradorsal cuspidate spine on segment 1, their cuspidate spine pattern in the lateral series also differs considerably. *Condyloderes shirleyi* differs by having cuspidate spines in the lateral series of segments 2, 6, and 7, but not on segment 1 (Neuhaus *et al.* 2019), and *C. shirleyi* by having lateral accessory cuspidate spines on segment 4 (Martorelli & Higgins 2004; Neuhaus *et al.* 2019).

If compared with the remaining *Condyloderes* species without cuspidate spines in the dorsal series, *C. notios* sp. nov. shows most resemblance with *C. clarae* Dal Zotto *et al.*, 2019 and *C. flosfimbriatus*

Fig. 4. Scanning electron micrographs showing overviews and details of male *Condyloderes notios* sp. nov. **A**. Right lateral overview. **B**. Ventral overview. **C**. Partly retracted introvert focused on midventral sector 1. **D**. Close-up of neck region, showing midventral and ventromedial placids. **E**. Segments 1 to 4, dorsal view; note that the paradorsal cuspidate spine broke off in this specimen. **F**. Segments 1 to 2, left lateral view. **G**. Segments 1 to 2, ventral view. **H**. Segments 4 to 7, dorsal view. **I**. Segments 5 to 6, left lateral view. **J**. Segments 5 to 6, ventral view. **K**. Segments 7 to 9, dorsal view. **L**. Segments 7 to 8, left lateral view. **M**. Segments 7 to 8, ventral view. **N**. Segments 9 to 11, dorsal view. **O**. Segments 9 to 11, left lateral view; inset shows close-up of laterodorsal sensory spot (left) and nephridiopore (right). **P**. Segments 10 to 11, ventral view. Scale bars: A – B = 100 µm; C, E – P = 20 µm; D = 10 µm.

Sørensen *et al.*, 2019, as they also have cuspidate spines in the lateral or ventral series of segments 5, 8 and 9, but none of them have lateral accessory cuspidate spines on segment 1 (Dal Zotto *et al.* 2019; Sørensen *et al.* 2019). Among its ten congeners, *C. notios* clearly shows greatest resemblance with *C. storchi*, which also happens to be the only other species of *Condyloderes* described from the southern hemisphere.

<div align="center">

Order Echinorhagata Sørensen *et al.*, 2015
Family Echinoderidae Carus, 1885
Genus *Polacanthoderes* Sørensen, 2008

***Polacanthoderes grzelakae* sp. nov**
urn:lsid:zoobank.org:act:3966DEF9-01C9-4294-AAFB-DCDB56648067
Figs 5–8, Tables 7–8

</div>

Diagnosis

Polacanthoderes with regular acicular spines in middorsal positions on segments 4 to 8, and in lateroventral positions on segments 6 to 9; lateroventral spines on segments 8 (in particular) and 9 are conspicuously stronger than other acicular spines, and the one on segment 8 is the strongest. Tubes are present in subdorsal and ventrolateral positions on segment 2, midlateral positions on segment 4, lateroventral positions on segment 5, and laterodorsal positions on segment 10. Small acicular spines are present in the following series: subdorsal positions on segments 4 and 5 (but missing in some specimens), laterodorsal positions on segments 6 to 8, midlateral positions on segments 5 to 9, sublateral positions on segment 7, lateral accessory positions on segments 6 and 8 to 9, ventrolateral positions on segments 8 to 10, and in ventromedial positions on segments 4 to 7. Glandular cell outlets type 2 are present in midlateral positions on segments 6 and 8. Dorsal glandular cell outlets type 1 are present in middorsal positions on segments 1 to 3 and 10, and in paradorsal positions on segments 4 to 9. Small sieve plates present on segment 9 in sublateral positions.

Etymology

The species is dedicated to Katarzyna Grzelak – a fabulous kinorhynch taxonomist and meiofauna ecologist.

Material examined

Holotype
ANTARCTICA • ♂ (mounted for LM in Fluoromount G on HS slide); Antarctic Peninsula, CRS 1706; 64°50.47′ S, 62°35.12′ W; 499 m b.s.l.; 1 Dec. 2015; FjordEco1; soft sediment; NHMD 1784249.

Paratypes
ANTARCTICA – **Antarctic Peninsula** • 1 ♀ (mounted as holotype); CRS 1769; 64°52.37′ S, 62°25.27′ W; 547 m b.s.l.; 5 Apr. 2016; FjordEco2; soft sediment; USNM 1740027 • 1 ♂ (mounted as holotype); CRS 1773; 64°52.35′ S, 62°25.88′ W; 553 m b.s.l.; 6 Apr. 2016; FjordEco2; soft sediment; NHMD 1784250 • 1 ♂ (mounted as holotype); CRS 1776; 64°52.53′ S, 62°33.90′ W; 551 m b.s.l.; 7 Apr. 2016; FjordEco2; soft sediment; USNM 1740028 • 3 ♀♀ (mounted as holotype); CRS 1793; 64°39.53′ S, 62°55.03′ W; 701 m b.s.l.; 11 Apr. 2016; FjordEco2; soft sediment; NHMD 1784251, 1784284, 1784303 • 2 ♂♂, 1 ♀ (mounted as holotype); CRS 1809; 64°39.59′ S, 62°55.09′ W; 694 m b.s.l.; 15 Apr. 2016; FjordEco2; soft sediment; NHMD 1784304 to 1784306.

Additional material
ANTARCTICA – **Antarctic Peninsula** • 1 ♀ (mounted for SEM); same data as for holotype; MVS • 1 ♂ (mounted for SEM); CRS 1776; 64°52.53′ S, 62°33.90′ W; 551 m b.s.l.; 7 Apr. 2016; FjordEco2; soft sediment; MVS • 4 ♂♂, 1 ♀ (mounted for SEM); CRS 1793; 64°39.53′ S, 62°55.03′ W; 701 m b.s.l.;

11 Apr. 2016; FjordEco2; soft sediment; MVS • 3 ♂♂, 1 ♀ (mounted for SEM); CRS 1809; 64°39.59′ S, 62°55.09′ W; 694 m b.s.l.; 15 Apr. 2016; FjordEco2; soft sediment; MVS • 4 ♂♂, 5 ♀♀ (mounted for SEM); CRS 1832; 64°39.30′ S, 62°55.98′ W; 631 m b.s.l.; 21 Apr. 2016; FjordEco2; soft sediment; MVS.

Description

GENERAL. Adults with head, neck and eleven trunk segments (Figs 5A–B, 6, 7A, 8B). The species is large for an Echinoderidae, 467 to 488 µm in trunk length, and the segments are completely devoid of regular, cuticular hairs. An overview of measurements and dimensions is given in Table 7. Distributions of cuticular structures, i.e., sensory spots, glandular cell outlets, spines, and tubes, are summarized in Table 8.

HEAD. Consists of a retractable mouth cone and an introvert (Figs 6, 8A). Inner oral styles of mouth cone are arranged in three rings: 10 styles are present in the outermost ring and 5 in the following. The innermost ring could not be examined. The external mouth cone armature consists of nine outer oral styles; bases of outer oral styles each flanked by a transverse fringe row consisting of very short spikes and a V-shaped row with considerably longer tips.

INTROVERT. The sectors are defined by the ten primary spinoscalids in Ring 01. Each primary spinoscalid consists of a basal sheath and a distal end piece with a blunt tip. The sheaths have, described from proximal towards distal parts: a transverse fringe with ca 10 long fringe tips; a slightly more distal fringe with four, terminally bifurcated fringe tips; and numerous short fringe tips along the distal margin of the sheath. End pieces are flexible and smooth. Rings 02 and 04 have 10 spinoscalids, and Rings 03 and 05 have 20 spinoscalids. All spinoscalids in these rings are well-developed, and consist of a basal sheath and a pointed end piece. Ring 06 has only 6 spinoscalids, located in sectors 1, 3, 5, 6, 7, and 9; they resemble those in preceding sectors, but without the distinct differentiation into sheath and end piece. Ring 07 has 8 spinoscalids, located as pairs in sectors 1, 3, and 9, and unpaired but laterally displaced in sectors 5 and 7 (trichoscalids take up the space in the opposite side of each sector); ring 07 spinoscalids appear very simplified and resemble thin fringes rather than actual scalids (Figs 6, 8A). Described sector-wise (Fig. 6), sectors 1, 3, and 9 are similar, having spinoscalids arranged as two double diamonds anterior to an additional pair of Ring 07 spinoscalids. Sectors 2, 4, 8, and 10 all have spinoscalids arranged as a quincunx, located in between an anterior spinoscalid in Ring 02 and a trichoscalid plate. Sectors 5 and 7 have spinoscalids forming double diamonds, anterior to an unpaired, lateral spinoscalid; the lateral spinoscalid is unpaired because a trichoscalid plate takes up the space in the opposite side of the sector. Sector 6 has its trichoscalids arranged as double diamonds. Regular trichoscalids with trichoscalid plates are present in sectors 2, 4, 5, 7, 8, and 10.

NECK. Consists of 16 placids. Midventral placid broadest, 17 µm in width and 18 µm in length, whereas all others are narrower, measuring 9 µm in width at their bases (Fig. 7B–C). The trichoscalid plates are well-developed.

SEGMENT 1. Consists of a complete cuticular ring. Sensory spots are present in subdorsal, laterodorsal sublateral, and ventromedial positions; sensory spots on this and following segments are small, slightly depressed into the cuticle, rounded, and composed of a central pore surrounded by a few micropapillae. Glandular cell outlets type 1 are present in middorsal and ventromedial positions. Posterior segment margin with very fine denticles in middorsal to midlateral positions and hardly any denticles or fringe tips at all in sublateral to ventromedial positions; ventromedial to midventral positions though with 11 to 13 strongly developed, dagger-shaped fringe tips (Figs 5A–B, 7B–C, 8C–D).

Table 7. Measurements from light microscopy of *Polacanthoderes grzelakae* sp. nov. (in µm), including number of measured specimens (*n*) and standard deviation (SD).

Character	*n*	Range	Mean	SD	Character	*n*	Range	Mean	SD
TL	5	467–488	475	8.58	ML4 (tu)	6	17–18	17	0.41
TL (CUM)	6	589–611	603	7.69	ML5 (sac)	6	20–22	21	1.03
MSW-6	5	84–86	85	1.10	ML6 (sac)	6	22–26	23	1.60
MSW-6/TL	4	17.8–18.4%	18.0%	0.28%	ML7 (sac)	6	23–27	25	1.60
SW-10	5	65–69	68	1.67	ML8 (sac)	6	22–25	23	1.37
SW-10/TL	4	13.9–14.6%	14.3%	0.28%	ML9 (sac)	6	20–24	22	1.41
S1	6	41–46	45	1.86	SL7 (sac)	6	22–26	24	1.86
S2	6	42–47	45	2.07	LAS6 (sac)	5	14–18	17	1.79
S3	6	42–46	44	1.67	LAS8 (sac)	6	20–22	21	1.10
S4	6	47–51	48	1.75	LAS9 (sac)	6	17–22	20	1.87
S5	6	48–54	52	2.51	LV5 (tu)	5	14–15	15	0.45
S6	6	54–59	56	2.83	LV6 (ac)	6	25–30	27	2.10
S7	6	56–63	60	2.42	LV7 (ac)	6	27–32	29	2.07
S8	6	66–72	68	2.32	LV8 (ac)	6	38–52	45	5.79
S9	6	65–71	68	2.14	LV9 (ac)	6	37–44	40	2.71
S10	6	64–74	70	4.40	VM3 (sac)	2	16	16	0.71
S11	6	43–54	48	4.22	VM4 (sac)	5	11–15	13	1.67
–					VM5 (sac)	5	12–16	14	1.58
MD4 (ac)	5	52–77	65	9.04	VM6 (sac)	5	13–16	15	1.30
MD5 (ac)	6	74–92	85	6.13	VM7 (sac)	4	16–19	17	1.41
MD6 (ac)	4	96–109	104	5.50	VL8 (sac)	6	15–19	17	1.47
MD7 (ac)	6	119–129	126	3.60	VL9 (sac)	6	17–18	18	0.55
MD8 (ac)	6	145–159	156	5.43	VL10 (sac)	5	14–21	17	2.51
VL2 (tu)	2	15–17	16	1.41	LD10 (tu)	5	16–17	16	0.55
SD2 (tu)	6	16–17	17	0.52	LTS	6	197–264	242	24.43
SD4 (tu)	5	16–20	18	1.48	LTAS	3	90–94	91	2.65
SD5 (sac)	5	16–19	17	1.14	LTS/TL	5	49.3–54.3%	52.9%	2.08%
LD6 (sac)	6	24–29	26	1.86	PE1	3	90–102	98	6.66
LD7 (sac)	6	25–30	27	1.90	PE2	2	44–63	54	13.44
LD8 (sac)	6	25–29	27	1.64	PE3	3	90–107	98	8.54

SEGMENT 2. As remaining segments, consists of a tergal and two sternal plates. Tubes are present in subdorsal and ventrolateral positions. Sensory spots are present in middorsal position, as two pairs in laterodorsal positions and in ventromedial positions. Glandular cell outlets type 1 are present in middorsal position and ventromedial positions; ventromedial outlets are located close, but anterior to the ventromedial sensory spots. The posterior segment margin is straight, with small denticles along the tergal plate and slightly longer but also thinner fringe tips along the margins of the sternal plates (Figs 5A–B, 7B–C, 8C–D).

SEGMENT 3. With sensory spots present in subdorsal, laterodorsal, midlateral and ventromedial positions, and glandular cell outlets type 1 in middorsal and ventromedial positions. A single specimen had small acicular spines in ventromedial positions. Posterior segment margin as on preceding segment (Figs 5A–B, 7C, 8C–E).

SEGMENT 4. With regular, acicular spine in middorsal position and small acicular spines in subdorsal and ventromedial positions; small subdorsal acicular spines were missing in five specimens. Tubes present midlateral positions; tubes missing in one specimen. Sensory spots present in subdorsal and ventromedial positions; subdorsal sensory spots slightly more lateral than subdorsal acicular spines.

Table 8. Summary of nature and location of sensory spots, glandular cell outlets, tubes, and spines arranged by series in *Polacanthoderes grzelakae* sp. nov. $^{-x}$ indicates number of specimens (out of 30 examined) in which the character trait is missing. Characters in parentheses are interpreted as abnormalities, present in only a single specimen.

Segment	Position									
	MD	PD	SD	LD	ML	SL	LA	LV	VL	VM
1	gco1	–	ss	ss	–	ss	–	–	–	gco1,ss
2	gco1,ss	–	tu	ss,ss	–	–	–	–	tu	gco1,ss
3	gco1	–	ss	ss	ss	–	–	–	–	gco1,(sac^{-29}),ss
4	ac	gco1	sac^{-5},ss	–	tu^{-1}	–	–	–	–	gco1,sac,ss
5	ac	gco1	sac^{-5},ss	–	sac,ss	–	–	tu	–	gco1,sac,ss
6	ac	gco1,ss	–	sac,(sac^{-29}),ss	sac,gco2	–	sac^{-1}	ac	–	gco1,sac,ss, pa(♀)
7	ac	gco1,ss	–	sac,ss	sac,ss	sac	(sac^{-29})	ac	pa(♀)	gco1,sac,ss
8	ac	gco1,ss	–	sac^{-2},ss	sac,gco2	–	sac	ac	sac,ss	gco1
9	–	gco1,ss	ss	–	sac,ss	si	sac	ac	sac,ss	gco1
10	gco1,gco1	–	ss	tu	–	–	–	–	sac,ss	gco1
11	–	–	ss	–	pex3(♂)	–	ltas(♀)	lts	–	–

Glandular cell outlets type 1 present in paradorsal and ventromedial positions. Posterior segment margin as on preceding segment (Figs 5A–B, 7B–C, 8D–F).

SEGMENT 5. With regular, acicular spine in middorsal position and small acicular spines in subdorsal, midlateral, and ventromedial positions; small subdorsal acicular spines were missing in five specimens. Tubes present lateroventral positions. Sensory spots present in subdorsal, midlateral, and ventromedial positions; subdorsal sensory spots slightly more lateral than subdorsal acicular spines, as on preceding segment. Glandular cell outlets type 1 present in paradorsal and ventromedial positions. Posterior segment margin as on preceding segment (Figs 5A–B, 7D–E, 8D–F).

SEGMENT 6. With regular, acicular spines in middorsal and lateroventral positions, and small acicular spines in laterodorsal, midlateral, lateral accessory, and ventromedial positions; one specimen had an extra set of laterodorsal small acicular spines, whereas another specimen lacked short lateral accessory acicular spines. Well-developed glandular cell outlets type 2, located in midlateral positions, slightly posterior to the short acicular spines. Females with ventromedial female papillae, forming small funnel-shaped intracuticular structures. Sensory spots present in paradorsal, laterodorsal and ventromedial positions; laterodorsal sensory spots slightly more dorsal than laterodorsal acicular spines. Glandular cell outlets type 1 present in paradorsal and ventromedial positions. Posterior segment margin as on preceding segment (Figs 5A–B, D, 7D–E, H, 8F, H–I).

SEGMENT 7. With regular, acicular spines in middorsal and lateroventral positions, and small acicular spines in laterodorsal, midlateral, sublateral and ventromedial positions; one specimen also with a pair of small acicular spines in lateral accessory positions. Females with ventrolateral female papillae, forming small funnel-shaped intracuticular structures. Sensory spots present in paradorsal, laterodorsal, midlateral, and ventromedial positions. Glandular cell outlets type 1 and posterior segment margin as on preceding segment (Figs 5A–B, D, 7F–H, 8F, H–I).

SEGMENT 8. With regular, acicular spines in middorsal and lateroventral positions, and small acicular spines in laterodorsal, midlateral, lateral accessory, and ventrolateral positions; lateroventral acicular spines are conspicuously strong on this segment and nearly twice as thick as the lateroventral spines on the two preceding segments; small laterodorsal acicular spines were missing in two specimens. Well-developed glandular cell outlets type 2, located in midlateral positions, slightly posterior to the short

acicular spines. Sensory spots present in paradorsal, laterodorsal, and ventrolateral positions. Glandular cell outlets type 1 and posterior segment margin as on preceding segment (Figs 5A–B, 7F–G, J, 8G, I).

Segment 9. With regular, acicular spines in lateroventral positions and small acicular spines in midlateral, lateral accessory and ventrolateral positions; lateroventral spine considerably stronger than those in same positions on segments 6 and 7, although not as strong as the spine on segment 8. Small rounded sieve plates present in sublateral positions. Sensory spots present in paradorsal, subdorsal, midlateral, and ventrolateral positions. Glandular cell outlets type 1 and posterior segment margin as on preceding segment (Figs 5A–B, 7I–J, 8G,).

Segment 10. With laterodorsal tubes located near, but not at, posterior segment margin and small acicular spines in ventrolateral positions. Sensory spots present in subdorsal and ventrolateral positions. Glandular cell outlets type 1 present as two longitudinally arranged outlets in middorsal position and a pair in ventromedial positions. Posterior segment margin with thin but longer fringe tips between the laterodorsal tubes and along the concave margins of the sternal plates (Figs 5A–C, 7I, K, 8J–K).

Segment 11. With lateral terminal spines. Females with thin lateral terminal accessory spines; males with three pairs of conspicuously long penile spines; especially the flexible and pointed dorsal and ventral pair are long, occasionally exceeding 100 μm, whereas the truncate and slightly more rigid median pair is shorter, around 54 μm. Sensory spots present in subdorsal positions, on inferior margins of tergal extensions. Glandular cell outlets type 1 were not observed. As is the case with all preceding segments, regular cuticular hairs are absent, but patches of very short triangular hairs are present on the sternal extensions. Tergal and sternal extensions are triangular with fine marginal fringes; tergal extensions are slightly longer than the sternal ones. A pair of rigid setae attaches on the outer lateral margins of the tergal extensions (Figs 5A–C, 7K–M, 8J–K).

Distribution

Antarctic Peninsula: Gerlache Strait and Andvord Bay MBA and IBB, 499 to 701 m b.s.l. See Fig. 1 for geographic overview of stations and Table 1 for station and specimen information.
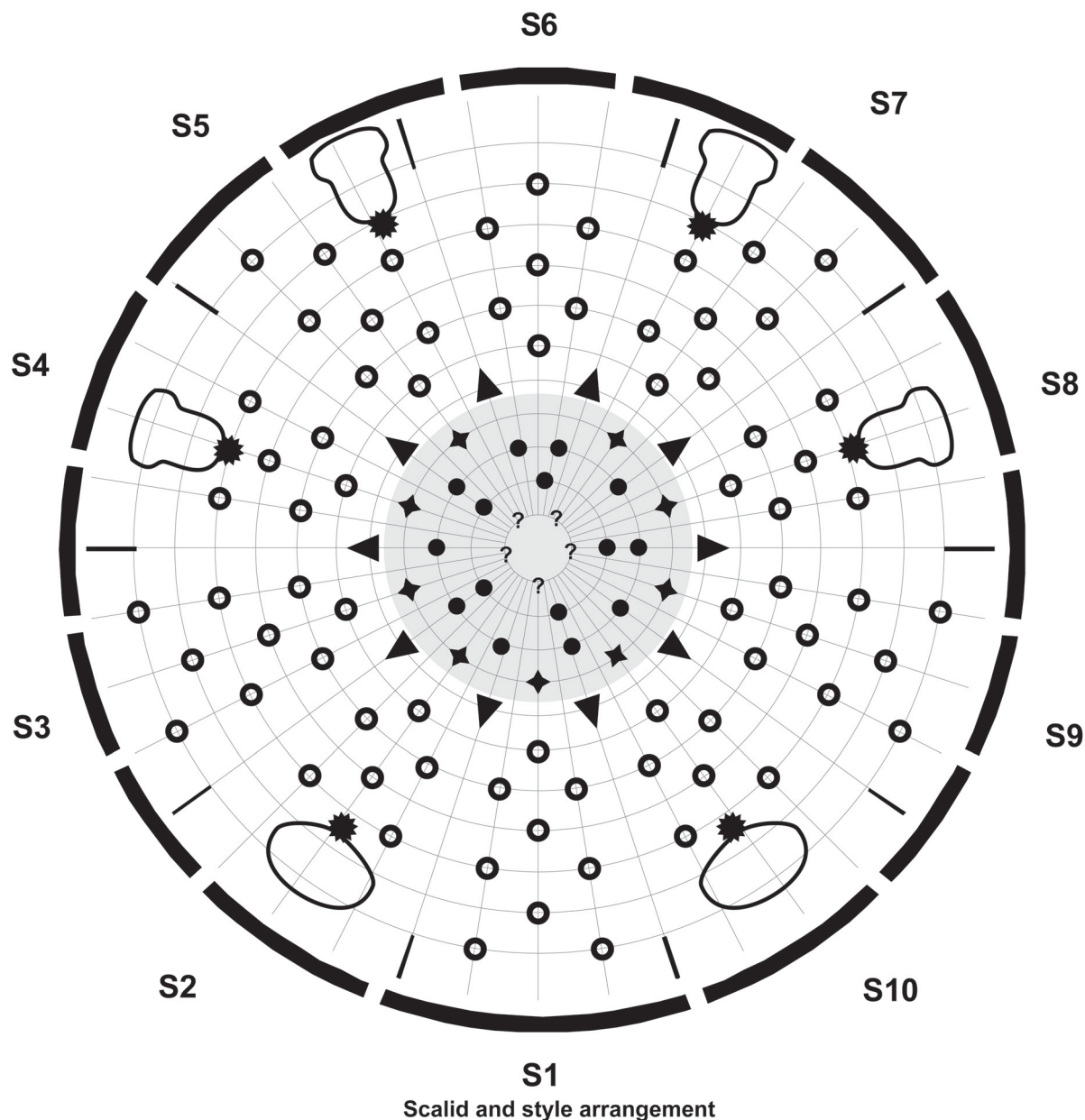
Polymorphism

The species shows a relatively high level of polymorphism, expressed in the relatively frequent absence of small acicular spines and, less frequently, in the presence of additional small acicular spines. It is not possible to provide a complete overview of the polymorphism in the 30 examined specimens of *P. grzelakae* sp. nov., because some specimens were damaged and others (SEM specimens) were mounted in a way that prevented observation of all relevant characters. It is, however, still possible to get some indications. Out of the 30 specimens, eight showed a confirmed, identical distribution of tubes and spines (except for the sexually dimorphic ones). The two most frequent 'abnormalities' were the lack of small acicular spines in subdorsal positions, on either segment 4 or 5. Interestingly, the spines were never missing on both segments in the same specimen. Five specimens (paratype NHMD 1784250 from stn 1773, two SEM specimens from stn 1793, and two from stn 1832) were lacking subdorsal spines on segment 5, but showed otherwise no variation from the most common spine pattern. Another five (SEM specimens from stn 1706, 1793, 1809 and 1832) lacked subdorsal spines on segment 4, but only one of these (a male from stn 1793) showed additional variation by also lacking small acicular spines in midlateral positions of segment 4. Two SEM specimens from stn 1832 lacked small acicular spines in laterodorsal positions on segment 8, but otherwise all remaining observed variation was restricted to three specimens with their own unique spine combinations, expressed either as lack of spines or presence of additional spines. For example, one specimen (paratype USNM 1740027 from stn 1769) had a set of small acicular spines in ventromedial positions on segment 3, although such spines were absent in all other specimens, and another (SEM specimen from stn 1909) was missing small acicular
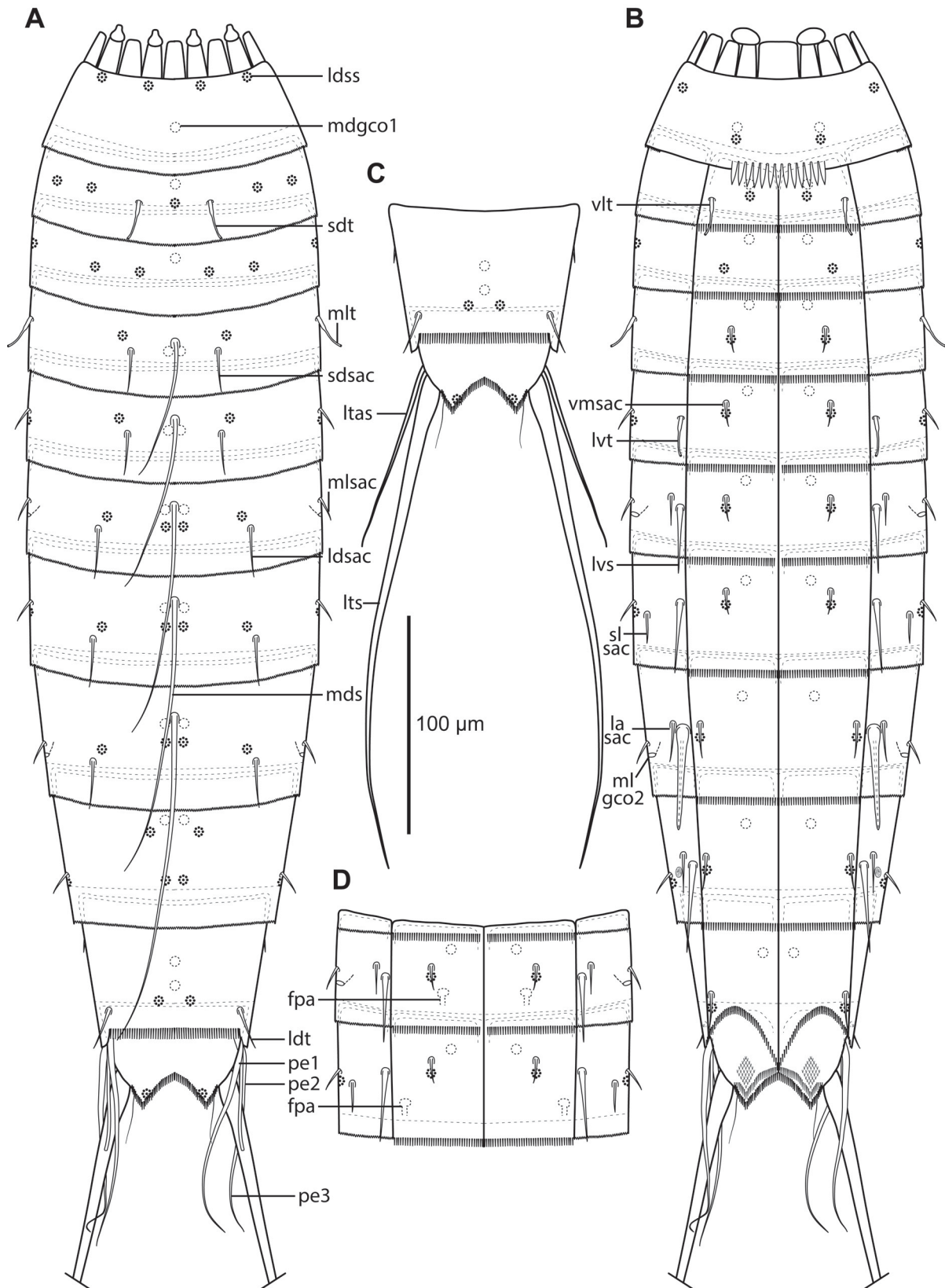
Fig. 5. Line art illustrations of *Polacanthoderes grzelakae* sp. nov. **A**. Male, dorsal view. **B**. Male, ventral view. **C**. Female, segments 10 to 11, dorsal view, with lateral terminal spines drawn to full length. **D**. Female, segments 6 to 7, ventral view.

S6 **S7** **S5** **S8** **S4** **S3** **S9** **S2** **S10**

S1
Scalid and style arrangement

Ring/Section		1	2	3	4	5	6	7	8	9	10	Total
00 outer oral styles	✦	1	1	1	1	1	0	1	1	1	1	9
01 primary spinoscalids	▼	1	1	1	1	1	1	1	1	1	1	10
02 spinoscalids	O	1	1	1	1	1	1	1	1	1	1	10
03 spinoscalids	O	2	2	2	2	2	2	2	2	2	2	20
04 spinoscalids	O	1	1	1	1	1	1	1	1	1	1	10
05 spinoscalids	O	2	2	2	2	2	2	2	2	2	2	20
06 spinoscalids	O	1	0	1	0	1	1	1	0	1	0	6
07 spinoscalids	O	2	0	2	0	1	0	1	0	2	0	8
Total scalids		9	6	9	6	8	7	8	6	9	6	74
trichoscalids	✸	0	1	0	1	1	0	1	1	0	1	6

Fig. 6. Diagram of mouth cone (grey area), introvert, and placids in *Polacanthoderes grzelakae* sp. nov., showing distribution of inner oral styles (closed dots), outer oral styles, scalids, and trichoscalids. Table shows the scalid arrangement by sector (S1 to S10); single-lined boxes mark quincunxes, double-lined boxes mark "double diamonds".
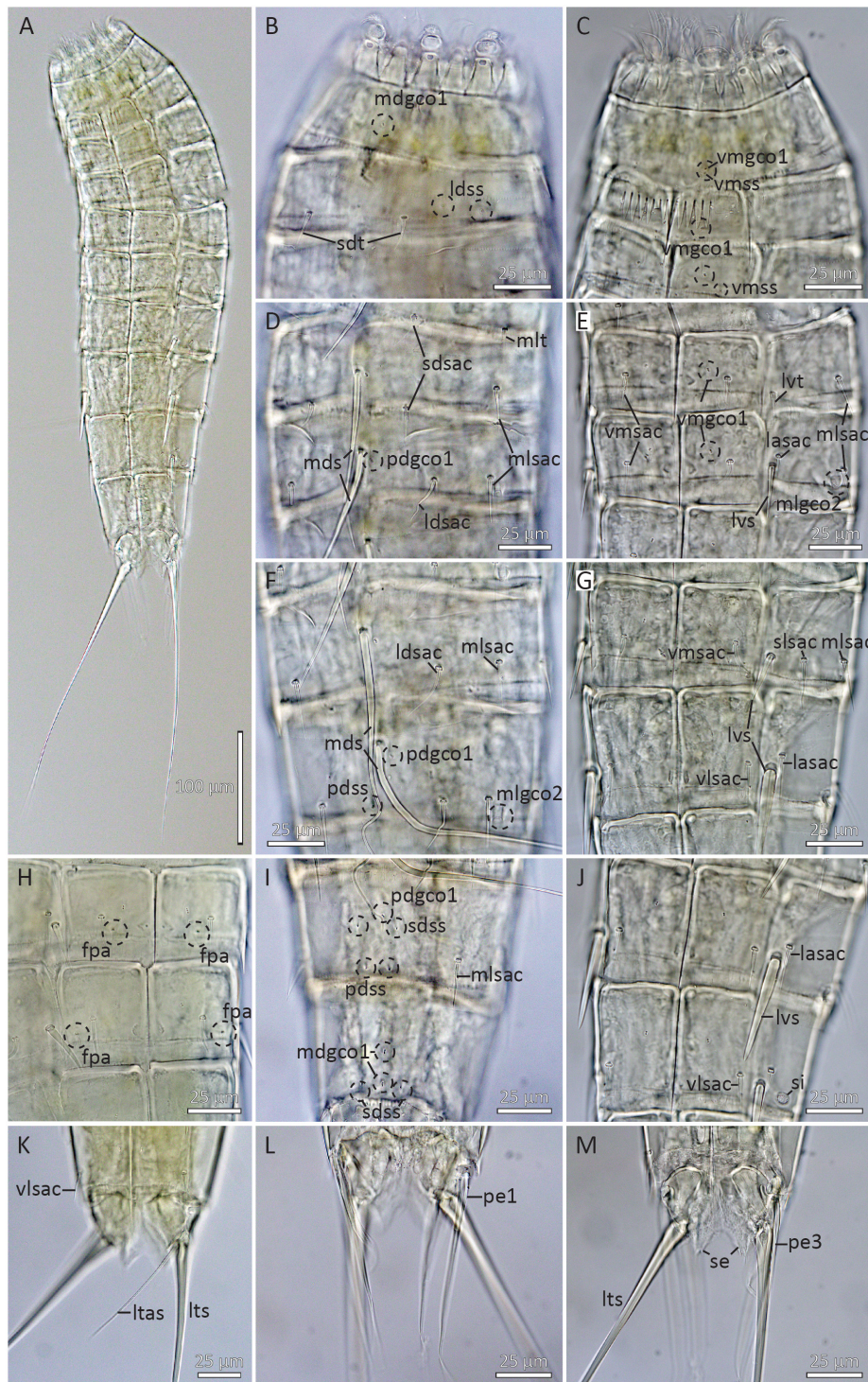
Fig. 7. Light micrographs showing overviews and details of *Polacanthoderes grzelakae* sp. nov. **A–G, I–J, L–M**. Male, holotype (NHMD 1784249). **H, K**. Female, paratype (NHMD 1784284). **A**. Ventral overview. **B**. Segments 1 to 3, dorsal view. **C**. Segments 1 to 3, ventral view. **D**. Segments 5 to 6, dorsal view. **E**. Segments 5 to 6, ventral view. **F**. Segments 7 to 8, dorsal view. **G**. Segments 7 to 8, ventral view. **H**. Tergal plates on segments 6 to 7, showing female sexual dimorphism. **I**. Segments 9 to 10, dorsal view. **J**. Segments 8 to 9, ventral view. **K**. Segments 10 to 11, ventral view, showing female sexual dimorphism. **L**. Segment 11, dorsal view, showing male sexual dimorphism. **M**. Segment 11, ventral view, showing male sexual dimorphism. Scale bars: A = 100 µm; B–M = 25 µm.
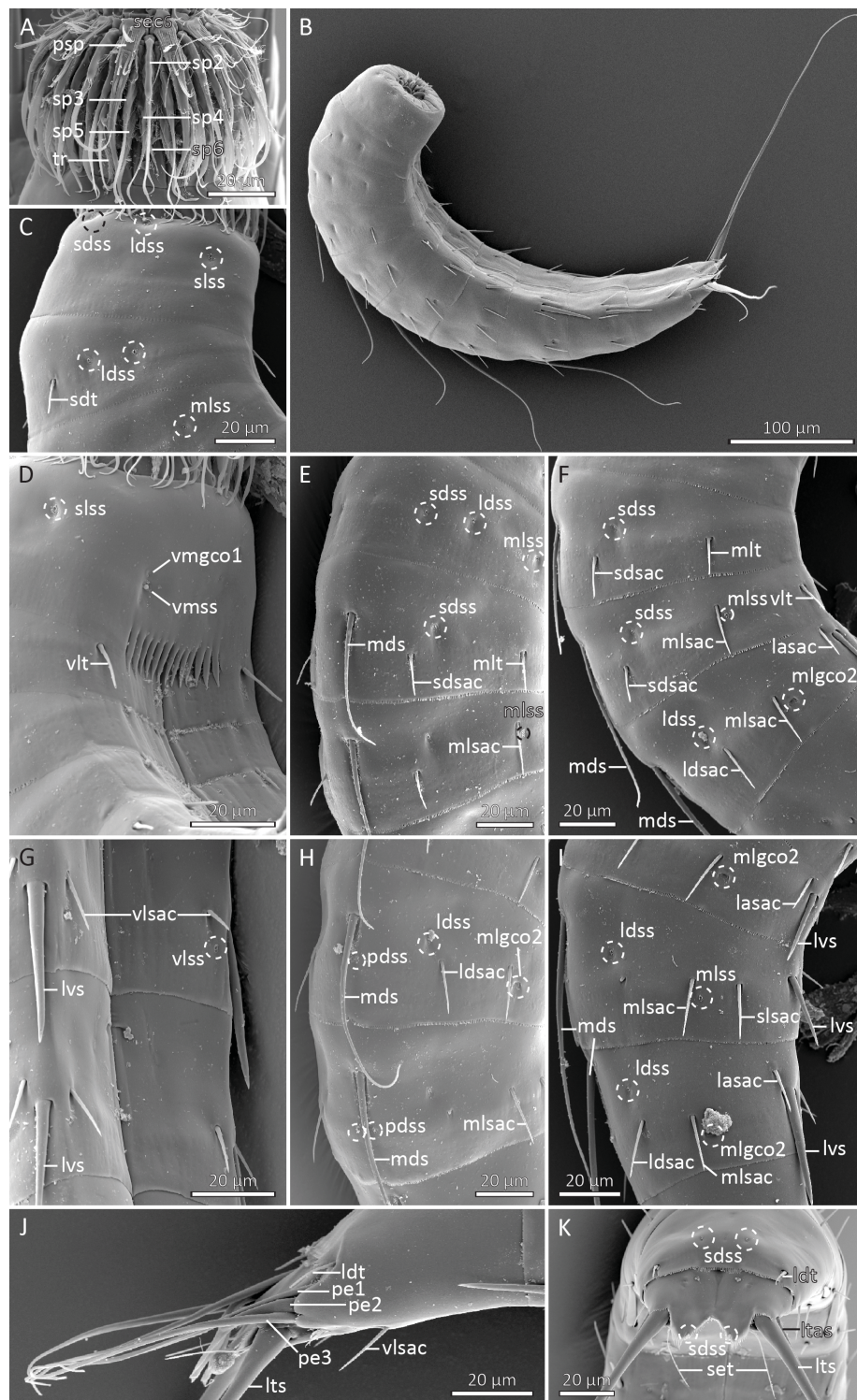
Fig. 8. Scanning electron micrographs showing overviews and details of *Polacanthoderes grzelakae* sp. nov. **A**. Introvert focused on the middorsal sector 6. **B**. Lateroventral overview of female. **C**. Segments 1 to 2, right lateral view. **D**. Segments 1 to 3, ventrolateral view. **E**. Segments 3 to 5, subdorsal view. **F**. Segments 4 to 6, right lateral view. **G**. Segments 8 to 9, ventrolateral view. **H**. Segments 8 to 9, subdorsal view. **I**. Segments 6 to 8, right lateral view. **J**. Segments 10 to 11, right lateral view, showing male sexual dimorphism. **K**. Segments 10 to 11, dorsocaudal view, showing female sexual dimorphism. Scale bars: A, C–K = 20 µm; B = 100 µm.

spines in lateral accessory positions on segment 6, but had instead double pairs of small acicular spines in laterodorsal positions on this segment. A third specimen (SEM specimen from stn 1793) followed the most common spine pattern for *P. grzelakae*, but had in addition – as the only *Polacanthoderes* in all samples – small acicular spines in lateral accessory positions on segment 7. The seven remaining specimens also appeared to follow the common pattern but had, due to their condition or mounting orientation, characters that could not be confirmed visually.

<center>*Polacanthoderes shiraseae* Yamasaki *et al.*, 2022</center>

Material examined

ANTARCTICA – **Antarctic Peninsula** • 1 ♂, 1 ♀ (mounted for LM in Fluoromount G on HS slide); CRS 1763; 64°48.41′ S, 65°21.82′ W; 593 m b.s.l.; 3 Apr. 2016; FjordEco2; soft sediment; NHMD 1784624, 1784625 • 2 ♀♀ (mounted for LM in Fluoromount G on HS slide); CRS 1846; 64°47.93′ S, 65°21.23′ W; 572 m b.s.l.; 25 Apr. 2016; FjordEco2; soft sediment; NHMD 1784626, 1784627.

Short description

Four adult specimens (one male and three females) from two different stations (stn 1763 and stn 1846) were measured and examined with light microscopy. All four specimens perfectly fit the species diagnosis of *P. shiraseae* (see Yamasaki *et al.* 2022), i.e., without tubes on segment 2 and with the short acicular spines on segment 7 placed in sublateral rather than lateral accessory positions. None of the specimens had short subdorsal acicular spines on segments 4 or 5. On segment 8, two specimens had short acicular spines in positions corresponding to subdorsal sensu Yamasaki *et al.* (2022), whereas such spines were missing in the other two specimens. All measurements were within the ranges of those reported in the original description of *P. shiraseae*.

Distribution

Antarctic Peninsula: only on the open continental shelf off the Peninsula, 572 to 593 m b.s.l. (Fig. 1C, Table 1). The species has in addition been recorded at Lützow-Holm Bay, Cape Damley, and near Totten Glacier (Yamasaki *et al.* 2022), i.e., on the opposite side of the Antarctic continent (see red dots in Fig. 1A).

<center>*Polacanthoderes* sp. 1</center>

Material examined

ANTARCTICA – **Antarctic Peninsula** • 1 ♂ (mounted for SEM); CRS 1767; 64°47.99′ S, 65°20.55′ W; 590 m b.s.l.; 4 Apr. 2016; FjordEco2; soft sediment; MVS • 1 ♂ (mounted for SEM); CRS 1776; 64°52.53′ S, 62°33.90′ W; 551 m b.s.l.; 7 Apr. 2016; FjordEco2; soft sediment; MVS • 1 ♂ (mounted for SEM); CRS 1809; 64°39.59′ S, 62°55.09′ W; 694 m b.s.l.; 15 Apr. 2016; FjordEco2; soft sediment; MVS.

Short description

Three adult males were examined with scanning electron microscopy. The morphology of the specimens closely follows the species diagnosis of *P. grzelakae* sp. nov., except for the missing ventrolateral tubes on segment 2. Short subdorsal acicular spines on segment 4 are missing in all three specimens but are present on segment 5. On segment 8, laterodorsal short acicular spines are present in two specimens and missing in one.

Distribution

Antarctic Peninsula: open continental shelf, Gerlache Strait, and Andvord Bay IBB, 551 to 694 m b.s.l. See Fig. 1 for geographic overview of stations and Table 1 for station and specimen information.

Polacanthoderes sp. 2

Material examined

ANTARCTICA • 1 ♂ (mounted for SEM); Antarctic Peninsula, CRS 1776; 64°52.53′ S, 62°33.90′ W; 551 m b.s.l.; 7 Apr. 2016; FjordEco2; soft sediment; MVS.

Short description

One adult male was examined with scanning electron microscopy. The morphology of the specimens closely follows the species diagnosis of *P. grzelakae* sp. nov., except for the missing subdorsal tubes on segment 2. Subdorsal short acicular spines are present on segment 4, but missing on segment 5. Short laterodorsal acicular spines are present on segment 8.

Distribution

Antarctic Peninsula: Andvord Bay IBB, 551 m b.s.l. See Fig. 1 for geographic overview of stations and Table 1 for station and specimen information.

Diagnostic remarks on *Polacanthoderes grzelakae* sp. nov.

With the addition of *P. grzelakae* sp. nov., *Polacanthoderes* now accommodates three species that all are restricted to the Antarctic continent (Sørensen 2008a; Yamasaki *et al.* 2022). The genus and its first described species, *Polacanthoderes martinezi* Sørensen, 2008, was described from the South Shetland Islands (Sørensen 2008a), and a phylogenetic analysis supported that *Polacanthoderes* represents a separate evolutionary linage within Echinoderidae (Sørensen 2008b). One of the characters that makes *Polacanthoderes* stand out from other echinoderids is the numerous small acicular spines in rather unusual positions, i.e., subdorsal, laterodorsal, midlateral, and ventromedial (Sørensen 2008a).

Some years later, Yamasaki *et al.* (2022) described the second species of the genus, *P. shiraseae*. The species was described from Lützow-Holm Bay, Cape Damley, and near Totten Glacier, i.e., from Antarctic areas that geographically are pretty much opposite to the Antarctic Peninsula and South Shetland Island. Besides contributing with a new species, Yamasaki *et al.* (2022) also provided a redescription of *P. martinezi* and, in addition, shed light on the exceptionally high level of morphological variation within the two species (see following section for further discussion of polymorphism in species of *Polacanthoderes*). In a group like Echinoderidae, where much of the taxonomy traditionally has been based on the presence and position of spines and tubes, such variation can obviously lead to some taxonomic challenges. Yet, Yamasaki *et al.* (2022) explained how *P. martinezi* and *P. shiraseae* fairly easily could be distinguished by the conspicuously stronger lateroventral spines on segments 8 and 9 in *P. shiraseae*, and by the position of short acicular spines on segment 7, which appear in lateral accessory positions in *P. martinezi* and in sublateral positions in *P. shiraseae*. The latter character might seem like a very subtle alteration, open for subjective interpretation, but when observed the difference is in fact very distinct, and since both species otherwise have a series of short lateral accessory acicular spines on segments 6 to 9, it is easy to detect the sublateral displacement of the spines on segment 7 in *P. shiraseae*.

The new species, *P. grzelakae* sp. nov., very clearly shares most characters with *P. shiraseae*, including the strong lateroventral spines on segments 8 and 9, and the sublateral short acicular spines on segment 7. Thus, *P. grzelakae* is easily distinguished from *P. martinezi*. The characters that separate *P. grzelakae* from both congeners are the presence of subdorsal and ventrolateral tubes on segment 2. In the present

study, a total of 38 specimens of *Polacanthoderes* were examined. Out of these, four specimens had no tubes on segment 2 and were thus identified as *P. shiraseae*. Thirty other specimens had both subdorsal and ventrolateral tubes on segment 2, and were assigned to *P. grzelakae*. Of the remaining four specimens, three had only subdorsal tubes on segment 2, whereas a single specimen had only ventrolateral tubes.

In light of the known morphological variation within species of *Polacanthoderes* (and without access to molecular barcoding data), it is obviously not straightforward to determine whether *P. grzelakae* sp. nov. is a distinct species or a morphological variation of *P. shiraseae*. However, a strong argument favours the first option. Recently, Anguas-Escalante *et al.* (2023) demonstrated with molecular barcoding that the presence or absence of tubes on segment 2 in otherwise very similar species of *Echinoderes* actually should be seen as species diagnostic. In *P. grzelakae* the species diagnostic trait is exactly expressed as the presence of tubes on segment 2, and these tubes are consistently present within the type series of the species, whereas the morphological variation we observe is mostly expressed in the presence/absence of short acicular spines in the dorsal series on segments 4, 5, and 8 (see below for further discussion of this).

Based on these arguments, we propose *P. grzelakae* sp. nov. as a new species showing close resemblance with *P. shiraseae*, but distinguished by the presence of subdorsal and ventrolateral tubes on segment 2. This proposal seems fair, but it is admittedly challenged by the four remaining specimens, *Polacanthoderes* sp. 1 and *P.* sp. 2, that show variation in their tubes on segment 2. With tubes only in either subdorsal or ventrolateral positions on segment 2, the four specimens fall in between the two species, and the number of potential explanations are too numerous to allow a final conclusion. The two morphotypes could represent the bridging between *P. shiraseae* and *P. grzelakae*, suggesting that they are all conspecific; they could represent another two distinct species; or they could be results of hybridisation between *P. shiraseae* and *P. grzelakae*. It would require molecular barcoding to solve this question, and any other conclusion at this point would be nothing but speculation. However, based on the arguments above, we find it justified to consider *P. grzelakae* as a new, easily distinguishable species of *Polacanthoderes*.

The distribution pattern of glandular cell outlets type 1 in *P. grzelakae* sp. nov. follows the MD Seg. 1–3, PD 4–9 pattern (see table with summary of species with this pattern described up to 2020 in Sørensen *et al.* 2020). The same pattern is present in both *Polacanthoderes* congeners (Sørensen 2008a; Yamasaki *et al.* 2022).

Remarks on polymorphism in *Polacanthoderes* spp.

The description of *P. shiraseae* also includes a careful re-examination of available *P. martinezi* specimens (eleven in total), and from both species Yamasaki *et al.* (2022) reported a relatively high level of intraspecific variation regarding tubes and short acicular spines. Among specimens of *P. martinezi* they found that a few specimens would have subdorsal tubes on segment 2, subdorsal tubes or short acicular spines on segment 5, and short subdorsal acicular spines on segment 8, whereas the majority of the available specimens would lack these structures. Likewise, they reported the occasional, but yet rather rare, presence of short subdorsal acicular spines on segments 4, 5, and 8 in *P. shiraseae*.

The new species, *P. grzelakae* sp. nov., also shows intraspecific variation, which contributes further to the taxonomic challenges. As with *P. shiraseae*, the polymorphism in *P. grzelakae* also appears to be expressed mostly in the dorsal series on segments 4, 5, and 8. Of 30 examined specimens, five lacked short subdorsal spines on segment 4, whereas five different specimens had no such spines on segment 5. In addition, another two specimens (of which neither showed spine loss on segments 4 or 5) lacked short laterodorsal acicular spines on segment 8. Additional spine variation was restricted to singletons and included: one specimen with short ventromedial acicular spines on segment 3; one without midlateral tubes on segment 4; one with two pairs of closely positioned, short laterodorsal acicular spines on

segment 6; one without short lateral accessory acicular spines on segment 6 (same specimen as the one with double pairs of segment 6 laterodorsal spines); and one specimen with both short sublateral and short lateral accessory acicular spines on segment 7 (all other specimens have no lateral accessory spine on this segment).

The present description of *P. grzelakae* sp. nov. is based on 30 specimens, whereas Yamasaki *et al.* (2022) examined around 50 specimens for their description of *P. shiraseae*. One could obviously always wish for even larger sample sizes, but they still represent enough specimens to provide some hints about where the variation is most expressed and where the differences should be seen as rarities. The data leaves the impression that while all regular acicular spines occur consistently across specimens of *Polacanthoderes*, nearly all tubes and small acicular spines can potentially vary. However, much of this variation is restricted to singletons and is therefore to some extent neglectable. In both species, higher frequencies of variation are only reached in the occurrence of small acicular spines in the dorsal series of segments 4, 5, and 8. For instance, small subdorsal acicular spines were absent on either segment 4 or 5 in one third of the *P. grzelakae* specimens.

As mentioned previously, such levels of morphological variation obviously represent a taxonomic challenge for present and future studies of *Polacanthoderes*, but understanding this polymorphism also makes it easier to comprehend. Thus, we need to acknowledge that eventual future species descriptions of *Polacanthoderes* spp. have to be based on a sufficiently high number of specimens to be able to detect polymorphic characters. In addition, it can be helpful to keep in mind that we can expect more variation on segments 4, 5, and 8, which in turn makes characters on these particular segments less suitable as species diagnostic.

Genus *Echinoderes* Claparède, 1863

***Echinoderes ahlfeldae* sp. nov**
urn:lsid:zoobank.org:act:E59B6DA9-45BD-4DE8-80E6-16529FBEC3A1
Figs 9–12, Tables 9–10

Diagnosis

Echinoderes with acicular spines in middorsal position on segments 4, 6, and 8, and in lateroventral positions on segments 6 to 9. Tubes present in subdorsal and ventrolateral positions on segment 2, in lateroventral positions on segment 5, in sublateral positions on segment 8, and in laterodorsal positions on segment 10; tubes on segment 10 show sexual dimorphism and are longer in males. Sieve plates on segment 9 in sublateral positions. Males with flare-like extensions from secondary fringe of sternal plates on segment 10. Female papillae or glandular cell outlets type 2 not present. Dorsal glandular cell outlets type 1 are present in middorsal positions on segments 1 to 3, 5, 7, and 10, and in paradorsal positions on segments 4, 6, 8, and 9.

Etymology

The species name is dedicated to Katie Ahlfeld, museum specialist at the USNM, in appreciation of her work maintaining the Smithsonian invertebrate collections and of the numerous kinorhynch loans she has issued to the first author.

Material examined

Holotype
ANTARCTICA • ♀ (mounted for LM in Fluoromount G on HS slide); Antarctic Peninsula, CRS 1792; 64°51.40′ S, 62°34.01′ W; 525 m b.s.l.; 11 Apr. 2016; FjordEco2; soft sediment; NHMD 1784759.

Paratypes
ANTARCTICA – **Antarctic Peninsula** • 7 ♂♂ (mounted as holotype); CRS 1698; 64°51.60′ S, 62°33.80′ W; 541 m b.s.l.; 28 Nov. 2015; FjordEco1; soft sediment; NHMD 1784762 to 1784766, USNM 1740029 to 1740030 • 1 ♂ (mounted as holotype); CRS 1769; 64°52.37′ S, 62°25.27′ W; 547 m b.s.l.; 5 Apr. 2016; FjordEco2; soft sediment; NHMD 1784768 • 4 ♂♂, 2 ♀♀ (mounted as holotype); CRS 1790; 64°51.49′ S, 62°34.01′ W; 532 m b.s.l.; 10 Apr. 2016; FjordEco2; soft sediment; NHMD 1784770 to 1784773, USNM 1740031 to 1740032 • 1 ♂, 2 ♀♀ (mounted as holotype); same data as for holotype; NHMD 1784760 to 1784761, USNM 1740033 • 1 ♂ (mounted as holotype); CRS 1793; 64°39.53′ S, 62°55.03′ W; 701 m b.s.l.; 11 Apr. 2016; FjordEco2; soft sediment; NHMD 1784774 • 6 ♂♂, 5 ♀♀ (mounted as holotype); CRS 1809; 64°39.59′ S, 62°55.09′ W; 694 m b.s.l.; 15 Apr. 2016; FjordEco2; soft sediment; NHMD 1784775 to 1784782, USNM 1740034 to 1740036.

Additional material
ANTARCTICA – **Antarctic Peninsula** • 2 ♂♂, 1 ♀ (mounted for SEM); CRS 1698; 64°51.60′ S, 62°33.80′ W; 541 m b.s.l.; 28 Nov. 2015; FjordEco1; soft sediment; MVS • 1 juv. (mounted as holotype); CRS 1698; 64º51.60′ S, 62°33.80′ W; 541 m b.s.l.; 28 Nov. 2015; FjordEco1; soft sediment; NHMD 1784767 • 1 ♂ (mounted for SEM); CRS 1773; 64°52.35′ S, 62°25.88′ W; 553 m b.s.l.; 6 Apr. 2016; FjordEco2; soft sediment; MVS • 4 ♂♂, 2 ♀♀ (mounted for SEM); same data as for holotype; MVS • 12 ♂♂, 7 ♀♀ (mounted for SEM); CRS 1793; 64°39.53′ S, 62°55.03′ W; 701 m b.s.l.; 11 Apr. 2016; FjordEco2; soft sediment; MVS • 4 ♂♂, 1 ♀ (mounted for SEM); CRS 1799; 64°51.51′ S, 62°33.83′ W; 541 m b.s.l.; 13 Apr. 2016; FjordEco2; soft sediment; MVS • 11 ♂♂, 6 ♀♀ (mounted for SEM); CRS 1809; 64°39.59′ S, 62°55.09′ W; 694 m b.s.l.; 15 Apr. 2016; FjordEco2; soft sediment; MVS • 1 ♂, 7 ♀♀ (mounted for SEM); CRS 1832; 64°39.30′ S, 62°55.98′ W; 631 m b.s.l.; 21 Apr. 2016; FjordEco2; soft sediment; MVS.

Description

General. Adults with head, neck and eleven trunk segments (Figs 9, 10, 11A, 12A–B). An overview of measurements and dimensions is given in Table 9. Distributions of cuticular structures, i.e., sensory spots, glandular cell outlets, spines, and tubes, are summarized in Table 10.

Head. Consists of a retractable mouth cone and an introvert (Figs 10, 12C–D). Mouth cone with nine outer oral styles composed of two units; all oral styles with uniform morphology, but differ alternatingly in length, with styles in uneven numbered sectors being ca 15% longer than those in even numbered (Fig. 12C). A partly folded structure with seven spikes (lateral ones longest) is present at the base of each outer oral style. A set of double fringes is located more basally, at the base of the mouth cone and in between the attachment points of the outer oral styles. Inner oral styles could not be examined.

Introvert. With ten primary spinoscalids in Ring 01 (Fig. 10). Each primary spinoscalid consists of a basal sheath and a distal end piece with a blunt tip (Fig. 12D). The sheaths have two transverse fringes; the most proximal fringe has the strongest fringe tips. End-pieces are flexible, with two longitudinal fringes on their proximal parts, whereas they are smooth on their distal halves. Rings 02 and 04 have 10 spinoscalids, and Rings 03 and 05 have 20. All spinoscalids in these rings are well-developed and consist of a basal sheath and a pointed end-piece. Ring 06 has only six spinoscalids, located in sectors 1, 3, 5, 6, 7, and 9; they resemble those in preceding sectors, but the distal end-pieces are much shorter, only slightly longer than their proximal sheaths. Ring 07 has two kinds of scalids: one kind resembles those in Ring 06 and are located as pairs in sectors 3 and 9; the other kind resembles trichoscalids (Fig. 12D). They have the same bushy appearance, but are much smaller than the actual trichoscalids. These trichoscalid-like scalids are present as pairs in sectors 1, 2, 4, 8, and 10, and as single, laterally

Table 9. Measurements from light microscopy of *Echinoderes ahlfeldae* sp. nov. (in µm), including number of measured specimens (*n*) and standard deviation (SD).

Character	*n*	Range	Mean	SD
TL	15	275–354	314	27.34
TL (CUM)	15	442–493	472	16.38
MSW-6	15	58–72	65	3.60
MSW-6/TL	15	18.4–23.2%	20.9%	1.51%
SW-10	15	54–62	58	2.53
SW-10/TL	15	16.4–21.1%	18.7%	1.30%
S1	15	32–39	36	2.39
S2	15	28–35	31	1.73
S3	15	32–37	34	1.83
S4	15	34–42	37	2.42
S5	15	38–46	41	2.54
S6	15	38–49	44	3.44
S7	15	44–52	48	2.43
S8	15	47–57	53	2.35
S9	15	55–60	57	1.24
S10	15	52–58	55	2.21
S11	15	30–40	35	2.67
—				
MD4 (ac)	15	42–52	47	2.95
MD6 (ac)	15	70–89	76	4.83
MD8 (ac)	15	88–99	92	2.97
—				
SD2 (tu)	10	12–19	16	1.84
VL2 (tu)	8	13–17	15	1.64
—				
LV5 (tu)	7	14–18	16	1.38
LV6 (ac)	15	35–41	37	1.89
LV7 (ac)	15	41–48	44	2.12
LV8 (ac)	15	48–57	52	2.37
LV9 (ac)	15	48–58	53	2.59
—				
SL8 (tu)	8	14–17	16	0.99
LD10 (tu) ♂	8	13–24	15	3.38
LD10 (tu) ♀	1	4	N/A	N/A
—				
LTAS	5	40–43	41	1.22
LTS	15	147–173	158	7.36
LTS/TL	15	43.2–58.9%	50.7%	5.29%

displaced ones in sectors 5 and 7 (Fig. 10). Described sector-wise (Fig. 10), sector 1 has its scalids arranged as two double diamonds, anterior to a pair of trichoscalid-like scalids. Sectors 3 and 9 are similar, and also have their spinoscalids arranged as two double diamonds but anterior to a pair of regular scalids. Sectors 2, 4, 8, and 10 all have spinoscalids arranged as a quincunx, located in between an anterior spinoscalid in Ring 02, a posterior pair of trichoscalid-like scalids, and a trichoscalid plate. Sectors 5 and 7 have spinoscalids forming double diamonds, anterior to an unpaired, lateral trichoscalid-like scalid and a trichoscalid plate. Regular trichoscalids with trichoscalid plates are present in sectors 2, 4, 5, 7, 8, and 10.

Table 10. Summary of nature and location of sensory spots, glandular cell outlets, tubes, and spines arranged by series in *Echinoderes ahlfeldae* sp. nov.

Segment	Position									
	MD	PD	SD	LD	ML	SL	LA	LV	VL	VM
1	gco1	–	ss	ss	–	–	–	–	gco1	ss
2	gco1,ss	–	tu	ss	–	–	–	–	tu	gco1,ss
3	gco1	–	ss	–	–	ss	–	–	–	gco1
4	ac	gco1	–	–	–	–	–	–	–	gco1
5	gco1	–	ss	–	–	ss	–	tu	–	gco1,ss
6	ac	gco1,ss	ss	–	–	ss	–	ac	–	gco1,ss
7	gco1	ss	–	–	–	ss	–	ac	–	gco1,ss
8	ac	gco1,ss	–	–	–	tu	–	ac	–	gco1
9	–	gco1,ss	ss	ss	–	si	–	ac	ss	gco1
10	gco1,gco1	–	ss	tu	–	–	–	–	ss	gco1
11	gco1,pr	–	–	–	pex3(♂)	–	ltas(♀)	lts	–	ss

NECK. With 16 placids. Midventral placid broadest, 17 µm in width and length, whereas all others are narrower, measuring 10 µm in width at their bases. The trichoscalid plates are well-developed and hat-shaped.

SEGMENT 1. Consists of a complete cuticular ring. Sensory spots are present in subdorsal, laterodorsal, and ventromedial positions; subdorsal and laterodorsal sensory spots are present on the anterior half of the segment, but not immediately at the anterior margin. They are composed of a dense tuft of micropapillae around a central pore and are flanked by four to five, irregularly arranged, strong and bristle-like cuticular hairs; ventromedial sensory spots are more posterior, with same appearance as the dorsal ones, but with only two or three cuticular hairs. Glandular cell outlets type 1 are present in middorsal and ventrolateral positions. Besides the few hairs around the sensory spots, the segment has either no cuticular hairs at all, or only very few rigid and bristle-like hairs on the dorsal side. The posterior segment margin is straight and terminates in a well-developed pectinate fringe with broad fringe tips (Figs 9A–B, 11B–C, 12E–G).

SEGMENT 2. Consists of a complete cuticular ring; some specimens mounted for SEM had indications of a weak, superficial tergosternal line (Fig. 12F), but this line did not occur consistently in all SEM specimens, and none of the specimens mounted for LM had any indications of plate differentiation. Tubes are located in subdorsal and ventrolateral positions; missing tubes in some specimens were evidently broken off. Sensory spots present in middorsal, laterodorsal, and ventromedial positions. The micropapillary areas around the sensory spots on this, and all following segments, are more oval; the micropapillae along the posterior margins of the areas are slightly longer, and one to three very long, hair-like micropapillae extend from the posterior part of the areas. Glandular cell outlets type 1 are present in middorsal and ventromedial positions. Bracteate cuticular hairs are arranged in three transverse rows from the middorsal to the midlateral positions; hairs in the two anteriormost rows are rather short, whereas those of the third row are considerably longer, reaching the pectinate fringe at the posterior segment margin; the ventral half of the segment is devoid of cuticular hairs. The posterior segment margin is straight along the dorsal and lateral sides, but extends in a small midventral V-shaped flap. Pectinate fringe as on preceding segment (Figs 9A–B, 11B–C, 12E–G).

SEGMENT 3. As remaining segments, consisting of one tergal and two sternal plates. Sensory spots are present in subdorsal and sublateral positions, and glandular cell outlets type 1 in middorsal and ventromedial positions. The hair covering of the tergal and lateral halves of sternal plates is dense on the

anterior half of the segment, except in hair-less midlateral areas; bracteate cuticular hairs are arranged in six to seven rows, with hairs getting gradually longer in the more posterior rows; the hairs in the most posterior row are considerably longer than the others. Paraventral areas without bracteate hairs, but with fine, short hair-like extensions. Posterior segment margin straight and pectinate fringe as on preceding segment (Figs 9A–B, 11B–C, 12E).

Segment 4. With spine in middorsal position. Sensory spots are not present. Glandular cell outlets type 1 are present in paradorsal and ventromedial positions. Cuticular hairs as on preceding segment, but in addition to the hairless midlateral areas, the mid- and paradorsal areas are also devoid of hairs. Posterior segment margin and pectinate fringe as on preceding segment (Figs 9A–B, 11B–C, 12E).

Segment 5. With tubes in lateroventral positions. Sensory spots present in subdorsal, sublateral and ventromedial positions, and glandular cell outlets type 1 in middorsal and ventromedial positions. Cuticular hairs, posterior segment margin, and pectinate fringe as on preceding segment (Figs 9A–B, 11B–C, 12E).

Segment 6. With spines in middorsal and lateroventral positions. Sensory spots present in paradorsal, subdorsal, sublateral, and ventromedial positions. Glandular cell outlets type 1 present in paradorsal and ventromedial positions. Cuticular hairs, posterior segment margin, and pectinate fringe as on preceding segment (Figs 9A–B, 11B–C).

Segment 7. With spines in lateroventral positions. Sensory spots present in paradorsal, sublateral, and ventromedial positions. Glandular cell outlets type 1 present in middorsal and ventromedial positions. Cuticular hairs, posterior segment margin, and pectinate fringe as on preceding segment (Figs 9A–B, 11B–E, 12I–J).

Segment 8. With spines in middorsal and lateroventral positions, and tubes in sublateral positions. Sensory spots present in paradorsal positions only. Glandular cell outlets type 1 present in paradorsal and ventromedial positions. Cuticular hairs, posterior segment margin, and pectinate fringe as on preceding segment (Figs 9A–B, 11D–E, G, 12H–J).
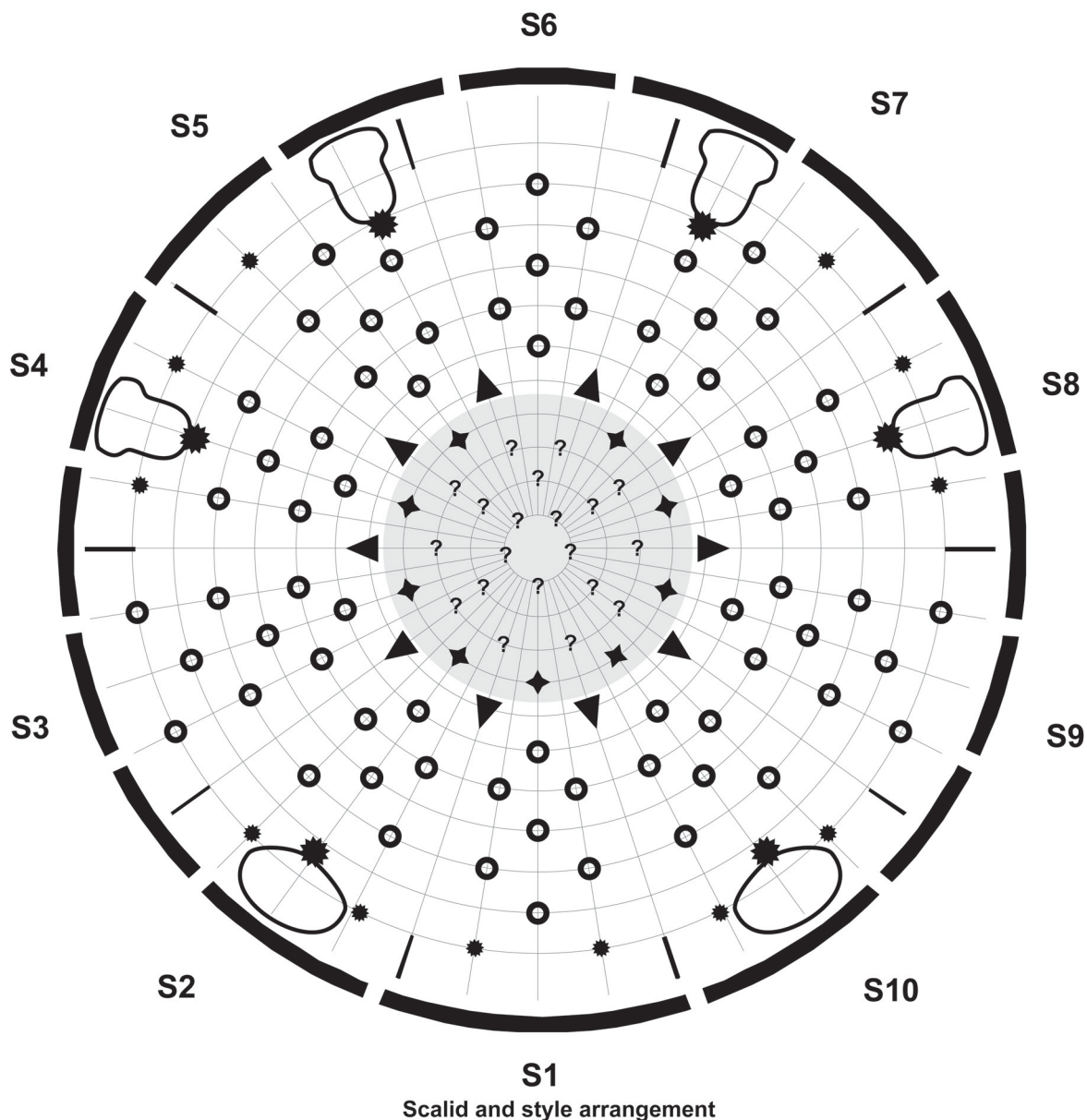
Segment 9. With spines in lateroventral positions. Sensory spots present in paradorsal (posterior on segment), subdorsal (anterior on segment), laterodorsal (medial on segment), and ventrolateral (medial on segment) positions. Glandular cell outlets type 1 present in paradorsal and ventromedial positions. Small rounded sieve plates located in sublateral positions; gaps between sieve plates and lateroventral spines are distinct. The cuticular hair covering is similar to that on preceding segments, but hairless middorsal area is broader, and the hairless lateral areas are in laterodorsal, rather than midlateral positions. Posterior segment margin and pectinate fringe as on preceding segment (Figs 9A–B, 11D–E, G–H, 12H).

Segment 10. With sexually dimorphic laterodorsal tubes located near, but not at, the posterior segment margin; female tubes are extremely small, hardly projecting from attachment site; male tubes of more regular size, reaching beyond the segment margin. An additional sexually dimorphic trait is expressed in the secondary fringe, enwrapping the anterior part of the segment; at most other segments the secondary fringe is covered by the free flap of the preceding segment, but in male specimens, a tuft of long setae expands from the secondary fringe on each sternal plate and reaches more than halfway down the exposed part of the segment (Figs 9D, 11F, H–I, 12K). In some specimens, the setal extensions appear rather disorganised, but in others they are very well-arranged and spread out from a common shaft, forming a fan- or flare-like structure. Due to this appearance, the structures will be referred to as
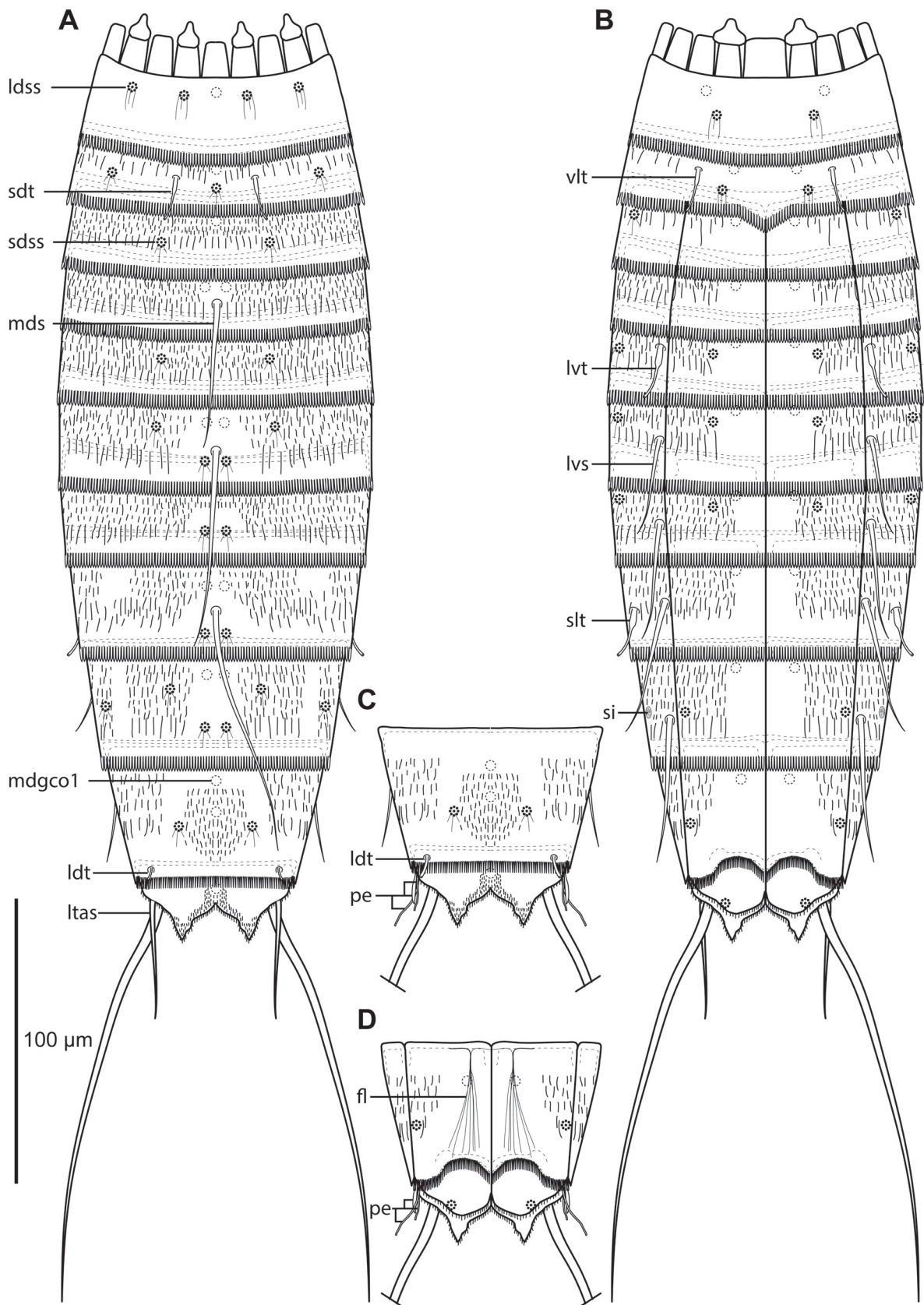
Fig. 9. Line art illustrations of *Echinoderes ahlfeldae* sp. nov. **A.** Female, dorsal view. **B.** Female, ventral view. **C.** Male, segments 10 to 11, dorsal view. **D.** Male, segments 10 to 11, ventral view.

S1
Scalid and style arrangement

Ring/Section		1	2	3	4	5	6	7	8	9	10	Total
00 outer oral styles	✦	1	1	1	1	1	0	1	1	1	1	9
01 primary spinoscalids	▼	1	1	1	1	1	1	1	1	1	1	10
02 spinoscalids	◯	1	1	1	1	1	1	1	1	1	1	10
03 spinoscalids	◯	2	2	2	2	2	2	2	2	2	2	20
04 spinoscalids	◯	1	1	1	1	1	1	1	1	1	1	10
05 spinoscalids	◯	2	2	2	2	2	2	2	2	2	2	20
06 spinoscalids	◯	1	0	1	0	1	1	1	0	1	0	6
07 spinoscalids	◯	0	0	2	0	0	0	0	0	2	0	4
07 trichoscalid-like	✴	2	2	0	2	1	0	1	2	0	2	12
Total scalids		9	8	9	8	8	7	8	8	9	8	82
trichoscalids	✴	0	1	0	1	1	0	1	1	0	1	6

Fig. 10. Diagram of mouth cone (grey area), introvert, and placids in *Echinoderes ahlfeldae* sp. nov., showing distribution of inner oral styles (closed dots,) outer oral styles, scalids, and trichoscalids. Table shows the scalid arrangement by sector (S1 to S10); single-lined boxes mark quincunxes, double-lined boxes mark "double diamonds".
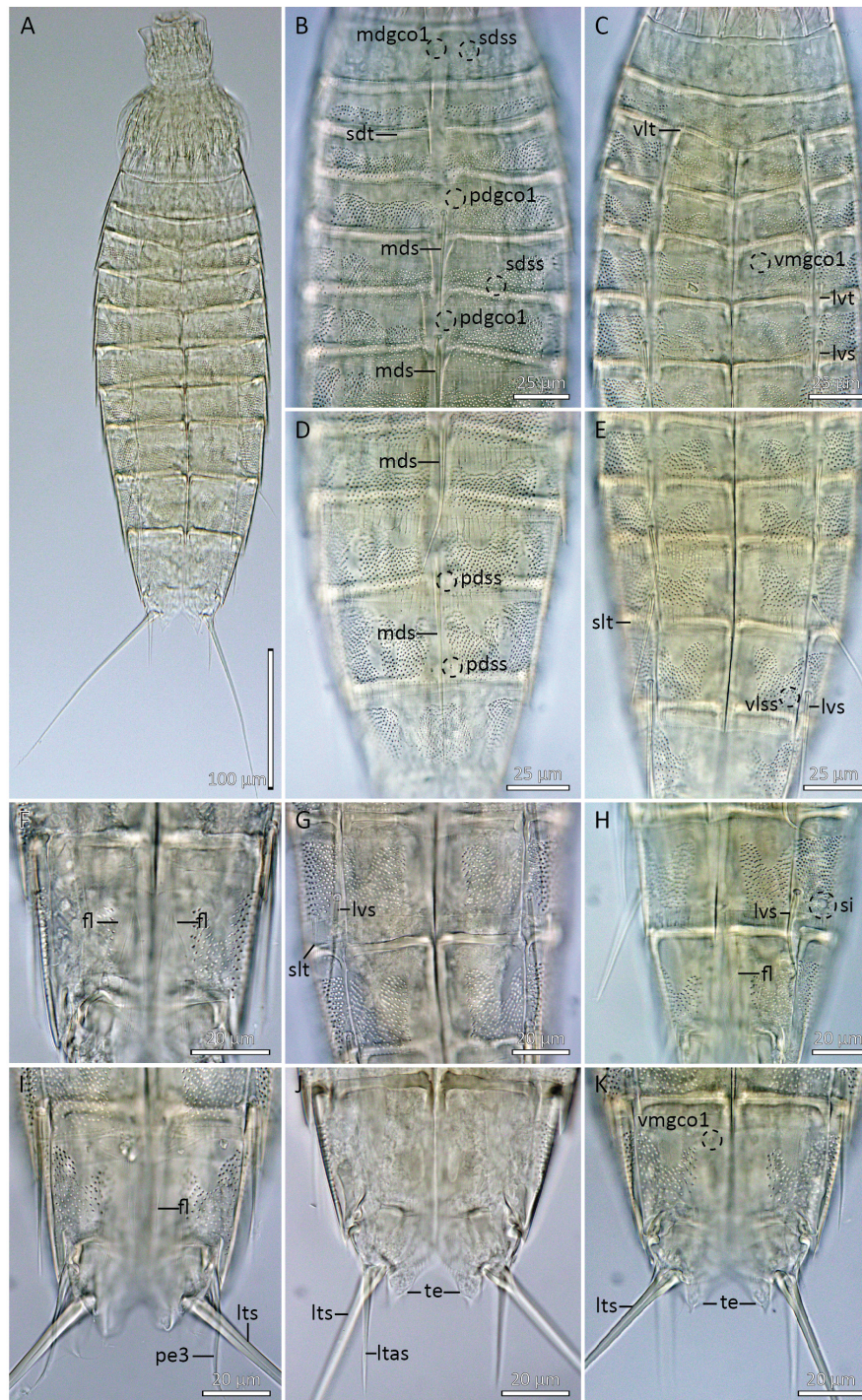
Fig. 11. Light micrographs showing overviews and details of *Echinoderes ahlfeldae* sp. nov. **A–E, J–K**. Female, holotype (NHMD 1784759). **F**. Male, paratype (NHMD 1784764). **G**. Female, paratype (NHMD 1784760). **H**. Male paratype (NHMD 1784768). **I**. Male paratype (NHMD 1784775). **A**. Ventral overview. **B**. Segments 1 to 6, dorsal view. **C**. Segments 1 to 6, ventral view. **D**. Segments 7 to 10, dorsal view. **E**. Segments 6 to 10, ventral view. **F**. Segment 10, ventral view, showing male sexual dimorphism. **G**. Segments 8 to 9, ventral view. **H**. Segments 9 to 10, ventral view, showing male sexual dimorphism. **I**. Segments 10 to 11, ventral view, showing male sexual dimorphism. **J**. Segments 10 to 11, focused on tergal extensions, showing female sexual dimorphism. **K**. Segments 10 to 11, ventral view, showing female sexual dimorphism. Scale bars: A = 100 μm; B–E = 25 μm; F–K = 20 μm.
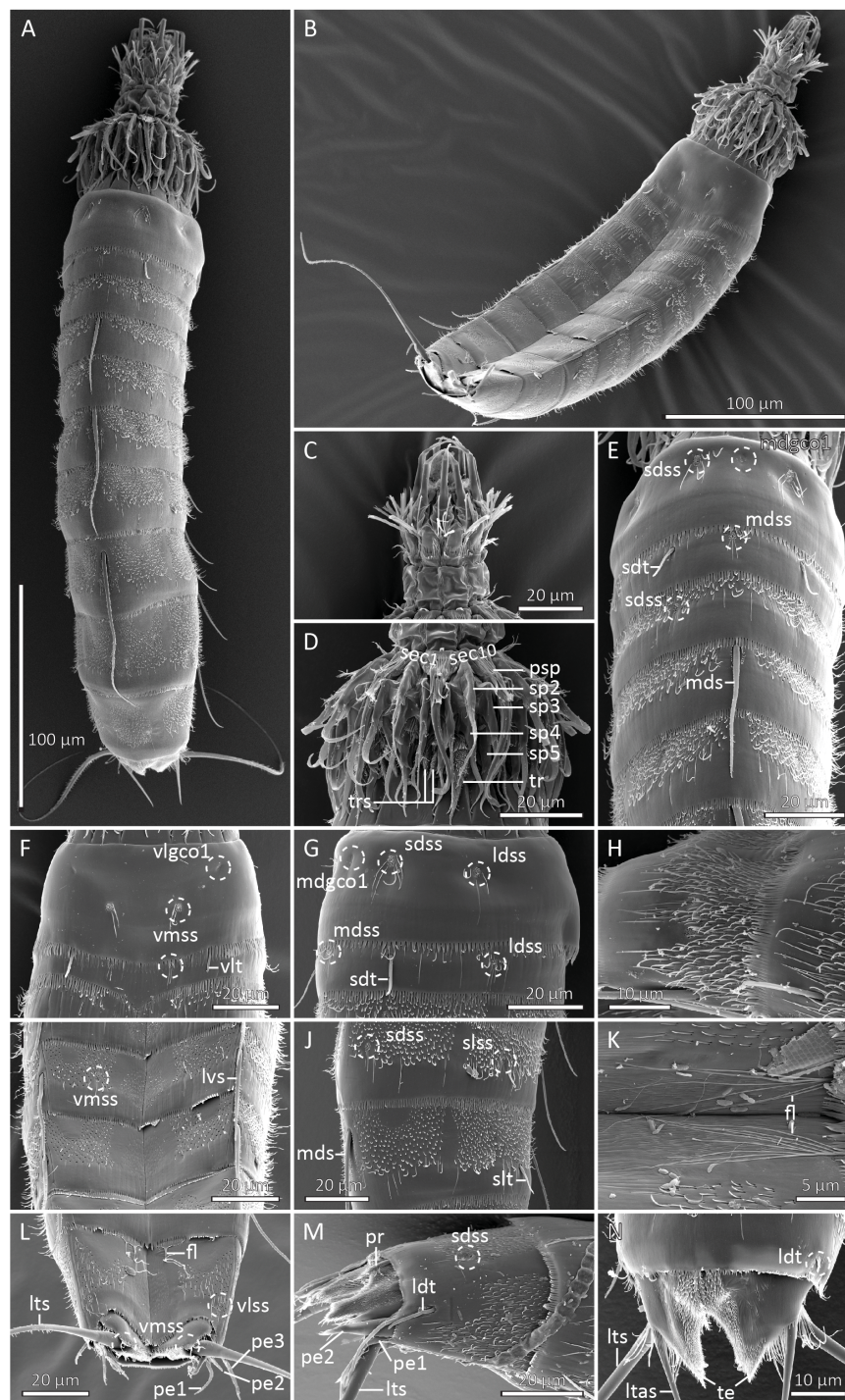
Fig. 12. Scanning electron micrographs showing overviews and details of *Echinoderes ahlfeldae* sp. nov. **A**. Dorsal overview of female. **B**. Ventrolateral overview of male. **C**. Mouth cone, ventral view. **D**. Introvert focused on the midventral sector 1 and sector 10. **E**. Segments 1 to 5, dorsal view. **F**. Segments 1 to 2, ventral view. **G**. Segments 1 to 2, right lateral view. **H**. Segments 8 to 9, right lateral view. **I**. Segments 7 to 8, ventral view. **J**. Segments 7 to 8, right lateral view. **K**. Detail of sternal plates of segment 10 with male dimorphic flare-like extensions from the secondary fringe. **L**. Segments 10 to 11, ventral view, showing male sexual dimorphism. **M**. Segments 10 to 11, right lateral view, showing male sexual dimorphism. **N**. Segments 10 to 11, dorsal view, showing female sexual dimorphism. Scale bars: A–B = 100 µm; C–G, I–J, L–M = 20 µm; H, N = 10 µm; K = 5 µm.

'flare-like extensions from secondary fringe'. No indication of a similar structure is evident in females. Sensory spots present in subdorsal and ventrolateral positions. Glandular cell outlets type 1 present as two longitudinally arranged outlets in middorsal position and in ventromedial positions. Cuticular hairs of uniform length, covering the tergal plate, except in two hairless subdorsal areas; cuticular hairs on sternal plates as on preceding segments. The posterior segment margin of the tergal plate is straight, with very minute fringe tips; the margins of the sternal plates are concave, reaching the posterior margin of the terminal segment, also with very short fringe tips (Figs 9A–D, 11D–F, H–K, 12K–N).

SEGMENT 11. With lateral terminal spines. Females with lateral terminal accessory spines; males with thin, tubular dorsal and ventral penile spines, and a well-developed, cone-shaped medial pair of penile spines. Sensory spots present in ventromedial positions, near margins of sternal extensions. A single glandular cell outlet type 1 present in middorsal position. A minute middorsal protuberance-like structure extends from the intersegmentary joint in some specimens (Fig. 12M), whereas it is evidently absent in others (Fig. 12N); holotype without middorsal protuberance. The segment is devoid of cuticular hairs, but with very short cuticular hair-like structures covering the mid- and paradorsal areas, and the inferior margins of the tergal extensions. Tergal extensions are short and triangular with slightly offset tips. Sternal extensions short, broadly rounded, and not extending beyond tergal extensions (Figs 9A–D, 11I–K, 12L–N).

Distribution

Antarctic Peninsula: Gerlache Strait and Andvord Bay MBA, IBB and OBA, 525 to 701 m b.s.l. See Fig. 1 for geographic overview of stations and Table 1 for station and specimen information.

Diagnostic remarks

The composition of segments 1 and 2 forming closed cuticular rings easily assigns the new species to *Echinoderes*. This generic assignment could, if genus diagnoses of Echinoderidae are used in the strictest possible way, be challenged by the presence of superficial markings on segment 2, which could indicate the presence of partial tergosternal junctions. However, several previous descriptions have demonstrated that a weak indication of a partially developed midventral fissure on segment 2 does not bring the generic assignments to *Echinoderes* into question (Sørensen *et al.* 2012; Herranz *et al.* 2018; Yamasaki & Dal Zotto 2019; Grzelak *et al.* 2023). In the case of *E. ahlfeldae* sp. nov. the superficial fissures on segment 2 are lateroventral rather than midventral, which to our knowledge has not been observed previously among species of Echinoderidae, but since the indications are only superficial lines on the cuticle, never observable with LM, and not even occurring in all specimens, we would not put any taxonomic value into this trait. Instead, it only confirms that the ring-like composition of segment 2 might show a certain level of variation within *Echinoderes*.

Among species of *Echinoderes*, *E. ahlfeldae* sp. nov. shares the common pattern with middorsal spines on segments 4, 6, and 8, and lateroventral tubes or spines on segments 5 to 9, with no less than 27 congeners (Yamasaki *et al.* 2020b). However, if this tube-spine pattern is combined with the presence of sublateral tubes on segment 8 and the complete lack of glandular cell outlets type 2, the list of similar candidates is shortened dramatically to only three species, i.e., *E. hispanicus* Pardos *et al.*, 1998, *E. leduci* Grzelak & Sørensen, 2022, and *E. newcaledoniensis* Higgins, 1967. These three species certainly show great resemblance to each other and to *E. ahlfeldae*, but still they can be distinguished from the latter by carrying additional pairs of tubes in various positions. Likewise, *E. newcaledoniensis* has laterodorsal and sublateral tubes on segment 2, whereas subdorsal tubes are lacking, and it has in addition midlateral tubes on segment 9 and lateral accessory tubes on segments 6 to 8 (Higgins 1967). Also *E. hispanicus* differs, by having sublateral tubes on segment 2 and lateral accessory tubes or spines on segment 8 (Pardos *et al.* 1998). The species showing the closest resemblance to *E. ahlfeldae* is

E. leduci. However, *E. leduci* differs by its uncommon lack of regular cuticular hairs that have been replaced by minute scales, by having laterodorsal tubes on segment 9, and by having its dorsal tubes on segment 2 in laterodorsal rather than subdorsal positions (Grzelak & Sørensen 2022). Even without taking the lack of glandular cell outlets type 2 into account, the combined spine and tube pattern in *E. ahlfeldae* is unique within the genus, which makes identification of the species fairly easy.

The distribution of glandular cell outlets type 1 in *E. ahlfeldae* sp. nov. follows the MD Seg. 1–3, 5, 7, PD 4, 6, 8–9 pattern (see table with summary of species with this pattern described up to 2020 in Sørensen *et al.* 2020). Among species described after 2020, this pattern is also found in *E. leduci*, which stresses the close resemblance between the two species.

Two other noteworthy characters in *E. ahlfeldae* sp. nov. are the position of the sieve plates and the uncommon flare-like extensions from the secondary fringes of the sternal extensions of segment 10 in males. The sieve plates in species of *Echinoderes* are most commonly located in lateral accessory positions on segment 9, but a slight relocation to sublateral positions is not uncommon either. Therefore, the sieve plate positions rarely play an important role as a diagnostic character. However, during the species identification phase of the present study, their positions turned out to be an extremely handy character when distinguishing between *E. ahlfeldae* and *E. nataliae* sp. nov. (see description below). The two species have a rather similar appearance, especially when it comes to specimens mounted for SEM, with only the ventral and parts of the lateral sides exposed. However, in *E. nataliae* the sieve plates sit in lateral accessory positions, very close to the lateroventral spines, and soon during the identification phase the position of the sieve plates became the easy way to distinguish between the two species when other diagnostic characters were hidden. This example shows that even the most unexpected character trait can suddenly become useful in species recognition.

Another subtle, but yet significant trait of *E. ahlfeldae* sp. nov. is the flare-like extensions from the secondary fringes of the sternal plates on segment 10 in male specimens. When first observed, the flare-like structures were considered to be unique for the species, because something like this was certainly never reported previously. The most similar, and also the only, published example of a structure like this are the tufts of long hairs reported from *Echinoderes pterus* Yamasaki *et al.*, 2018a. However, the structures in *E. pterus* differ in several points: they are much stronger and appear more like a brush; they are present on the tergal plate and on segment 9; and they are present in both sexes. Thus, the similarities between the hairy tufts in *E. pterus* and the flare-like extensions in *E. ahlfeldae* are only superficial, and the structures in the latter species were therefore initially considered to be limited to this particular species. However, as discussed above, the similarities between *E. ahlfeldae* and *E. leduci* led to a closer examination of unpublished SEM images of the latter species and, surprisingly, similar structures were found in this species. In *E. leduci* they also appear on the sternal plates of segment 10 and were found in two males mounted for SEM (their presence in females could not be confirmed though, as the only available female mounted for SEM was mounted on its ventral side). Their appearance and position in *E. leduci* clearly suggest that the structures are homologous with the flare-like extensions in *E. ahlfeldae*, but they also showed clear differences. Whereas the flares in *E. ahlfeldae* consist of six to eight setal threads, only one to three threads were present in *E. leduci*. This obviously makes the structure much more indistinct, which also explains why they were not mentioned in the original description (Grzelak & Sørensen 2022). In addition to the occurrence in these two species, similar setal threads was found in one of the new species, *E. nataliae* sp. nov. (see following description). In this species, the setal threads are also restricted to males and are formed as extensions from the secondary fringe of the sternal plates of segment 10. However, in *E. nataliae* only a single thread is present on each sternal plate, in contrast to the more numerous threads found in *E. ahlfeldae*.

Echinoderes nataliae sp. nov
urn:lsid:zoobank.org:act:B64378E9-7DF2-481E-BAE4-9B76D26E4819
Figs 13–15, Tables 11–12

Diagnosis

Echinoderes with acicular spines in middorsal position on segments 4, 6, and 8, and in lateroventral positions on segments 6 to 9. Tubes present in subdorsal (almost paradorsal), laterodorsal, sublateral, and ventrolateral positions on segment 2, in lateroventral positions on segment 5, in sublateral positions on segment 8, and in laterodorsal positions on segment 10; tubes on segment 10 show sexual dimorphism and are larger in males. Laterodorsal glandular cell outlet type 2 with short, broad, projecting rectangular flap present on segment 9. Dorsal glandular cell outlets type 1 are present in middorsal positions on segments 1 to 3, 5, 7, and 10, and in paradorsal positions on segments 4, 6, 8, and 9. Sieve plates on segment 9 in lateral accessory positions, very close to base of lateroventral spine. Segment 1 completely devoid of cuticular hairs, except for those flanking the sensory spots. Males with single setal extension from secondary fringe of sternal plates on segment 10. Female papillae not present.

Etymology

The first author dedicates this species to his wife, Natalia Pouchkina-Stantcheva.

Material examined

　Holotype
ANTARCTICA • ♂ (mounted for LM in Fluoromount G on HS slide); Antarctic Peninsula, CRS 1778; 64°47.01′ S, 62°43.90′ W; 567 m b.s.l.; 8 Apr. 2016; FjordEco2; soft sediment; NHMD 1786668.

　Paratypes
ANTARCTICA – **Antarctic Peninsula** • 1 ♂ (mounted as holotype); CRS 1706; 64°50.47′ S, 62°35.12′ W; 499 m b.s.l.; 1 Dec. 2015; FjordEco1; soft sediment; NHMD 1786672 • 1 ♂ (mounted as holotype); CRS 1716; 64°52.36′ S, 62°25.49′ W; 551 m b.s.l.; 6 Dec. 2015; FjordEco2; soft sediment; NHMD 1786673 • 1 ♀ (mounted as holotype); CRS 1773; 64°52.35′ S, 62°25.88′ W; 553 m b.s.l.; 6 Apr. 2016; FjordEco2; soft sediment; NHMD 1786674 • 3 ♂♂, 2 ♀♀ (mounted as holotype); same data as for holotype; NHMD 1784769 to 1784771, USNM 1740037 to 1740038 • 2 ♂♂, 1 ♀, 1 juv. (mounted as holotype); CRS 1790; 64°51.49′ S, 62°34.01′ W; 532 m b.s.l.; 10 Apr. 2016; FjordEco2; soft sediment; NHMD 1786675 to 1786676, USNM 1740039 • 1 ♂ (mounted as holotype); CRS 1792; 64°51.40′ S, 62°34.01′ W; 525 m b.s.l.; 11 Apr. 2016; FjordEco2; soft sediment; NHMD 1786679 • 1 ♂ (mounted as holotype); CRS 1799; 64°51.51′ S, 62°33.83′ W; 541 m b.s.l.; 13 Apr. 2016; FjordEco2; soft sediment; NHMD 1786680.

　Additional material
ANTARCTICA – **Antarctic Peninsula** • 1 ♀ (mounted for SEM); CRS 1698; 64°51.60′ S, 62°33.80′ W; 541 m b.s.l.; 28 Nov. 2015; FjordEco1; soft sediment; MVS • 2 ♂♂, 1 ♀ (mounted for SEM); CRS 1702; 64°51.15′ S, 62°34.44′ W; 502 m b.s.l.; 30 Nov. 2015; FjordEco1; soft sediment; MVS • 1 ♂, 2 ♀♀ (mounted for SEM); CRS 1773; 64°52.35′ S, 62°25.88′ W; 553 m b.s.l.; 6 Apr. 2016; FjordEco2; soft sediment; MVS • 4 ♂♂, 1 ♀ (mounted for SEM); CRS 1790; 64°51.49′ S, 62°34.01′ W; 532 m b.s.l.; 10 Apr. 2016; FjordEco2; soft sediment; MVS • 1 ♂, 3 ♀♀ (mounted for SEM); CRS 1792; 64°51.40′ S, 62°34.01′ W; 525 m b.s.l.; 11 Apr. 2016; FjordEco2; soft sediment; MVS • 5 ♂♂, 1 ♀ (mounted for SEM); CRS 1793; 64°39.53′ S, 62°55.03′ W; 701 m b.s.l.; 11 Apr. 2016; FjordEco2; soft sediment; MVS • 1 ♀ (mounted for SEM); CRS 1799; 64°51.51′ S, 62°33.83′ W; 541 m b.s.l.; 13 Apr. 2016; FjordEco2; soft sediment; MVS • 5 ♂♂, 1 ♀ (mounted for SEM); CRS 1809; 64°39.59′ S, 62°55.09′ W; 694 m b.s.l.; 15 Apr. 2016; FjordEco2; soft sediment; MVS.

Description

General. Adults with head, neck, and eleven trunk segments (Figs 13A–B, 14A, 15A–B). An overview of measurements and dimensions is given in Table 11. Distributions of cuticular structures, i.e., sensory spots, glandular cell outlets, spines, and tubes, are summarized in Table 12.

Head. Consists of a retractable mouth cone and an introvert (Fig. 15C–D). Mouth cone with nine outer oral styles composed of two units; all oral styles with uniform morphology, but differ alternately in length, with styles in uneven numbered sectors being ca 15% longer than those in even numbered. Bases of outer oral styles with row of six slender spikes, flanked by pair of stronger spikes. A single fringe is located more basally, at the base of the mouth cone and in between the attachment points of the outer oral styles. Inner oral styles could not be examined.

Introvert. The arrangement of scalids follows the pattern of *P. grzelakae* nov. sp., thus see Fig. 6 for scalid arrangement. The introvert has ten primary spinoscalids in Ring 01. Each primary spinoscalid consists of a basal sheath and a distal end piece with a blunt tip (Fig. 15D). Rings 02 and 04 have 10 spinoscalids, and Rings 03 and 05 have 20. All spinoscalids in these rings are well-developed and consist of a basal sheath with fringed distal margins and a pointed end-piece. Ring 06 has only six spinoscalids, located in sectors 1, 3, 5, 6, 7, and 9; they resemble those in preceding sectors, but the distal end-pieces are slightly shorter. Ring 07 has eight scalids with very short end-pieces, i.e., shorter than the basal sheaths, located as pairs in sectors 1, 3, and 9, and as single, laterally displaced ones in sectors 5 and 7 (Fig. 6). Described sector-wise (Fig. 6), sectors 1, 3, and 9 are similar, having spinoscalids arranged as two double diamonds anterior to an additional pair of Ring 07 spinoscalids. Sectors 2, 4, 8, and 10 all have spinoscalids arranged as a quincunx, located in between an anterior spinoscalid in Ring 02 and a trichoscalid plate. Sectors 5 and 7 have spinoscalids forming double diamonds, anterior to an unpaired, lateral spinoscalid; the lateral spinoscalid is unpaired because a trichoscalid plate takes up the space on the opposite side of the sector. Sector 6 has its spinoscalids arranged as double diamonds. Regular trichoscalids with trichoscalid plates are present in sectors 2, 4, 5, 7, 8, and 10 (Figs 6, 15D).

Neck. With 16 placids. Midventral placid broadest, 13 μm in width and length, whereas all others are narrower, measuring 8 μm in width at their bases. The trichoscalid plates are well-developed and hat-shaped.

Segment 1. Consists of a complete cuticular ring. Sensory spots are present in subdorsal, laterodorsal, and ventromedial positions; subdorsal and laterodorsal sensory spots are present on the anterior half of the segment, but not immediately at the anterior margin. They are composed of a dense tuft of micropapillae around a central pore and are flanked by three to five long, bristle-like cuticular hairs, arranged along the lower margin of the micropapillary area; ventromedial sensory spots are more posterior on the segment, with same appearance as the dorsal ones, but with only two or three cuticular hairs. Glandular cell outlets type 1 are present in middorsal and ventrolateral positions. Besides the few hairs around the sensory spots, the segment is completely devoid of cuticular hairs. The posterior segment margin is straight and terminates in a pectinate fringe with narrow and slender fringe tips (Figs 13A–B, 14B–C, 15E–G).

Segment 2. Consists of a complete cuticular ring. Tubes are located in subdorsal, laterodorsal, sublateral, and ventrolateral positions; subdorsal tubes are located very close to the paradorsal positions. Sensory spots present in middorsal, midlateral, and ventromedial positions; the micropapillary areas around the sensory spots on this, and all following segments, are rounded. The micropapillae along the posterior margin of the areas are longer, and several conspicuously long micropapillae extend from the posterior part of the areas. Glandular cell outlets type 1 are present in middorsal and ventromedial positions. Bracteate cuticular hairs are arranged in three to four transverse rows; hairs in the two to three anteriormost rows are rather short, whereas those of the most posterior row are considerably longer,

Table 11. Measurements from light microscopy of *Echinoderes nataliae* sp. nov. (in µm), including number of measured specimens (*n*) and standard deviation (SD).

Character	*n*	Range	Mean	SD
TL	13	240–312	271	21.51
TL (CUM)	13	372–452	400	22.59
MSW-6	13	50–55	53	1.66
MSW-6/TL	13	16.0–22.1%	19.7%	1.78%
SW-10	13	43–47	46	1.00
SW-10/TL	13	14.7–18.8%	17.0%	1.36%
S1	13	29–35	33	1.98
S2	13	24–31	27	2.10
S3	13	27–33	30	1.91
S4	13	29–40	33	3.01
S5	13	32–42	36	3.21
S6	13	34–46	39	3.31
S7	13	37–48	41	3.20
S8	13	40–51	44	3.33
S9	13	44–52	47	1.98
S10	13	37–43	40	2.18
S11	13	26–34	29	2.18
–				
MD4 (ac)	13	49–60	55	3.53
MD6 (ac)	13	71–79	75	2.78
MD8 (ac)	12	77–91	83	4.942
–				
SD2 (tu)	3	9–11	10	1.15
LD2 (tu)	5	9–12	11	1.30
SL2 (tu)	4	9–11	10	1.15
VL2 (tu)	7	9–14	11	1.95
–				
LA5 (tu)	4	12–14	13	0.96
LV6 (ac)	13	23–31	28	2.59
LV7 (ac)	13	28–34	32	1.52
LV8 (ac)	13	32–37	34	1.61
LV9 (ac)	13	31–38	34	2.03
–				
SL8 (tu)	7	9–15	12	2.14
LD10 (tu) ♂	1	12	N/A	N/A
–				
LTAS	4	28–32	30	1.83
LTS	12	120–136	126	5.90
LTS/TL	12	38.5–51.3%	46.5%	3.75%

reaching the pectinate fringe at the posterior segment margin. The posterior segment margin is straight along the dorsal and lateral sides, but extends into a small midventral V-shaped flap. Pectinate fringe from middorsal to ventromedial areas with narrow and slender fringe tips as on preceding segment; however, from ventromedial to midsternal positions the fringe tips are conspicuously shorter and narrower (Figs 13A–B, 14B–C, 15E–G).

SEGMENT 3. As remaining segments, consisting of one tergal and two sternal plates. Sensory spots are present in subdorsal and sublateral positions, and glandular cell outlets type 1 in middorsal and ventromedial positions. The hair covering of the tergal and lateral halves of sternal plates is dense

Table 12. Summary of nature and location of sensory spots, glandular cell outlets, tubes, and spines arranged by series in *Echinoderes nataliae* sp. nov.

Segment	MD	PD	SD	LD	ML	SL	LA	LV	VL	VM
					Position					
1	gco1	–	ss	ss	–	–	–	–	gco1	ss
2	gco1,ss	–	tu	tu	ss	tu	–	–	tu	gco1,ss
3	gco1	–	ss	–	–	ss	–	–	–	gco1
4	ac	gco1	–	–	–	–	–	–	–	gco1
5	gco1	–	ss	–	–	ss	–	tu	–	gco1,ss
6	ac	gco1,ss	–	–	–	ss	–	ac	–	gco1,ss
7	gco1	ss	–	–	–	ss	–	ac	–	gco1,ss
8	ac	gco1,ss	–	–	–	tu	–	ac	–	gco1
9	–	gco1,ss	–	gco2,ss	–	–	si	ac	ss	gco1
10	gco1,gco1	–	ss	tu	–	–	–	–	ss	gco1
11	pr	ss	–	–	pex3(♂)	–	ltas(♀)	lts	–	ss

on the anterior half of the segment, except in hair-less midlateral areas; bracteate cuticular hairs are arranged in five to six rows; hairs in the two anteriormost rows are conspicuously short, only 1–2 μm; hairs in the median rows are longer, 5–6 μm, and hairs in the posteriormost row are very long, reaching the pectinate fringe. Paraventral areas without bracteate hairs, but with a rhomboid patch of fine, short hair-like extensions. Posterior segment margin straight and pectinate fringe as on preceding segment (Figs 13A–B, 14B–C, 15H, J).

SEGMENT 4. With spine in middorsal position. Sensory spots are not present. Glandular cell outlets type 1 are present in paradorsal and ventromedial positions. Cuticular hairs as on preceding segment, but in addition to the hairless midlateral areas, the middorsal area is also devoid of hairs. Posterior segment margin and pectinate fringe as on preceding segment (Figs 13A–B, 14B–C, 15H, J).

SEGMENT 5. With tubes in lateroventral positions. Sensory spots present in subdorsal, sublateral, and ventromedial positions, and glandular cell outlets type 1 in middorsal and ventromedial positions. Cuticular hairs, posterior segment margin, and pectinate fringe as on preceding segment (Figs 13A–B, 14B–C, 15I–J).

SEGMENT 6. With spines in middorsal and lateroventral positions. Sensory spots present in paradorsal, sublateral, and ventromedial positions. Glandular cell outlets type 1 present in paradorsal and ventromedial positions. Cuticular hairs, posterior segment margin, and pectinate fringe as on preceding segment (Figs 13A–B, 14B–C, 15I).

SEGMENT 7. With spines in lateroventral positions. Sensory spots present in paradorsal, sublateral, and ventromedial positions, and glandular cell outlets type 1 in middorsal and ventromedial positions. Cuticular hairs arranged in seven to eight rows, and still differentiated into very short, uniform hairs in the three to four anteriormost, longer hairs in the three median rows, and very long hairs in the posteriormost row. Posterior segment margin and pectinate fringe as on preceding segment (Figs 13A–B, 14D–E).

SEGMENT 8. With spines in middorsal and lateroventral positions, and tubes in sublateral positions. Sensory spots present in paradorsal positions only, and glandular cell outlets type 1 in paradorsal and ventromedial positions. Cuticular hairs as on preceding segment, but the midlateral hairless areas have moved to more laterodorsal positions. Posterior segment margin and pectinate fringe as on preceding segment (Figs 13A–B, 14D–F, 15L–M).
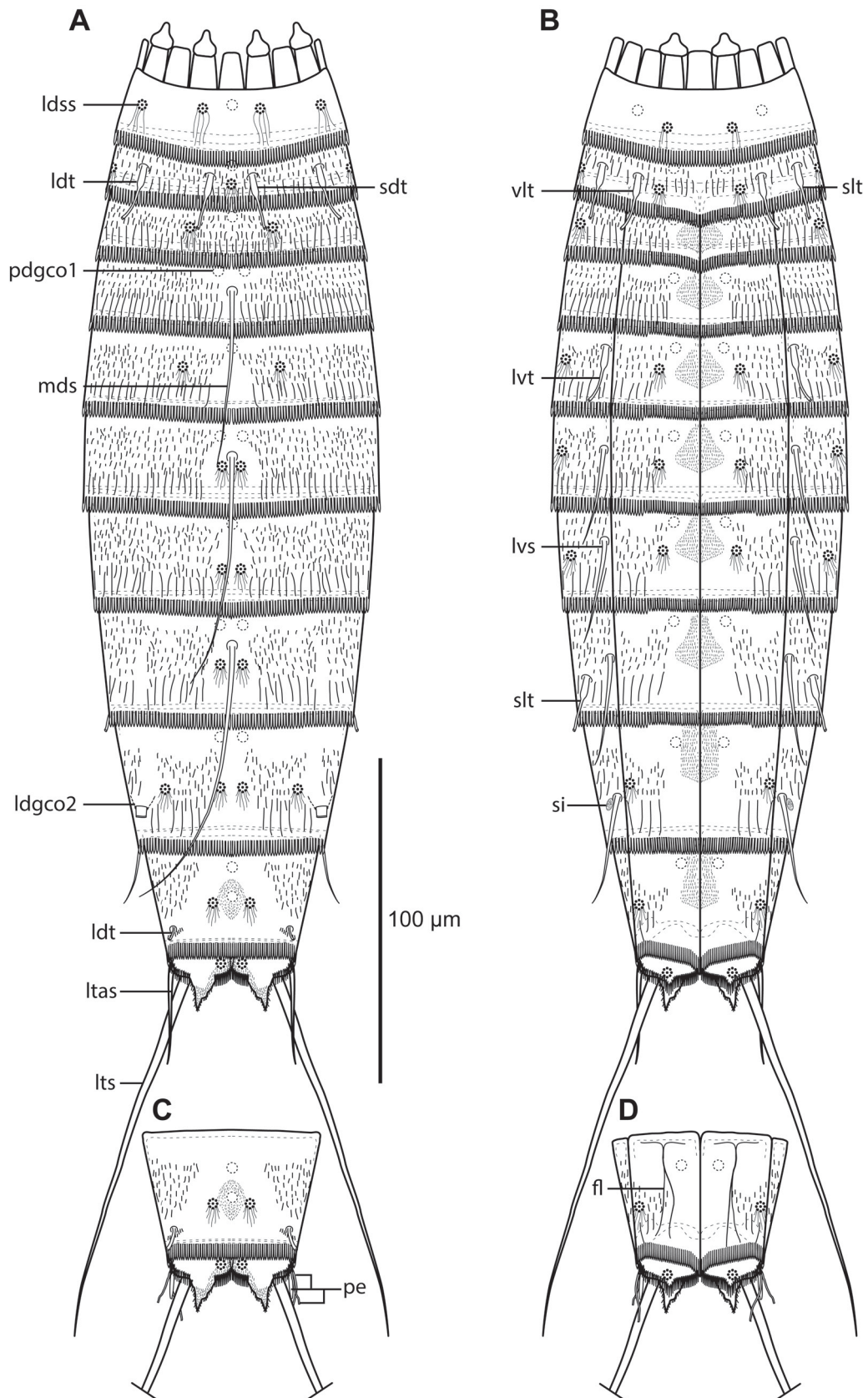
Fig. 13. Line art illustrations of *Echinoderes nataliae* sp. nov. **A.** Female, dorsal view. **B.** Female, ventral view. **C.** Male, segments 10 to 11, dorsal view. **D.** Male, segments 10 to 11, ventral view.
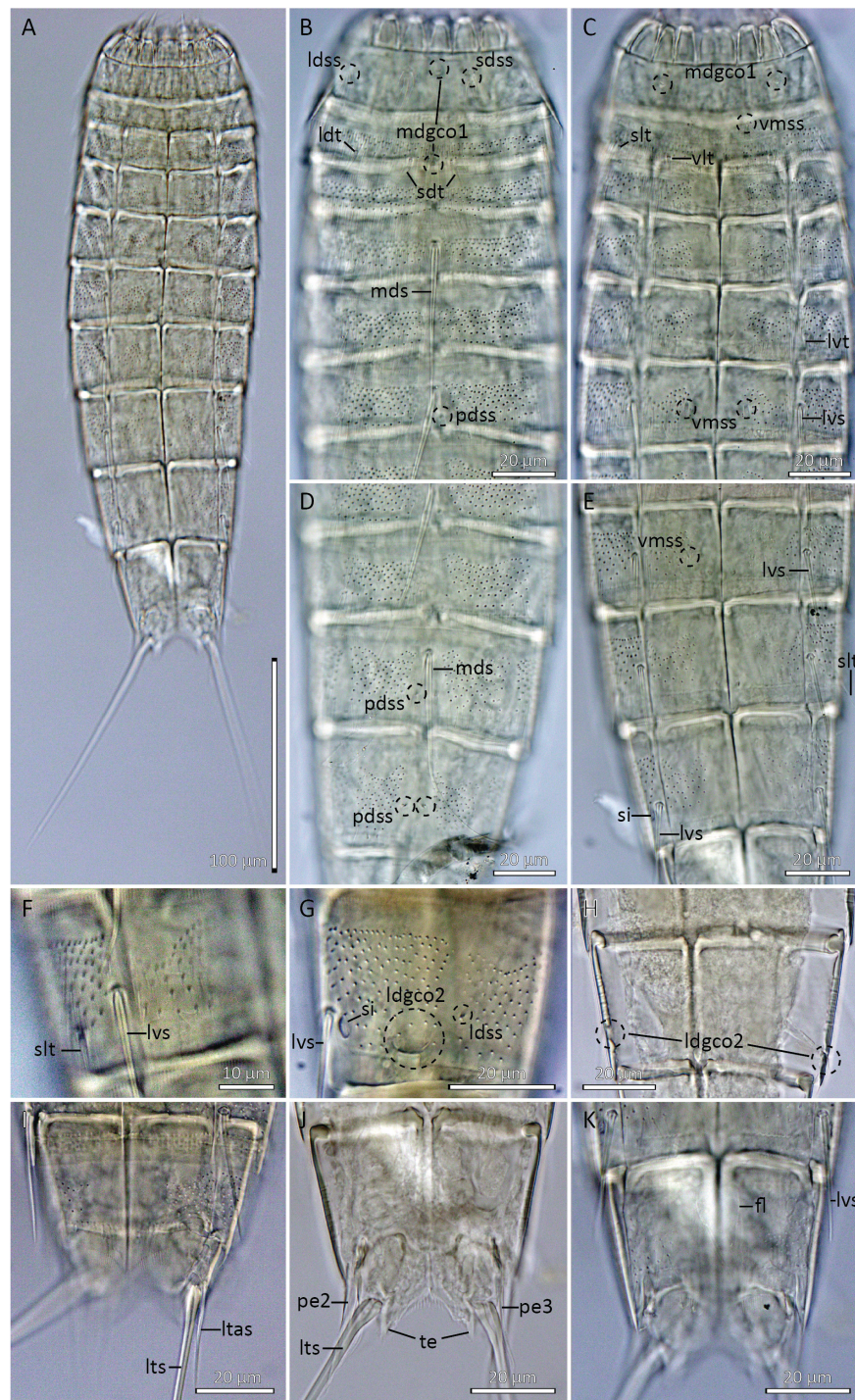
Fig. 14. Light micrographs showing overviews and details of *Echinoderes nataliae* sp. nov. **A–E, J–K**. Male, holotype (NHMD 1786668). **F**. Female, paratype (NHMD 1786671). **G**. Male, paratype (NHMD 1786669). **H**. Female, paratype (USNM 1740038). **I**. Female, paratype (NHMD 1786674). **A**. Ventral overview. **B**. Segments 1 to 6, dorsal view. **C**. Segments 1 to 6, ventral view. **D**. Segments 7 to 9, dorsal view. **E**. Segments 7 to 9, ventral view. **F**. Detail showing lateral half of segment 8, ventral view. **G**. Segments 9, lateral view, ventral is left. **H**. Segment 9, focused inside specimen. **I**. Segments 10 to 11, ventral view, showing female sexual dimorphism. **J**. Segments 10 to 11, focused on tergal extensions, showing male sexual dimorphism. **K**. Segments 10 to 11, ventral view, showing male sexual dimorphism. Scale bars: A = 100 µm; B–E, G–K = 20 µm; F = 10 µm.

Fig. 15. Scanning electron micrographs showing overviews and details of *Echinoderes nataliae* sp. nov. **A**. Laterodorsal overview of female. **B**. Ventral overview of male. **C**. Mouth cone, ventral view. **D**. Introvert focused on sectors 10 (left) and 9 (right). **E**. Segments 1 to 2, dorsal view. **F**. Segments 1 to 2, right lateral view. **G**. Segments 1 to 2, ventral view. **H**. Segments 3 to 4, laterodorsal view. **I**. Segments 5 to 6, right lateral view. **J**. Segments 3 to 5, ventral view. **K**. Segment 8, dorsal view, inset shows close-up of laterodorsal sensory spot and glandular cell outlet type 2 with protruding flap; scale = 3 μm. **L**. Segments 8 to 9, right lateral view. **M**. Segments 8 to 9, ventral view. **N**. Segments 10 to 11, dorsal view, showing male sexual dimorphism. **O**. Segments 10 to 11, ventral view, showing male sexual dimorphism. **P**. Segments 10 to 11, ventral view, showing female sexual dimorphism. Scale bars: A = 100 μm; B = 50 μm; C–D, J, L–P = 10 μm; E–I, K = 20 μm.

SEGMENT 9. With spines in lateroventral positions. Sensory spots present in paradorsal, laterodorsal, and ventrolateral positions. Very large glandular cell outlets type 2, with a broad rectangular flap projecting from the outlets, are present in laterodorsal positions. Glandular cell outlets type 1 present in paradorsal and ventromedial positions. Small rounded sieve plates located in lateral accessory positions, immediately next to the attachment point of the lateroventral spines. The cuticular hair covering is similar to that on the preceding segment, but hairless middorsal area is broader. Posterior segment margin and pectinate fringe as on preceding segment (Figs 13A–B, 14D–E, G–H, 15K–M).

SEGMENT 10. With sexually dimorphic laterodorsal tubes located near, but not at, the posterior segment margin; female tubes are extremely small, hardly projecting from attachment site; male tubes of more regular size, reaching beyond the segment margin. Males in addition with one to three flare-like setae extending from the secondary fringes of each sternal plate. Sensory spots present in subdorsal and ventrolateral positions. Glandular cell outlets type 1 present as two longitudinally arranged outlets in middorsal position and in ventromedial positions. Cuticular hairs with same size differentiation as on preceding segments, but only present from laterodorsal to ventromedial areas; middorsal and paradorsal areas with rhomboid patch of short, hair-like extensions. The posterior segment margin of the tergal plate is straight, with fringe tips as on preceding segments; however, the narrower ventromedial to midventral fringe tips are as long as the other fringe tips. Sternal plate margins straight, but slightly oblique (Figs 13A–D, 14I–K, 15N–P).

SEGMENT 11. With lateral terminal spines. Females with lateral terminal accessory spines; males with thin, tubular dorsal and ventral penile spines, and well-developed, cone-shaped medial pair of penile spines. Sensory spots present in paradorsal and ventromedial positions. Middorsal protuberance-like structure extends from intersegmentary joint. The segment is devoid of cuticular hairs, but has a dense covering of minute cuticular hair-like structures on the protuberance, in the paradorsal areas, and along the inferior margins of the tergal extensions. Tergal extensions are short and triangular, with a small denticle on the inferior margins. Sternal extensions short, broadly rounded, and not extending beyond tergal extensions (Figs 13 A–D, 14I–K, 15N–P).

Distribution

Antarctic Peninsula: Gerlache Strait and Andvord Bay MBA, IBB, and OBA, 499 to 701 m b.s.l. See Fig. 1 for geographic overview of stations and Table 1 for station and specimen information.

Diagnostic remarks

The new species can easily be assigned to *Echinoderes*, and when comparing the spine pattern combined with the presence of four pairs of tubes on segment 2, the number of similar congeners is narrowed down to two described species, *E. hakaiensis* Herranz *et al*., 2018 and *E. frodoi* Grzelak & Sørensen, 2022, and the undescribed *Echinoderes* sp. 3, reported from abyssal plains near the Atacama Trench by Grzelak *et al.* (2021). However, *E. nataliae* sp. nov. can be distinguished from *E. hakaiensis* and *Echinoderes* sp. 3 by the presence of large glandular cell outlets type 2 on segment 9. Glandular cell outlets type 2 are not present at all in *E. hakaiensis* or *Echinoderes* sp. 3 (Herranz *et al.* 2018; Grzelak *et al.* 2021).

The glandular cell outlets type 2 on segment 9 in *E. nataliae* sp. nov. are not only large. They also have a very particular morphology, with a rectangular flap projecting from the openings. Somewhat similar structures are present in *E. frodoi*, even though Grzelak & Sørensen (2022) reported the structures as "laterodorsal tubes". *Echinoderes frodoi* has large openings, resembling glandular cell outlets type 2, in lateral accessory positions on segment 8 and in laterodorsal positions on segment 9. On both segments, there are flattened, tubular structures projecting from the openings. The structures look like collapsed tubes and were interpreted as such by Grzelak & Sørensen (2022), but they could in fact also be flattened

flaps, as seen on segment 9 in *E. nataliae*. Although the structures in the two species are very similar, they are not identical. For instance, the flaps in *E. nataliae* are rectangular, close to quadratic (Fig. 15K), whereas they are clearly more elongate and slender in *E. frodoi* – at least on segment 8. On segment 9 in *E. frodoi*, the tubes vary between forming short but wide collars to forming elongate but yet rather wide tubes. We believe that the two species share a special and homologous variation of type 2 glandular cell outlets.

Besides the similar glandular cell outlets, and resemblance in tube and spine patterns, *E. frodoi* and *E. nataliae* sp. nov. also differ on several points. The most substantial difference between the two species is the midlateral tubes on segment 1, present in *E. frodoi* only. However, these tubes are not consistently present in all specimens of *E. frodoi*, and even though such tubes never occurred in the 50+ examined specimens of *E. nataliae*, their inconsistent occurrence in *E. frodoi* makes them less useful as a differential character. Another difference between the two species is expressed in their morphometrics. The trunk length of *E. frodoi* ranges from 161 to 202 μm, unlike the 240 to 312 μm in *E. nataliae*, and the general trunk shape of *E. frodoi* appears stouter or chubbier than the more slender *E. nataliae*. This difference is expressed in the differing Maximum Sternal Width to Trunk Length ratios, with an average of 24.7% in *E. frodoi* (Grzelak & Sørensen 2022) but only 19.7% in *E. nataliae*. Also all middorsal spines are longer in *E. nataliae*, and the ranges of the middorsal spine lengths in the two species never overlap. Small differences are also expressed in the position of tubes on segment 8, with the tubes of *E. frodoi* attaching in lateral accessory positions, whereas they are more dorsal in *E. nataliae* and sit in sublateral positions. There are also distinct differences in the cuticular hair covering of the two species. *Echinoderes nataliae* never has cuticular hairs on segment 1 (except those associated with the sensory spots), but has a relatively dense hair covering on the following nine segments. In contrast, most specimens of *E. frodoi* have plenty of hairs on segment 1, whereas the hair covering of the remaining segments is less dense compared to that of *E. nataliae*. Finally, *E. nataliae* has a pair of large and distinct ventromedial sensory spots on segment 1. Such sensory spots are lacking in *E. frodoi*. Thus, in conclusion, *E. nataliae* and *E. frodoi* are clearly two very similar species, and very likely also closely related, but they are also easily distinguished by several conspicuous as well as more subtle differences.

The distribution of glandular cell outlets type 1 in *E. nataliae* sp. nov. follows the MD Seg. 1–3, 5, 7, PD 4, 6, 8–9 pattern (see table with summary of species with this pattern described up to 2020 in Sørensen *et al.* 2020).

Echinoderes kathleenhannae sp. nov.
urn:lsid:zoobank.org:act:DD7B8B21-DE35-47FC-98F7-B0A8F3832421
Figs 16–18, Tables 13–14

Diagnosis

Echinoderes with acicular spines in middorsal position on segments 4, 6, and 8, and in lateroventral positions on segments 6 to 9. Tubes present in subdorsal, laterodorsal, sublateral, and ventrolateral positions on segment 2, in lateroventral positions on segment 5, in laterodorsal and lateral accessory positions on segment 8, and in laterodorsal positions on segment 10; tubes on segment 10 show sexual dimorphism and are largest in males. Female papillae or glandular cell outlets type 2 not present. Dorsal glandular cell outlets type 1 are present in middorsal positions on segments 1 to 3, 5, 7, and 10, and in paradorsal positions on segments 4, 6, 8, and 9. Sieve plates present on segment 9 in sublateral positions.

Etymology

The species is dedicated to the musician, artist, activist and rebel girl, Kathleen Hanna.

Material examined

Holotype

ANTARCTICA • ♂ (mounted for LM in Fluoromount G on HS slide); Antarctic Peninsula, CRS 1793; 64°39.53′ S, 62°55.03′ W; 701 m b.s.l.; 11 Apr. 2016; FjordEco2; soft sediment; NHMD 1786779.

Additional material

ANTARCTICA • 1 ♀ (mounted for SEM); same data as for holotype; MVS • 3 ♂♂, 1 ♀ (mounted for SEM); Antarctic Peninsula, CRS 1832; 64°39.30′ S, 62°55.98′ W; 631 m b.s.l.; 21 Apr. 2016; FjordEco2; soft sediment; MVS.

Description

General. Adults with head, neck and eleven trunk segments (Figs 16A–B, 17A, 18A–C). An overview of measurements and dimensions is given in Table 13. Distributions of cuticular structures, i.e., sensory spots, glandular cell outlets, spines and tubes, are summarized in Table 14.

Head. All specimens had their heads fully retracted; thus, information on head morphology is not available.

Neck. With 16 placids. Midventral placid broadest, 12 µm in width and 13 µm in length, whereas all others are narrower, measuring 8 µm in width at their bases. The trichoscalid plates are well-developed and hat-shaped.

Segment 1. Consists of a complete cuticular ring. Sensory spots are present in subdorsal and laterodorsal positions; the sensory spots are small, with numerous micropapillae and two long cuticular hairs attached on the margin of the papillated area. Glandular cell outlets type 1 are present in middorsal and ventrolateral positions. Cuticular hairs emerge from rounded perforation sites and are arranged in four to five rows on the dorsal side, and only two to three rows on the ventral. The posterior segment margin is almost straight and terminates in a pectinate fringe with rather broad fringe tips (Figs 16A–B, 17B–C, 18D–F).

Segment 2. Consists of a complete cuticular ring. Tubes are located in subdorsal, laterodorsal, sublateral, and ventrolateral positions; all tubes are very slender, and the proximal thickenings are hardly visible. Sensory spots present in middorsal, laterodorsal, and ventromedial positions; the micropapillary areas around the sensory spots on this, and all following segments, are rounded, with up to five longer micropapillae extending from the posterior part of the papillated areas. Glandular cell outlets type 1 are present in middorsal and ventromedial positions. Bracteate cuticular hairs are arranged in three to four transverse rows; hairs in the first and second anterior rows are rather short, whereas those of the most posterior row are longer. The posterior segment margin is nearly straight. Pectinate fringe of dorsal and lateral margins well-developed, as on preceding segment; pectinate fringe of ventrolateral to midventral margins narrower and with extended, flexible tips (Figs 16A–B, 17B–C, 18D–F).

Segment 3. As remaining segments, consisting of one tergal and two sternal plates. Sensory spots are present in subdorsal and sublateral positions, and glandular cell outlets type 1 in middorsal and ventromedial positions. The hair covering of the tergal and lateral halves of sternal plates is dense on the anterior half of the segment, except in hair-less midlateral areas; bracteate cuticular hairs are arranged in five to six rows, and the hairs in each row get progressively longer towards the more posterior rows. Paraventral areas without bracteate hairs, but with rhomboid patch of well-developed hair-like extensions. Posterior segment margin straight, and pectinate fringe as on preceding segment (Figs 16A–B, 17B–C).

Segment 4. With spine in middorsal position; middorsal spines on this and segments 6 and 8 are uniform in length, rather than getting progressively longer towards the more posterior segments. Sensory spots are

Table 13. Measurements from light microscopy of *Echinoderes kathleenhannae* sp. nov. (in µm).

Character	NHMD- 1786779 (♂)		
TL	262	MD4 (ac)	36
TL (CUM)	387	MD6 (ac)	35
MSW-6	61	MD8 (ac)	36
MSW-6/TL	23.3%	–	
SW-10	48	SD2 (tu)	14
SW-10/TL	18.3%	LD2 (tu)	14
–		SL2 (tu)	15
S1	32	VL2 (tu)	15
S2	31	LV5 (tu)	15
S3	31	LV6 (ac)	27
S4	34	LV7 (ac)	30
S5	37	LV8 (ac)	32
S6	38	LV9 (ac)	34
S7	39	LD8 (tu)	15
S8	40	LA8 (tu)	16
S9	41	LD10(tu)	15
S10	39	LTS	169
S11	25	LTS/TL	64.5%

not present. Glandular cell outlets type 1 are present in paradorsal and ventromedial positions. Cuticular hairs, posterior segment margin, and pectinate fringe as on preceding segment (Figs 16A–B, 17D–E).

SEGMENT 5. With tubes in lateroventral positions. Sensory spots present in subdorsal, midlateral and ventromedial positions, and glandular cell outlets type 1 in middorsal and ventromedial positions. Cuticular hairs, posterior segment margin, and pectinate fringe as on preceding segment (Figs 16A–B, 17D–E, 18G–I).

SEGMENT 6. With spines in middorsal and lateroventral positions; lateroventral spines on this and following segments are almost uniform in length, rather than getting progressively longer towards the more posterior segments. Sensory spots present in paradorsal, midlateral and ventromedial positions, and glandular cell outlets type 1 in paradorsal and ventromedial positions. Cuticular hairs, posterior segment margin, and pectinate fringe as on preceding segment (Figs 16A–B, 17D–E, 18G–I).

SEGMENT 7. With spines in lateroventral positions. Sensory spots present in subdorsal, midlateral, and ventromedial positions, and glandular cell outlets type 1 in middorsal and ventromedial positions. Cuticular hairs, posterior segment margin, and pectinate fringe as on preceding segment (Figs 16A–B, 17F–G, 18L).

SEGMENT 8. With spines in middorsal and lateroventral positions, and tubes in laterodorsal and lateral accessory positions. Sensory spots present in paradorsal positions only, and glandular cell outlets type 1 in paradorsal and ventromedial positions. Cuticular hairs as on preceding segment, except for mid- and paradorsal areas, where the bracteate hairs are replaced by very fine hair-like extensions. Posterior segment margin and pectinate fringe as on preceding segment (Figs 16A–B, 17F–J, 18J–L).

SEGMENT 9. With spines in lateroventral positions. Sensory spots present in paradorsal, subdorsal, laterodorsal, and ventrolateral positions. Glandular cell outlets type 1 present in paradorsal and ventromedial positions. Small rounded sieve plates present in sublateral positions. Cuticular hairs, posterior segment margin, and pectinate fringe as on preceding segment (Figs 16A–B, 17H–K, 18J–K).

Table 14. Summary of nature and location of sensory spots, glandular cell outlets, tubes, and spines arranged by series in *Echinoderes kathleenhannae* sp. nov.

Segment	Position									
	MD	PD	SD	LD	ML	SL	LA	LV	VL	VM
1	gco1	–	ss	ss	–	–	–	–	gco1	–
2	gco1,ss	–	tu	tu,ss	–	tu	–	–	tu	gco1,ss
3	gco1	–	ss	–	–	ss	–	–	–	gco1
4	ac	gco1	–	–	–	–	–	–	–	gco1
5	gco1	–	ss	–	ss	–	–	tu	–	gco1,ss
6	ac	gco1,ss	–	–	ss	–	–	ac	–	gco1,ss
7	gco1	–	ss	–	ss	–	–	ac	–	gco1,ss
8	ac	gco1,ss	–	tu	–	–	tu	ac	–	gco1
9	–	gco1,ss	ss	ss	–	si	–	ac	ss	gco1
10	gco1,gco1	–	ss	tu	–	–	–	–	ss	gco1
11	pr	–	–	–	pex3(♂)	–	ltas(♀)	lts	–	ss

SEGMENT 10. With sexually dimorphic laterodorsal tubes; male tubes well-developed, located near, but not at, the posterior segment margin; female tubes shorter and attaching at the posterior segment margin. Sensory spots present in subdorsal and ventrolateral positions. Glandular cell outlet type 1 present as two longitudinally arranged outlets in middorsal position, and in ventromedial positions. Cuticular hairs in two to three rows and only present from laterodorsal to ventromedial areas; middorsal and paradorsal areas with rhomboid patch of short, hair-like extensions. The posterior segment margin of the tergal plate is straight, with fringe tips as on preceding segments. Sternal plate margins oblique towards posteriormost midventral point; fringe tips well-developed, like those along the dorsal margin (Figs 16A–D, 17J–M, 18M–O).

SEGMENT 11. With lateral terminal spines. Females with lateral terminal accessory spines, measuring around 42 μm (measure estimated from SEM images); males with thin, tubular dorsal and ventral penile spines; medial pair of penile spines cone-shaped and well-developed. Sensory spots present in ventromedial positions. Middorsal protuberance-like structure extends from intersegmentary joint. The segment is devoid of cuticular hairs, but has a dense covering of minute, cuticular hair-like structures on the middorsal protuberance, in the paradorsal areas, and along the inferior margins of the tergal extensions. Tergal extensions are short and triangular with a small denticle on the inferior margins. Sternal extensions short, broadly rounded, and not extending beyond tergal extensions (Figs 16A–D, 17L–M, 18M–O).

Distribution

Antarctic Peninsula: Gerlache Strait, 631 to 701 m b.s.l. See Fig. 1 for geographic overview of stations and Table 1 for station and specimen information.

Diagnostic remarks

The new species clearly belongs to *Echinoderes*, and the presence of laterodorsal and lateral accessory tubes on segment 8 but otherwise absence of tubes on segments 6 and 7 makes the species unique among congeners. Only five species of *Echinoderes* have the combined presence of laterodorsal and lateral accessory tubes on segment 8, i.e., *E. abbreviatus* Higgins, 1983, *E. belenae* Pardos *et al*., 2016b, *E. brevipes* Cepeda *et al*., 2019b, *E. rociae* Pardos *et al*., 2016a, and *E. intermedius* Sørensen, 2006 (Higgins 1983; Sørensen 2006; Pardos *et al.* 2016a, 2016b; Cepeda *et al.* 2019b). However, the four first mentioned species all have short and stout lateral terminal spines, which makes them very easy to distinguish from *E. kathleenhannae* sp. nov. Only *E. intermedius* show some resemblance with the new
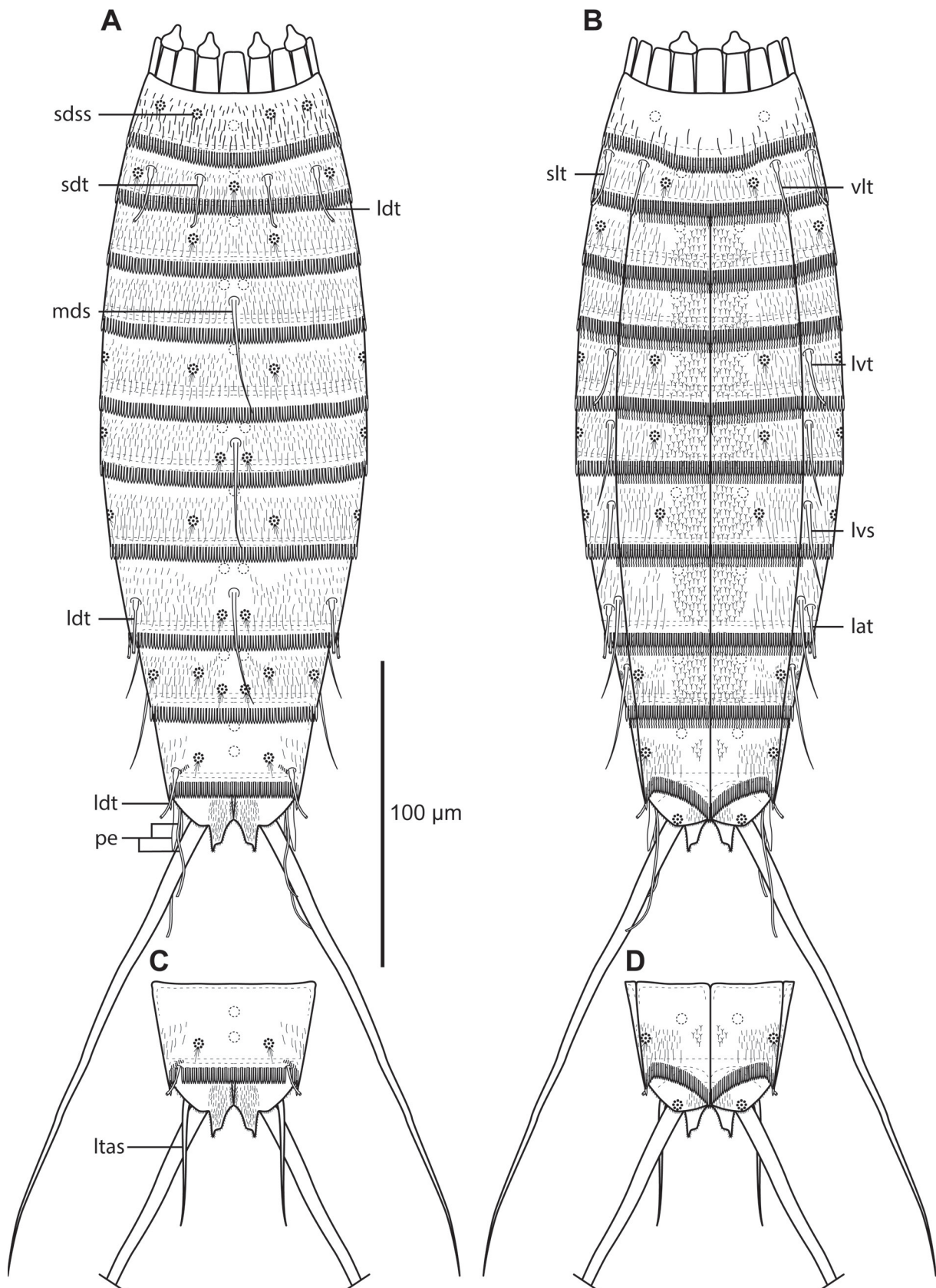
Fig. 16. Line art illustrations of *Echinoderes kathleenhannae* sp. nov. **A**. Male, dorsal view. **B**. Male, ventral view. **C**. Female, segments 10 to 11, dorsal view. **D**. Female, segments 10 to 11, ventral view.
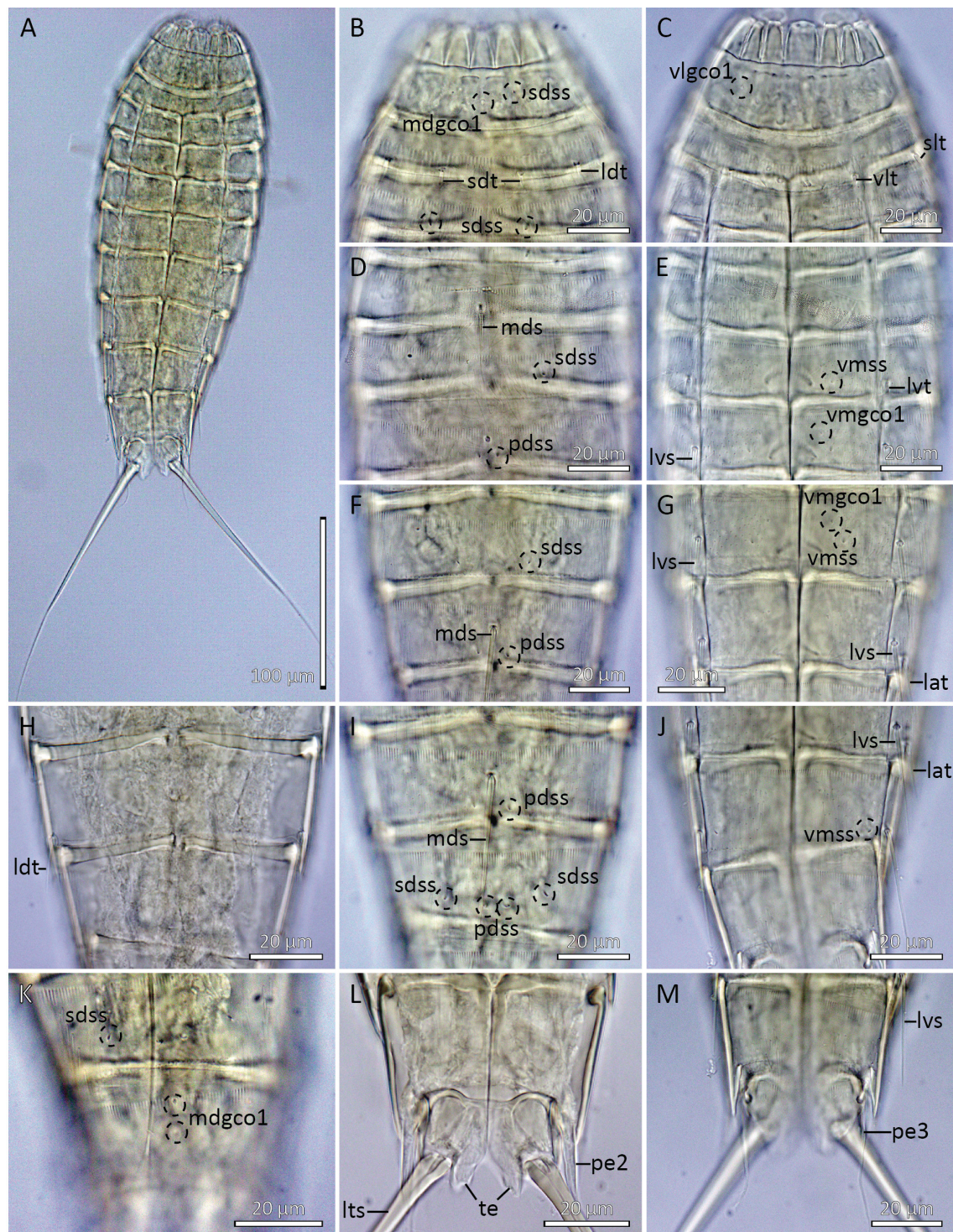
Fig. 17. Light micrographs showing overviews and details of *Echinoderes kathleenhannae* sp. nov., male, holotype (NHMD 1786779). **A**. Ventral overview. **B**. Segments 1 to 3, dorsal view. **C**. Segments 1 to 3, ventral view. **D**. Segments 4 to 6, dorsal view. **E**. Segments 4 to 6, ventral view. **F**. Segments 7 to 8, dorsal view. **G**. Segments 7 to 8, ventral view. **H**. Segments 8 to 9, focused on laterodorsal tube on segment 8. **I**. Segments 8 to 9, dorsal view. **J**. Segments 8 (posterior part) to 10. **K**. Segments 9 to 10, dorsal view. **L**. Segments 10 to 11, focused on tergal extensions, showing male sexual dimorphism. **M**. Segments 10 to 11, ventral view, showing male sexual dimorphism. Scale bars: A = 100 μm; B–M = 20 μm.
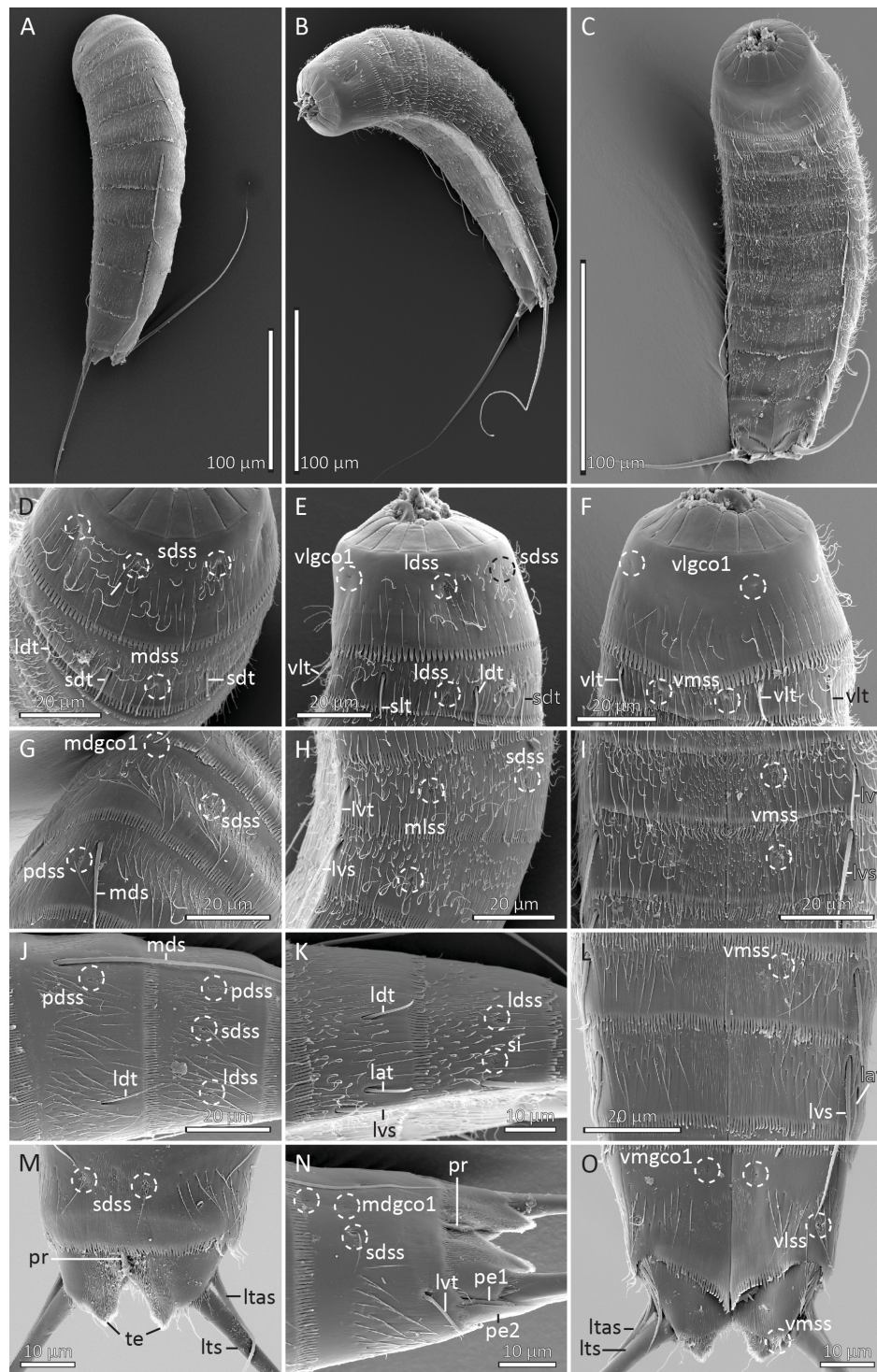
Fig. 18. Scanning electron micrographs showing overviews and details of *Echinoderes kathleenhannae* sp. nov. **A**. Dorsal overview of male. **B**. Left lateral overview of female. **C**. Ventral overview of female. **D**. Segments 1 to 2, dorsal view. **E**. Segments 1 to 2, left lateral view. **F**. Segments 1 to 2, ventral view. **G**. Segments 5 to 6, dorsal view. **H**. Segments 5 to 6, left lateral view. **I**. Segments 5 to 6, ventral view. **J**. Segments 8 to 9, laterodorsal view. **K**. Segments 8 to 9, left lateral view. **L**. Segments 7 to 8, ventral view. **M**. Segments 10 to 11, dorsal view, showing female sexual dimorphism. **N**. Segments 10 to 11, left lateral view, showing male sexual dimorphism. **O**. Segments 10 to 11, ventral view, showing female sexual dimorphism. Scale bars: A–C = 100 µm; D–J, L = 20 µm; K, M–O = 10 µm.

species, but the presence of midlateral glandular cell outlets type 2 on segment 2 and of lateral accessory tubes on segments 6 and 7 still makes it differ considerably from the new species.

Another species that could be confused with *E. kathleenhannae* sp. nov. is *E. hispanicus*. The two species share the same general habitus and spine pattern, and *E. hispanicus* also has two sets of tubes on segment 8. In *E. hispanicus* the tubes are located in midlateral and lateral accessory positions (Pardos *et al.* 1998), which differs slightly from the laterodorsal and lateral accessory tube positions in *E. kathleenhannae*. However, especially on the more posterior segments, the laterodorsal and midlateral positions are so close to each other that they can be difficult to distinguish; thus, the tube positions on segment 8 are not in themselves suitable for species differentiation. The easy way to distinguish the two species is by the number of tubes on segment 2, where *E. kathleenhannae* has four pairs, whereas *E. hispanicus* lacks the laterodorsal tubes and therefore has only three pairs of tubes.

The distribution of glandular cell outlets type 1 in *E. kathleenhannae* sp. nov. follows the MD Seg. 1–3, 5, 7, PD 4, 6, 8–9 pattern, as is the case with the two congeners described above.

Echinoderes antarcticus sp. nov.
urn:lsid:zoobank.org:act:940A9763-763D-4DBE-9A81-66F7A97312B8
Figs 19–21, Tables 15–16

Diagnosis
Echinoderes with acicular spines in middorsal position on segments 4, 6, and 8, and in lateroventral positions on segments 6 to 9. Tubes present in subdorsal, sublateral, and ventrolateral positions on segment 2, in lateroventral positions on segment 5, in sublateral positions on segment 8, and in laterodorsal positions on segment 10. Terminal segment with middorsal fissure, splitting the tergal plate in two. Male morphology unknown. Female papillae or glandular cell outlets type 2 not present. Dorsal glandular cell outlets type 1 are present in middorsal positions on segments 1 to 3, 5, 7 and 10, and in paradorsal positions on segments 4, 6, 8, and 9. Sieve plates present on segment 9 in lateral accessory positions.

Etymology
The species name '*antarcticus*' is derived from the Greek ανταρκτικός (antarcticos), meaning 'opposite to north' (masculine).

Material examined
Holotype
ANTARCTICA • ♀ (mounted for LM in Fluoromount G on HS slide); Antarctic Peninsula, CRS 1778; 64°47.01′ S, 62°43.90′ W; 567 m b.s.l.; 8 Apr. 2016; FjordEco2; soft sediment; NHMD 1786932.

Paratype
ANTARCTICA • 1 ♀ (mounted as holotype); Antarctic Peninsula, CRS 1809; 64°39.59′ S, 62°55.09′ W; 694 m b.s.l.; 15 Apr. 2016; FjordEco2; soft sediment; USNM 1740040.

Additional material
ANTARCTICA • 1 ♀ (mounted for SEM); Antarctic Peninsula, CRS 1832; 64°39.30′ S, 62°55.98′ W; 631 m b.s.l.; 21 Apr. 2016; FjordEco2; soft sediment; MVS.

Description
General. Adults with head, neck and eleven trunk segments (Figs 19A–B, 20A, 21A–B). The trunk is nearly parallel-sided from segment 2 to 7, and the cuticle of a thickness that makes all cuticular

structures appear very distinct. An overview of measurements and dimensions is given in Table 15. Distributions of cuticular structures, i.e., sensory spots, glandular cell outlets, spines and tubes, are summarized in Table 16.

HEAD. The available SEM specimen and the paratype had their heads fully retracted, whereas the head of the holotype was only partly extended; thus, information on head morphology is very limited. The presence of nine outer oral styles, each composed of two units, is evident though. The neck consists of 16 placids. Midventral placid broadest, 14 µm in width and 16 µm in length, whereas all others are narrower, measuring 9 µm in width at their bases. The trichoscalid plates are well-developed and hat-shaped.

SEGMENT 1. Consists of a complete cuticular ring. Sensory spots are present in subdorsal, laterodorsal, and ventromedial positions; the sensory spots are rounded to droplet-shaped, with numerous micropapillae around a central pore. Glandular cell outlets type 1 are present in middorsal and lateroventral positions. Cuticular hairs emerge from rounded perforation sites and are arranged in three diffuse rows on the dorsal side, a single row in the sublateral positions, and two rows ventrally, between the sensory spots. The posterior segment margin is almost straight and terminates in a pectinate fringe with tripartite tips (Figs 19A–B, 20B–C, 21C–D).

SEGMENT 2. Consists of a complete cuticular ring. Tubes are located in subdorsal, sublateral, and ventro-lateral positions; all tubes are very slender, and the proximal thickenings are hardly visible. Sensory spots present in middorsal, midlateral, and ventromedial positions; the micropapillary areas around the sensory spots on this, and all following segments, are rounded, with up to five longer micropapillae extending from the posterior part of the papillated areas. Glandular cell outlets type 1 are present in middorsal and ventromedial positions. Bracteate cuticular hairs are arranged in five transverse rows; hairs in the first anterior row are short, whereas those of the more posterior rows are considerably longer. The posterior segment margin is nearly straight, except at the small, midventral V-shaped extension. Pectinate fringe with well-developed, pointed fringe tips along dorsal and lateral margins; ventromedial fringe tips similar, but shorter and narrower (Figs 19A–B, 20B–C, 21C–D).

SEGMENT 3. As following seven segments, consisting of one tergal and two sternal plates. Sensory spots are present in subdorsal and sublateral positions, and glandular cell outlets type 1 in middorsal and ventromedial positions. The hair covering of the tergal and lateral halves of sternal plates is dense on the anterior half of the segment, except in hair-less midlateral areas, with bracteate cuticular hairs as on preceding segment. Paraventral areas without bracteate hairs, but with shield-shaped patch of well-developed hair-like extensions. Posterior segment margin straight, and pectinate fringe as on preceding segment (Figs 19A–B, 20B–C).

SEGMENT 4. With spine in middorsal position. Sensory spots are not present. Glandular cell outlets type 1 are present in paradorsal and ventromedial positions. Cuticular hairs from paradorsal to ventromedial positions arranged in seven to eight rows, with very short hairs in the anteriormost row, and hairs of remaining rows getting progressively longer towards the more posterior rows; middorsal area with triangular patch of short, hair-like extensions; paraventral areas as on preceding segment. Segment margin and pectinate fringe as on preceding segment (Figs 19A–B, 20B–C, 21E).

SEGMENT 5. With tubes in lateroventral positions. Sensory spots present in subdorsal, sublateral and ventromedial positions, and glandular cell outlets type 1 in middorsal and ventromedial positions. Cuticular hairs, posterior segment margin, and pectinate fringe as on preceding segment (Figs 19A–B, 20D–E, 21E–G).

Table 15. Measurements from light microscopy of *Echinoderes antarcticus* sp. nov. (in µm).

Character	NHMD-1786932 Holotype (♀)	USNM-1740040 Paratype (♀)
TL	318	377
TL (CUM)	464	488
MSW-7	63	74
MSW-7/TL	19.8%	19.6%
SW-10	54	62
SW-10/TL	17.0%	16.4%
–		
S1	38	44
S2	30	39
S3	31	40
S4	41	41
S5	44	46
S6	46	46
S7	51	52
S8	54	56
S9	54	56
S10	44	41
S11	31	27
–		
MD4 (ac)	55	48
MD6 (ac)	79	78
MD8 (ac)	92	105
–		
SD2 (tu)	21	16
SL2 (tu)	19	16
VL2 (tu)	18	16
LV5 (tu)	20	–
LV6 (ac)	35	31
LV7 (ac)	37	34
LV8 (ac)	43	34
LV9 (ac)	44	37
SL8 (tu)	22	–
LD10 (tu)	–	12
–		
LTS	171	213
LTS/TL	53.8%	56.5%
LTAS	46	55

SEGMENT 6. With spines in middorsal and lateroventral positions. Sensory spots present in paradorsal, sublateral and ventromedial positions, and glandular cell outlets type 1 in paradorsal and ventromedial positions. Cuticular hairs as on preceding segment, except for the dorsal patch of hair-like extensions that covers both the middorsal and paradorsal areas. Posterior segment margin and pectinate fringe as on preceding segment (Figs 19A–B, 20D–E, 21E–G).

SEGMENT 7. With spines in lateroventral positions. Sensory spots present in paradorsal, sublateral, and ventromedial positions, and glandular cell outlets type 1 in middorsal and ventromedial positions. Cuticular hairs, posterior segment margin, and pectinate fringe as on preceding segment (Figs 19A–B, 20D–E, 21G, I).

Table 16. Summary of nature and location of sensory spots, glandular cell outlets, tubes, and spines arranged by series in *Echinoderes antarcticus* sp. nov.

Segment	Position									
	MD	PD	SD	LD	ML	SL	LA	LV	VL	VM
1	gco1	–	ss	ss	–	–	–	gco1	–	ss
2	gco1,ss	–	tu	–	ss	tu	–	–	tu	gco1,ss
3	gco1	–	ss	–	–	ss	–	–	–	gco1
4	ac	gco1	–	–	–	–	–	–	–	gco1
5	gco1	–	ss	–	–	ss	–	tu	–	gco1,ss
6	ac	gco1,ss	–	–	–	ss	–	ac	–	gco1,ss
7	gco1	ss	–	–	–	ss	–	ac	–	gco1,ss
8	ac	gco1,ss	–	–	–	tu	–	ac	–	gco1
9	–	gco1,ss	ss	ss	–	–	si	ac	ss	gco1
10	gco1,gco1	–	ss	tu	–	–	–	–	ss	gco1
11	–	–	–	–	–	–	ltas(♀)	lts	–	–

Segment 8. With spines in middorsal and lateroventral positions, and tubes in sublateral positions. Sensory spots present in paradorsal positions only, and glandular cell outlets type 1 in paradorsal and ventromedial positions. Cuticular hairs, posterior segment margin, and pectinate fringe as on preceding segment (Figs 19A–B, 20F–H, 21I).

Segment 9. With spines in lateroventral positions. Sensory spots present in paradorsal, subdorsal, laterodorsal, and ventrolateral positions. Glandular cell outlets type 1 present in paradorsal and ventromedial positions. Small rounded sieve plates present in lateral accessory positions. Cuticular hairs as on preceding segment, but with midlateral hairless areas in more laterodorsal positions and dorsal area of hair-like extensions even broader, extending into the subdorsal areas. Posterior segment margin and pectinate fringe as on preceding segment (Figs 19A–B, 20J–K, 21H).

Segment 10. With short laterodorsal tubes of females attaching at the posterior segment margin. Potential sexual dimorphism in length of these laterodorsal tubes unknown. Sensory spots present in subdorsal and ventrolateral positions. Glandular cell outlet type 1 present as two longitudinally arranged outlets in middorsal position, and in ventromedial positions. Cuticular hairs in three rows and only present from laterodorsal to ventromedial areas; middorsal to subdorsal areas with patch of short, hair-like extensions. The posterior segment margin of the tergal plate is straight, whereas sternal plate margins are deeply concave; all fringe tips along the margins are narrow and slender (Figs 19A–B, 20J–K, 21H, J).

Segment 11. Consisting of two tergal and two sternal plates. Lateral terminal and lateral terminal accessory (the latter assumed female dimorphic) spines present. Sensory spots not observed. The segment is devoid of cuticular hairs, but has a dense covering of minute cuticular hair-like structures, only interrupted by smooth areas laterodorsally and lateroventral to ventromedially. Tergal extensions are triangular, and sternal extensions rounded, with deeply fringed margins (Figs 19A–B, 20I–K, 21H, J).
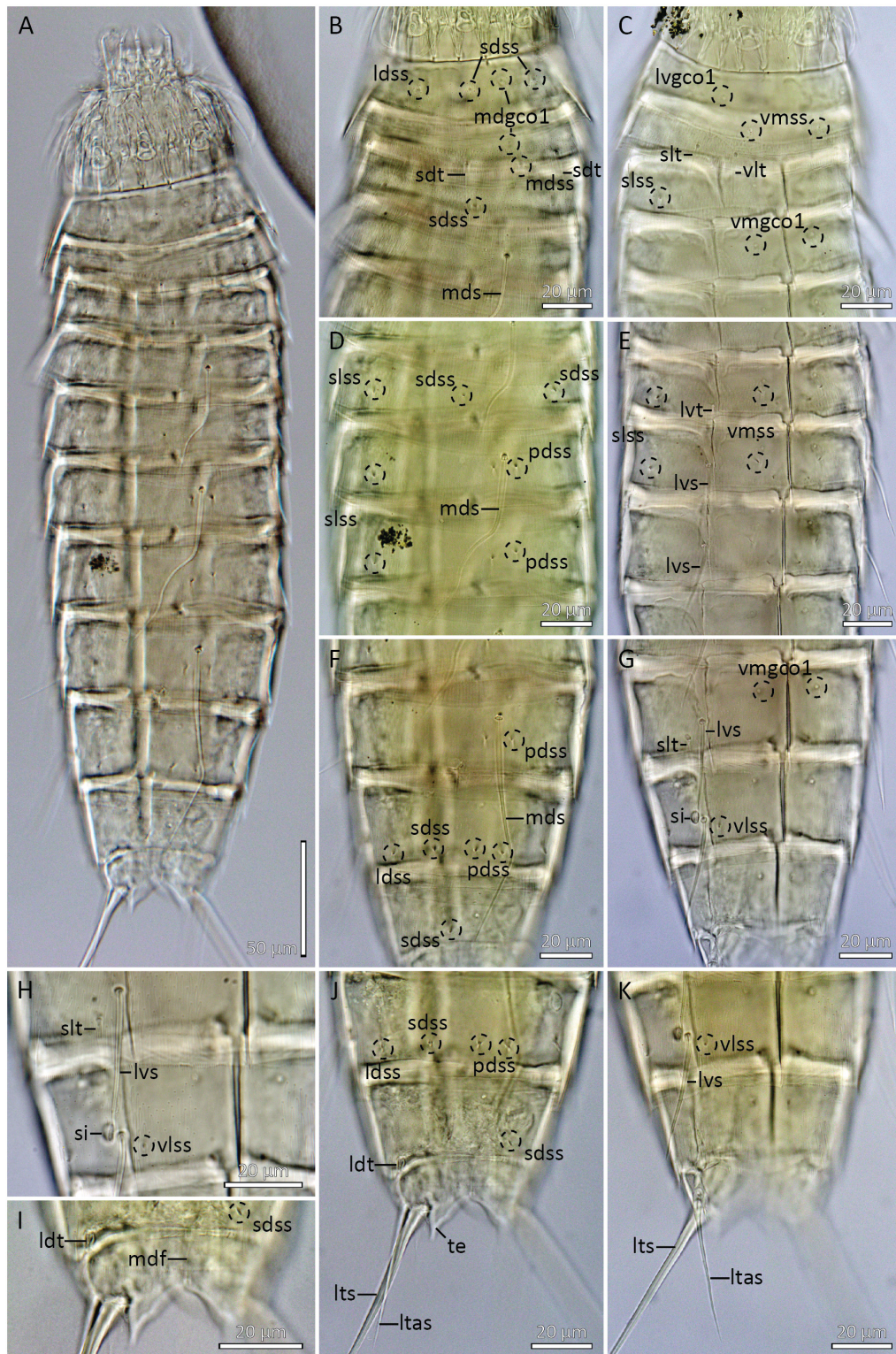
Distribution

Antarctic Peninsula: Gerlache Strait and Andvord Bay OBA, 567 to 694 m b.s.l. See Fig. 1 for geographic overview of stations and Table 1 for station and specimen information.
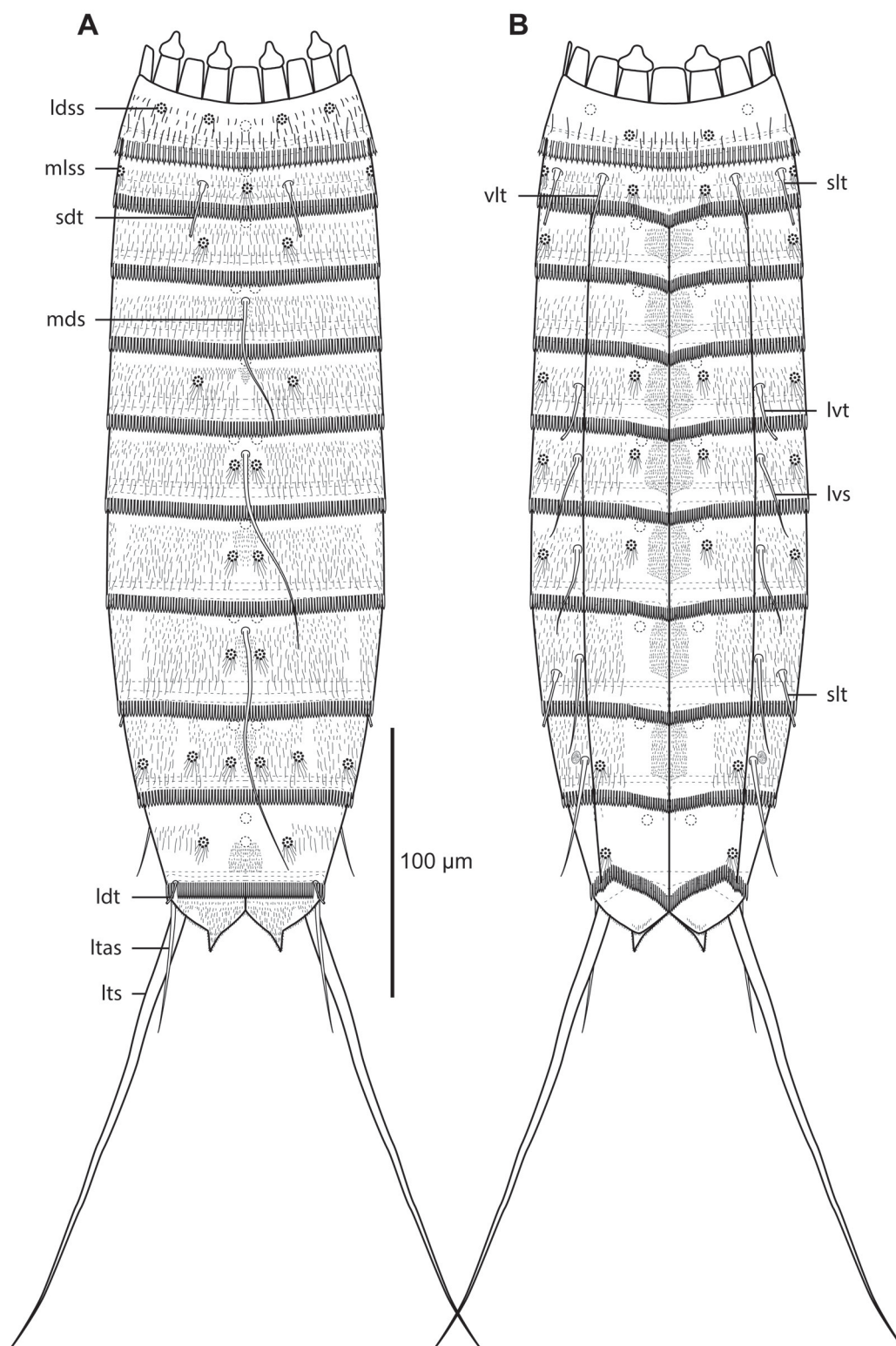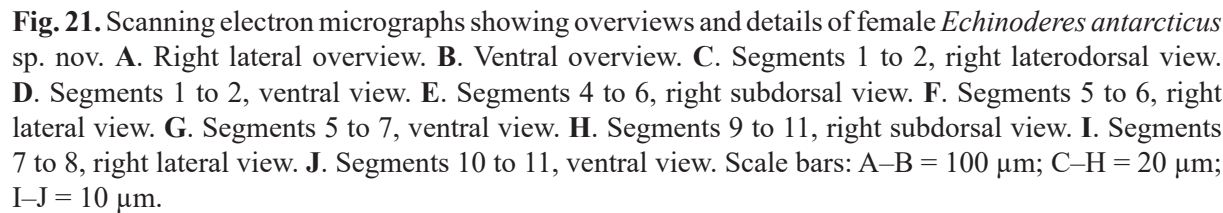
Fig. 19. Line art illustrations of *Echinoderes antarcticus* sp. nov. **A**. Female, dorsal view. **B**. Female, ventral view.

Fig. 20. Light micrographs showing overviews and details of *Echinoderes antarcticus* sp. nov., female, holotype (NHMD 1786932). **A**. Dorsal overview. **B**. Segments 1 to 4, dorsal view. **C**. Segments 1 to 4, ventral view. **D**. Segments 5 to 7, dorsal view. **E**. Segments 5 to 7, ventral view. **F**. Segments 8 to 10, dorsal view. **G**. Segments 8 to 10, ventral view. **H**. Detail showing lateroventral positions on segments 8 to 9. **I**. Segments 10 (posterior part) to 11, dorsal view. **J**. Segments 9 to 11, dorsal view. **K**. Segments 9 to 11, ventral view. Scale bars: A = 50 μm; B–K = 20 μm.

Fig. 21. Scanning electron micrographs showing overviews and details of female *Echinoderes antarcticus* sp. nov. **A**. Right lateral overview. **B**. Ventral overview. **C**. Segments 1 to 2, right laterodorsal view. **D**. Segments 1 to 2, ventral view. **E**. Segments 4 to 6, right subdorsal view. **F**. Segments 5 to 6, right lateral view. **G**. Segments 5 to 7, ventral view. **H**. Segments 9 to 11, right subdorsal view. **I**. Segments 7 to 8, right lateral view. **J**. Segments 10 to 11, ventral view. Scale bars: A–B = 100 µm; C–H = 20 µm; I–J = 10 µm.

Diagnostic remarks

The new species can easily be assigned to *Echinoderes* based on the composition of its trunk segments. The middorsal fissure that divides the tergal plate of segment 11 into two halves is not common in the genus, but it does occur in various species, such as *E. beringiensis*, *E. cernunnos* Sørensen *et al.*, 2012, *E. drogoni* Grzelak & Sørensen, 2018, *E. galadrielae* Grzelak & Sørensen, 2022, the recently described species *E. quasae* Herranz *et al.*, 2024 (Sørensen *et al.* 2012; Grzelak & Sørensen 2018, 2022; Adrianov & Maiorova 2022; Herranz *et al.* 2024), and in *E. angustus* as discussed below under *Echinoderes* aff. *angustus*. Besides the divided tergal plate, the four species do not share any particular similarities.

The character that most easily distinguishes the new species is the configuration of tubes on segment 2. Tubes on segment 2 are quite common among species of *Echinoderes*, but the presence of tubes in subdorsal, sublateral, and ventrolateral positions, and not in laterodorsal positions as well, is only shared between six species (Yamasaki *et al.* 2020b). Among these, just four species have middorsal spines on segments 4, 6 and 8 only. The four species in question are *E. belenae*, *E. hispanicus*, *E. peterseni* Higgins & Kristensen, 1988, and *E. xiphophorus* Adrianov & Maiorova, 2021. Among these species, *E. belenae* differs the most, with its short and stout lateral terminal spines and numerous tubes distributed over most trunk segments (Pardos *et al.* 2016b). Also *E. hispanicus* is easily distinguished from the new species by having both sublateral and lateral accessory tubes on segment 8 (Pardos *et al.* 1998) and *E. xiphophorus* by its long and slender tergal extensions (Adrianov & Maiorova 2021).

Interestingly, the species showing the closest resemblance to *E. antarcticus* sp. nov. is the Arctic species *E. peterseni*, known from West Greenland, NE Canada, and Svalbard (Higgins & Kristensen 1988; Sørensen & Kristensen 2000; Grzelak & Sørensen 2018). The two antipodean species basically share the same spine/tube distribution patterns, with the tube positions on segment 8 as the only minor difference. In *E. antarcticus*, the tubes are sublateral, whereas they are lateral accessory in *E. peterseni*, but this in itself is not sufficient to distinguish the two species. The easiest way to tell the species apart is morphometrically, where *E. antarcticus* generally is larger than *E. peterseni*. The trunk lengths of the two *E. antarcticus* types are 318 µm and 377 µm, whereas trunk lengths of *E. peterseni*, as reported by Higgins & Kristensen (1988), range between 250 µm and 325 µm. Likewise, the middorsal spines are longer in *E. antarcticus*, i.e., on segment 4: 48–55 µm vs 30–44 µm; on segment 6: 78–79 µm vs 45–60 µm; on segment 8: 92–105 µm vs 60–70 µm. Regarding cuticular structures, the sensory spot distribution patterns differ slightly between the two species, i.e., *E. antarcticus* has paradorsal sensory spots on segment 7, whereas these sensory spots in *E. peterseni* clearly sit in subdorsal positions (see Grzelak & Sørensen 2018: fig. 18f). Furthermore, *E. antarcticus* has three pairs of tergal sensory spots on segment 9, in paradorsal, subdorsal, and laterodorsal positions, whereas *E. peterseni* has only two pairs, in paradorsal and laterodorsal positions. Finally, the cuticular hair covering is generally denser in *E. antarcticus*, typically with hairs in seven to eight rows, as opposed to only five rows in *E. peterseni*, and the latter species also lacks patches of hair-like extensions in middorsal and paraventral positions, instead having regular bracteate hairs.

Thus, with help from these relatively subtle characters, it is possible to distinguish the two species. It is, however, still striking to observe two species with an antipodean distribution being so similar and putatively closely related. This clearly suggests that kinorhynch relationships are not always reflected in their biogeography.

The distribution of glandular cell outlets type 1 in *E. antarcticus* sp. nov. follows the MD Seg. 1–3, 5, 7, PD 4, 6, 8–9 pattern, as is the case with the all congeners described above.

***Echinoderes crux* sp. nov.**
urn:lsid:zoobank.org:act:7F3ECD36-A974-404A-9476-D1A3435F29D3
Figs 22–24, Tables 17–18

Diagnosis

Echinoderes with acicular spines in middorsal position on segments 4, 6, and 8, and in lateroventral positions on segments 6 to 9. Tubes present in lateroventral positions on segment 5. Minute slit-like openings (glandular cell outlets type 2?) present near the anterior margin of segment 1 in subdorsal (two pairs), laterodorsal, sublateral, and ventromedial positions. Numerous glandular cell outlets type 2 are present throughout segments 2 to 9: paradorsal positions on segment 3; subdorsal positions on segments 2 to 9 (two pairs on segments 2 and 9); laterodorsal positions on segments 2 to 9 (two pairs on segment 2); sublateral positions on segments 2 to 3 and 5 to 9 (two pairs on segments 2 and 8); lateral accessory positions on segments 3 and 5 to 7; lateroventral positions on segment 4; and ventrolateral positions on segment 2. Dorsal glandular cell outlets type 1 are present at least in middorsal positions on segments 1, 3, 5, 7, and 10, and in paradorsal positions on segments 4, 6, 8, and 9. Female papillae not present; male morphology unknown. Sieve plates present on segment 9 in lateral accessory positions.

Etymology

The species is named '*crux*', after the constellation Crux, also known as the Southern Cross.

Material examined

Holotype
ANTARCTICA • ♀ (mounted for SEM); Antarctic Peninsula, CRS 1760; 64°47.86′ S, 65°21.09′ W; 593 m b.s.l.; 21 Dec. 2015; FjordEco1; soft sediment; NHMD 1790632.

Paratype
ANTARCTICA • 1 ♀ (mounted for SEM); same data as for holotype; NHMD 1790633.

Description

General. Adults with head, neck and eleven trunk segments (Figs 22A–B, 23A–C). The species is characterised by numerous series of minute glandular cell outlets type 2. An overview of measurements and dimensions estimated from SEM is given in Table 17. Distributions of cuticular structures, i.e., sensory spots, glandular cell outlets, spines, and tubes, are summarized in Table 18.

Head. The two available specimens both had their heads fully retracted; thus, information on head morphology is not available.

Neck. Consists of 16 placids. Midventral placid broadest, 9 µm in width and 10 µm in length, whereas all others are narrower, measuring 6 µm in width at their bases. The trichoscalid plates are well-developed and hat-shaped.

Segment 1. Consists of a complete cuticular ring. Sensory spots are present in subdorsal and laterodorsal positions; the sensory spots are large, rounded, with numerous micropapillae around two pores; seven to eight long cuticular hairs emerge from the margin of the micropapillary area. 'Slit-like openings' are located near the anterior segment margin in subdorsal (two pairs), laterodorsal, sublateral and ventromedial positions; the openings are perfectly round rather than slit-like, but the term 'slit-like openings' is chosen to stress their clear homology with the corresponding structures in *Echinoderes aragorni* Grzelak & Sørensen, 2022. Glandular cell outlets type 1 are present in middorsal and lateroventral positions. Besides the cuticular hairs around the margins of the sensory spots, the segment is completely devoid of hairs. The posterior segment margin is straight along the dorsal and lateral

sides, but has a broadly rounded ventral extension. The fringe tips are long and have a broader basis that narrows abruptly into a slender distal tip (Figs 22A–B, 23D–F).

Segment 2. Consists of a complete cuticular ring. Glandular cell outlets type 2 are present in subdorsal (two pairs), laterodorsal (two pairs), sublateral (two pairs), and ventrolateral (one pair) positions; the outlets, on this and following segments, are minute (>1 μm in diameter) and have a collar of fringes projecting from the openings. Sensory spots present in middorsal, laterodorsal, and ventromedial positions; the micropapillary areas around the sensory spots on this, and all following segments, are rounded, and longer micropapillae extend from the posterior part of the papillated areas. Glandular cell outlets type 1 are present in ventromedial positions; the most anterior part of the middorsal line could not be examined in any of the specimens; thus, type 1 outlets could potentially be present there as well. Bracteate cuticular hairs are arranged in three transverse rows; hairs in the first anterior row are short, whereas those of the more posterior rows are fairly long. The posterior segment margin is almost straight. Pectinate fringe with well-developed, long, triangular fringe tips along all margins (Figs 22A–B, 23D–F).

Segment 3. As following seven segments, consisting of one tergal and two sternal plates. Glandular cell outlets type 2 are present in paradorsal, subdorsal, laterodorsal, sublateral, and lateral accessory positions. Sensory spots are present in subdorsal and sublateral positions, and glandular cell outlets type 1 in middorsal and ventromedial positions. The hair covering of the tergal and lateral halves of sternal plates is dense on the anterior half of the segment, except in hair-less midlateral areas, with bracteate cuticular hairs as on preceding segment. Paraventral areas without bracteate hairs, but with shield-shaped patch of well-developed hair-like extensions. Posterior segment margin straight and pectinate fringe as on preceding segment (Figs 22A–B, 23G–I).

Segment 4. With spine in middorsal position. Glandular cell outlets type 2 are present in subdorsal, laterodorsal, and lateroventral positions. Sensory spots are not present. Glandular cell outlets type 1 are present in paradorsal and ventromedial positions. Cuticular hairs, posterior segment margin, and pectinate fringe as on preceding segment (Figs 22A–B, 23G–I).

Segment 5. With tubes in lateroventral positions. Glandular cell outlets type 2 are present in subdorsal, laterodorsal, sublateral, and lateral accessory positions. Sensory spots present in subdorsal, sublateral, and ventromedial positions, and glandular cell outlets type 1 in middorsal and ventromedial positions. Cuticular hairs, posterior segment margin, and pectinate fringe as on preceding segment (Figs 22A–B, 24A–C).

Segment 6. With spines in middorsal and lateroventral positions. Glandular cell outlets type 2 as on preceding segment. Sensory spots present in paradorsal, sublateral, and ventromedial positions, and glandular cell outlets type 1 in paradorsal and ventromedial positions. Cuticular hairs as on preceding segment, but arranged in additional rows; middorsal area without hairs. Posterior segment margin and pectinate fringe as on preceding segment (Figs 22A–B, 24A–C).

Segment 7. With spines in lateroventral positions. Glandular cell outlets type 2 and sensory spots as on preceding segment. Glandular cell outlets type 1 present in middorsal and ventromedial positions. Cuticular hairs as on proceeding segment, but with middorsal hairless areas now also reaching the paradorsal positions. Posterior segment margin and pectinate fringe as on preceding segment (Figs 22A–B, 24D–F).

Segment 8. With spines in middorsal and lateroventral positions. Glandular cell outlets type 2 are present in subdorsal, laterodorsal, and sublateral (two pairs) positions. Sensory spots present in paradorsal positions only, and glandular cell outlets type 1 in paradorsal and ventromedial positions. Cuticular

Table 17. Measurements estimated from scanning electron microscopy of *Echinoderes crux* sp. nov. (in μm).

Character	NHMD-1790632 Holotype (♀)	NHMD-1790633 Paratype (♀)
TL	198	209
TL (CUM)	253	271
MSW-6	39	37
MSW-6/TL	19.7%	17.7%
SW-10	32	33
SW-10/TL	16.6%	15.8%
–		
S1	23	22
S2	15	14
S3	16	17
S4	18	21
S5	19	25
S6	24	29
S7	28	31
S8	28	31
S9	30	30
S10	30	30
S11	22	21
–		
MD4 (ac)	33	41
MD6 (ac)	52	70
MD8 (ac)	75	71
–		
LV5 (tu)	7	7
LV6 (ac)	24	23
LV7 (ac)	27	29
LV8 (ac)	33	31
LV9 (ac)	40	39
–		
LTS	82	99
LTS/TL	41.4%	47.4%
LTAS	27	38

hairs as on preceding segment, but hairless dorsal area also reaches into the subdorsal positions and has a covering of hair-like extensions. Posterior segment margin and pectinate fringe as on preceding segment (Figs 22A–B, 24F–H).

Segment 9. With spines in lateroventral positions. Glandular cell outlets type 2 are present in subdorsal (two pairs), laterodorsal, and sublateral positions. Sensory spots present in paradorsal, subdorsal, laterodorsal, and ventrolateral positions. Glandular cell outlets type 1 present in paradorsal and ventromedial positions. Very minute sieve plates present in lateral accessory positions, at base of spine. Cuticular hairs as on preceding segment, but with midlateral hairless areas in more laterodorsal positions and dorsal area of hair-like extensions even broader, extending well into the subdorsal areas. Posterior segment margin and pectinate fringe as on preceding segment (Figs 22A–B, 24I–L).

Segment 10. Without spines, tubes, or glandular cell outlets type 2. Male morphology, and thus potential presence of tubes, is so far unknown. Sensory spots present in subdorsal and ventrolateral positions. Glandular cell outlet type 1 present as a single outlet in middorsal position and as a pair in

Table 18. Summary of nature and location of sensory spots, glandular cell outlets, tubes, and spines arranged by series in *Echinoderes crux* sp. nov.

Segment	MD	PD	SD	LD	SL	LA	LV	VL	VM
					Position				
1	gco1	–	so,ss,so	so,ss	so	–	gco1	–	so
2	ss	–	gco2,gco2	gco2,gco2,ss	gco2,gco2	–	–	gco2	gco1,ss
3	gco1	gco2	ss,gco2	gco2	gco2,ss	gco2	–	–	gco1
4	ac	gco1	gco2	gco2	–	–	gco2	–	gco1
5	gco1	–	gco2,ss	gco2	ss,gco2	gco2	tu	–	gco1,ss
6	ac	gco1,ss	gco2	gco2	ss,gco2	gco2	ac	–	gco1,ss
7	gco1	ss	gco2	gco2	ss,gco2	gco2	ac	–	gco1,ss
8	ac	gco1,ss	gco2	gco2	gco2,gco2	–	ac	–	gco1
9	–	gco1,ss	gco2,ss,gco2	gco2,ss	gco2	si	ac	ss	gco1
10	gco1	–	ss	–	–	–	–	ss	gco1
11	–	–	–	–	–	ltas(♀)	lts	–	ss

ventromedial positions. Cuticular hairs in three rows and only present from laterodorsal to ventromedial areas; middorsal to subdorsal areas with patch of short, hair-like extensions between the sensory spots and as a distinct, oblique row below the laterodorsal cuticular hairs; paralateral areas without any kind of hairs or hair-like extensions. The posterior segment margin of the tergal plate is straight, whereas sternal plate margins are deeply concave; all fringe tips along the margins are narrow and slender (Figs 22A–B, 24L–O).

SEGMENT 11. With lateral terminal- and lateral terminal accessory (assumed female dimorphic) spines. Sensory spots present in ventromedial positions, at margins of sternal extensions. The segment is devoid of cuticular hairs, but has a dense covering of minute cuticular hair-like structures on tergal and sternal extensions. Tergal extensions are triangular and sternal extensions rounded, with fringed margins (Figs 22A–B, 24M–O).

Distribution

Antarctic Peninsula: Open continental shelf off the Antarctic Peninsula, 596 m b.s.l. See Fig. 1 for geographic overview of stations and Table 1 for station and specimen information.

Diagnostic remarks

We would usually hesitate to describe a species based only on SEM specimens. First of all, the SEM specimens deteriorate much faster than specimens mounted for LM, which shortens the available time span for re-examining the type material. Second, certain internal or intracuticular structures, such as pachycycli are difficult to visualise with SEM. However, we still chose to describe *E. crux* sp. nov. because of its very distinct morphology and clear phylogenetic affinities within the genus.

The most distinct character trait in *E. crux* sp. nov. is the numerous series of minute glandular cell outlets type 2, which sums up to 35 pairs in total. Such a morphology is only shared with a single congener, *E. aragorni*. Males of *E. aragorni* also have exactly 35 pairs of glandular cell outlets type 2, whereas the females have 34 (Grzelak & Sørensen 2022). Besides the type 2 outlets on segments 2 to 9, they also share the presence of openings near the anterior margin of segment 1. In *E. aragorni* these openings are elongate, which is why Grzelak & Sørensen (2022) referred to them as 'slit-like openings'. In *E. crux* the openings are perfectly round, but for the sake of terminological consistency, and in order to stress the homology between the structures in the two species, we also choose to refer to them as slit-like openings in *E. crux*. Grzelak & Sørensen (2022) discussed whether the openings on segment 1 should also be
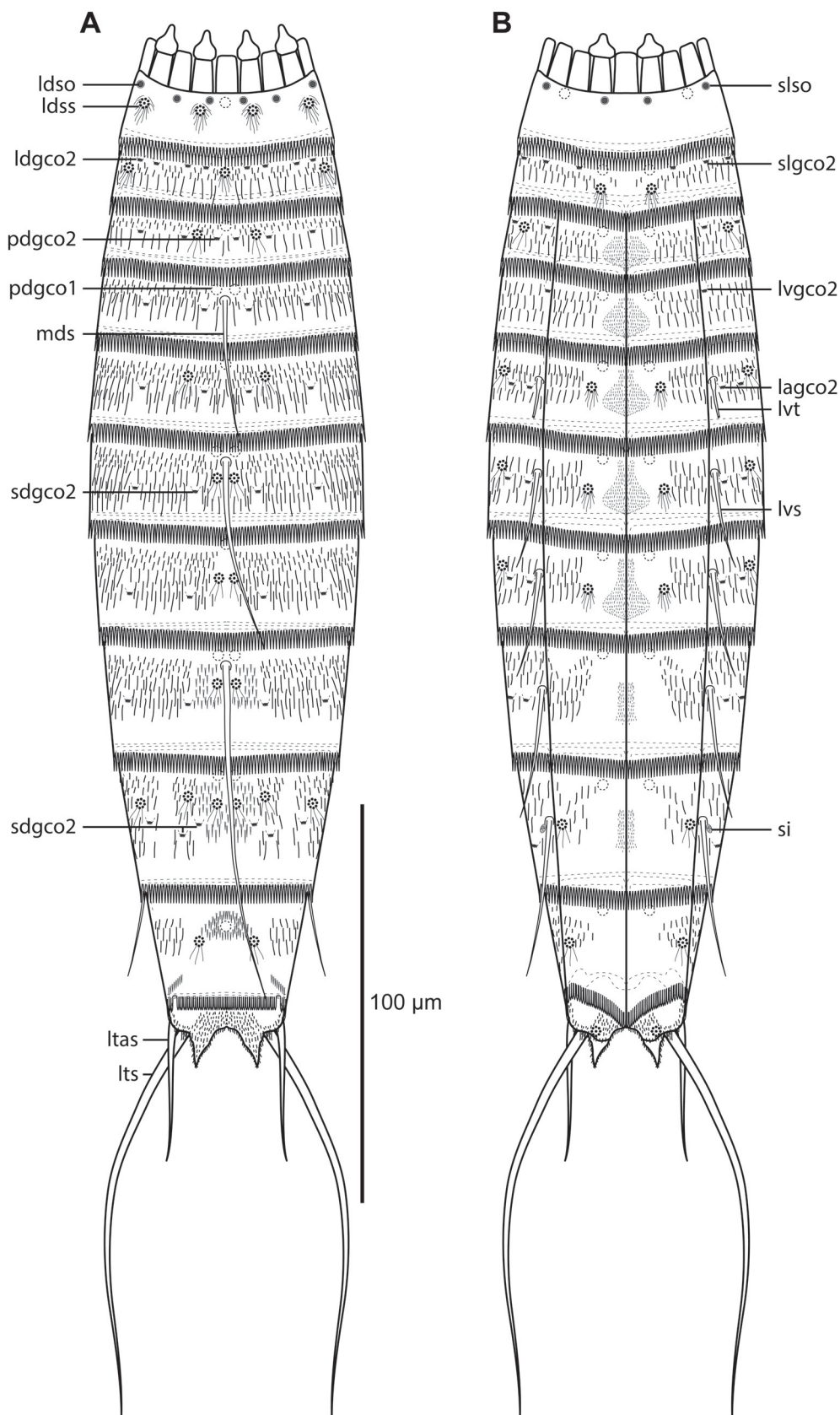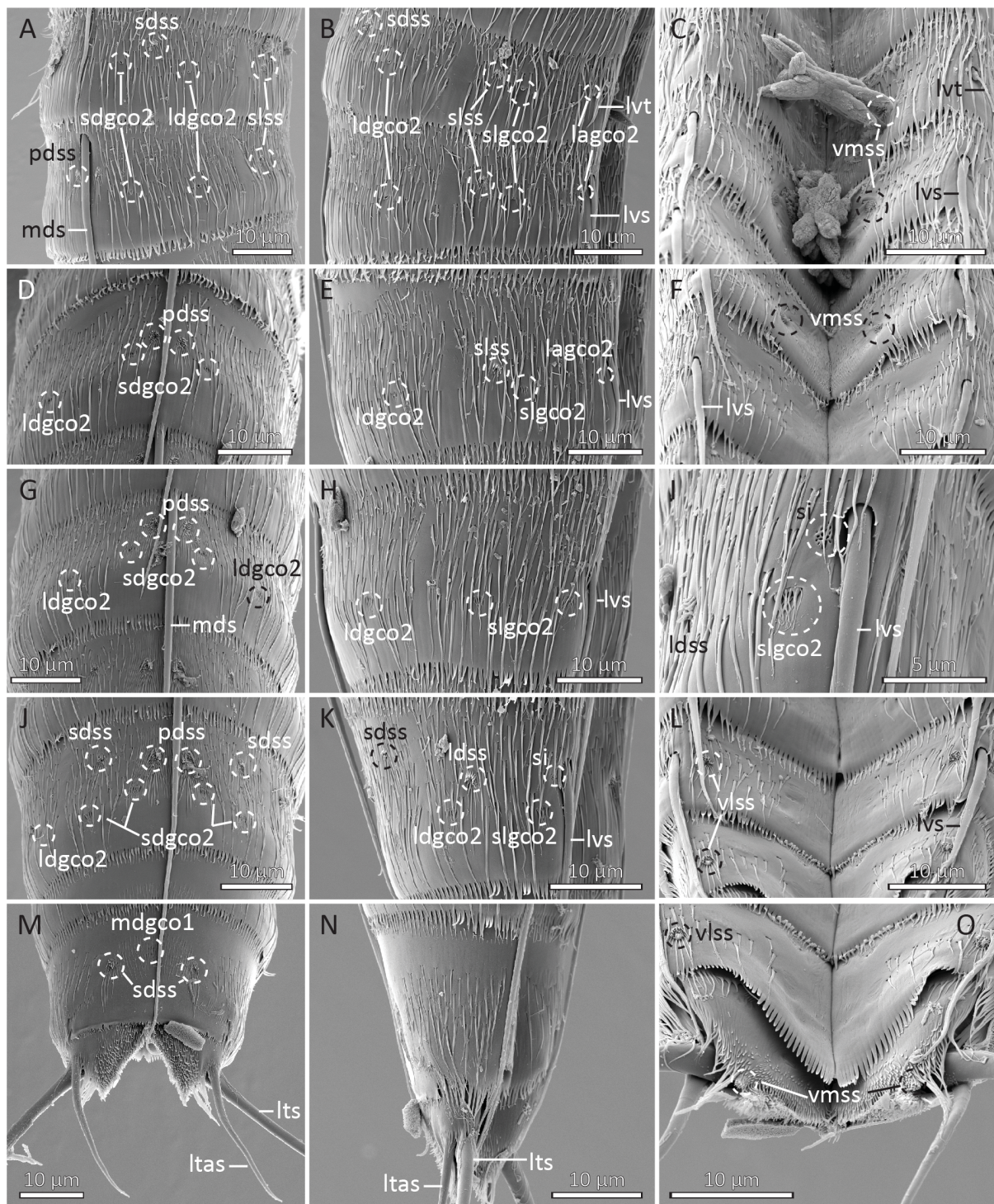
Fig. 22. Line art illustrations of *Echinoderes crux* sp. nov. **A**. Female, dorsal view. **B**. Female, ventral view.

Fig. 23. Scanning electron micrographs showing overviews and details of anterior segments in female *Echinoderes crux* sp. nov. **A**. Female, paratype (NHMD 1790633). **B–I**. Female, holotype (NHMD 1790632). **A**. Dorsal overview. **B**. Right lateral overview. **C**. Lateroventral overview. **D**. Segments 1 to 2, dorsal view. **E**. Segments 1 to 2, right lateral view. **F**. Segments 1 to 2, ventrolateral view. **G**. Segments 3 to 4, dorsal view. **H**. Segments 3 to 4, right lateral view. **I**. Segments 3 to 4, ventral view. Scale bars: A–C = 50 µm; D–I = 10 µm.

Fig. 24. Scanning electron micrographs showing details of posterior segments in female, holotype (NHMD 1790632) of *Echinoderes crux* sp. nov. **A**. Segments 5 to 6, subdorsal view. **B**. Segments 5 to 6, right lateral view. **C**. Segments 5 to 6, ventral view. **D**. Segment 7, dorsal view. **E**. Segment 7, right lateral view. **F**. Segments 7 to 8, ventral view. **G**. Segment 8, dorsal view. **H**. Segment 8, right lateral view. **I**. Close-up showing sublateral to lateroventral details on segment 9. **J**. Segment 9, dorsal view. **K**. Segment 9, right lateral view. **L**. Segments 9 to 10, ventral view. **M**. Segments 10 to 11, dorsal view. **N**. Segments 10 to 11, right lateral view. **O**. Segments 10 to 11, ventral view. Scale bars: A–H, J–O = 10 μm; I = 5 μm.

seen as a variation of glandular cell outlets type 2. It would require a comparative study of histological sections to confirm or reject this suggestion, and suitable material for a study like this is currently not available. However, we find it quite likely that there is a homology between the openings on segment 1, and the type 2 outlets on the following segments.

Thus, based on the presence of these openings on segment 1 and the numerous type 2 outlets on the following eight segments, the close relationship between the two species is undisputable. They are, however, still easily distinguished from each other. The most distinct difference between the two species is the lack of lateroventral spines on segments 6 and 7 in *E. aragorni*. In addition, there are several differences in the distribution of slit-like openings and glandular cell outlets type 2. Besides minor (interpretive) differences in longitudinal positioning, *E. crux* sp. nov. differs from *E. aragorni* by having one additional pair of slit-like openings on segment 1, and by having seven pairs of type 2 outlets on segment 2, unlike the 'only' five pairs in *E. aragorni*. In contrast, *E. aragorni* has four pairs of type 2 outlets on segment 4, whereas *E. crux* only has three. The number and approximate position of type 2 outlets on the remaining segments is the same for the two species and seems to be conserved. Males of *E. aragorni* have an additional pair of type 2 outlets in laterodorsal positions of segment 10, but since no males are yet available for *E. crux*, it is not possible to confirm whether this species shows the same sexual dimorphism.

The mapping of glandular cell outlets type 1 in the dorsal series of *E. crux* sp. nov. is not complete, but besides the uncertain appearance of a middorsal type 1 outlets on segment 2, the observed pattern fits the very common MD Seg. 1–3, 5, 7, PD 4, 6, 8–9 pattern, which is also present in most other species of the present study. The mapping of dorsal type 1 outlets in *E. aragorni* is very incomplete, but it is noteworthy that both *E. aragorni* and *E. crux* have only a single middorsal type 1 outlet on segment 10, unlike the otherwise extremely common presence of two, longitudinally aligned middorsal outlets.

Species with uncertain identities

***Echinoderes* aff. *angustus* Higgins & Kristensen, 1988**
Figs 25–26, Tables 19–20

Material examined
ANTARCTICA – **Antarctic Peninsula** • 1 ♂ (mounted for LM in Fluoromount G on HS slide); CRS 1698; 64°51.60′ S, 62°33.80′ W; 541 m b.s.l.; 28 Nov. 2015; FjordEco1; soft sediment; NHMD 1790691 • 1 ♀ (mounted for SEM); CRS 1702; 64°51.15′ S, 62°34.44′ W; 502 m b.s.l.; 30 Nov. 2015; FjordEco1; soft sediment; MVS • 1 ♂ (mounted for SEM); CRS 1773; 64°52.35′ S, 62°25.88′ W; 553 m b.s.l.; 6 Apr. 2016; FjordEco2; soft sediment; MVS • 1 ♂ (mounted for SEM); CRS 1776; 64°52.53′ S, 62°33.90′ W; 551 m b.s.l.; 7 Apr. 2016; FjordEco2; soft sediment; MVS • 1 ♀ (mounted for LM in Fluoromount G on HS slide); CRS 1792; 64°51.40′ S, 62°34.01′ W; 525 m b.s.l.; 11 Apr. 2016; FjordEco2; soft sediment; NHMD 1790692 • 1 ♂, 1 ♀ (mounted for SEM); CRS 1793; 64°39.53′ S, 62°55.03′ W; 701 m b.s.l.; 11 Apr. 2016; FjordEco2; soft sediment; MVS • 1 ♂ (mounted for LM in Fluoromount G on HS slide); CRS 1809; 64°39.59′ S, 62°55.09′ W; 694 m b.s.l.; 15 Apr. 2016; FjordEco2; soft sediment; NHMD 1790693 • 2 ♂♂ (mounted for SEM); CRS 1809; 64°39.59′ S, 62°55.09′ W; 694 m b.s.l.; 15 Apr. 2016; FjordEco2; soft sediment; MVS.

Concise description
Except when clearly specified, the following concise description applies to both the Antarctic population of *Echinoderes* aff. *angustus* and to the Arctic type material, as well as supplementary specimens of *E. angustus* mounted for SEM.

General. An overview of measurements and dimensions is given in Table 19. Distributions of cuticular structures, i.e., sensory spots, glandular cell outlets, spines and tubes, are summarized in Table 20.

Segment 1. Consists of a complete cuticular ring. Sensory spots are present in subdorsal, laterodorsal, and ventromedial positions; sensory spots are minute, and consist of relatively few, very short micropapillae arranged around two pores. Glandular cell outlets type 1 are present in middorsal and lateroventral positions. Cuticular hairs are arranged in three to four rows: anterior two to three rows are present only on the dorsal side, between midlateral positions, whereas the posteriormost row extends around the entire segment. The posterior segment margin is straight and terminates in a pectinate fringe with broad and well-developed slender fringe tips; fringe tips on ventral side are slightly longer than those on the lateral and dorsal sides (Figs 25A–D, 26A–C).

Segment 2. Consists of a complete cuticular ring. However, a partially developed, midventral fissure is visible in the Arctic type specimens of *E. angustus* (Fig. 25F). Indications of such a fissure were never observed in any of the Antarctic specimens (Fig. 25E). Glandular cell outlets type 2 are present in subdorsal, laterodorsal, sublateral, and ventrolateral positions. Sensory spots are present in middorsal, laterodorsal, midlateral, and ventromedial positions; the micropapillary areas around the sensory spots on this, and all following segments, are even smaller than those on segment 1 and form a slightly oval ring around a single pore; one or two long and rigid hairs (extremely extended micropapillae?) stick out from the micropapillary area. Glandular cell outlets type 1 are present in middorsal and ventromedial positions. Fairly long bracteate cuticular hairs are arranged in three to four transverse rows on the dorsal and lateral sides; ventromedial and paraventral areas without hairs. The posterior segment margin is straight, terminating in uniform, well-developed fringe tips (Figs 25A–F, 26A–C).

Segment 3. As following seven segments, consisting of one tergal and two sternal plates. Sensory spots are present in subdorsal and sublateral positions, and glandular cell outlets type 1 in middorsal and ventromedial positions. Cuticular hairs present in four rows on the tergal and lateral halves of the sternal plates, except in hair-less midlateral areas; paraventral areas and most ventral parts of ventromedial areas completely free of hairs and hair-like structures. Posterior segment margin straight and pectinate fringe as on preceding segment (Figs 25A–B, 26A–B, D).

Segment 4. With spine in middorsal position. Glandular cell outlets type 2 are present in subdorsal positions. Sensory spots are not present. Glandular cell outlets type 1 are present in paradorsal and ventromedial positions. Cuticular hairs as on preceding segment, but now arranged in five rows. Posterior segment margin and pectinate fringe as on preceding segment (Figs 25A–B, 26A–B, D).

Segment 5. With spine in middorsal position and tubes in lateroventral positions. Glandular cell outlets type 2 are present in midlateral positions. Sensory spots present in subdorsal and ventromedial positions, and glandular cell outlets type 1 in paradorsal and ventromedial positions. Cuticular hairs, posterior segment margin, and pectinate fringe as on preceding segment (Figs 25G–L, 26E–G).

Segment 6. With spines in middorsal and lateroventral positions. Sensory spots present in paradorsal, subdorsal, midlateral, and ventromedial positions; ventromedial sensory spots situated closer to midventral articulation than those on preceding segment. Glandular cell outlets type 1 present in paradorsal and ventromedial positions. Cuticular hairs, posterior segment margin, and pectinate fringe as on preceding segment (Figs 25G–J, 26E–G).

Segment 7. With spines in middorsal and lateroventral positions. Sensory spots present in paradorsal, midlateral, and ventromedial positions; ventromedial sensory spots situated more lateral than those on preceding segment and aligned with those on segment 5. Glandular cell outlets type 1 present in paradorsal and ventromedial positions. Cuticular hairs, posterior segment margin, and pectinate fringe as on preceding segment (Figs 25G–J, 26E–I).

**Table 19.** Measurements from light microscopy of *Echinoderes* aff. *angustus* Higgins & Kristensen, 1988 (in µm) from the Antarctic Peninsula, including number of measured specimens (*n*) and standard deviation (SD), and comparative measurements of *Echinoderes* aff. *angustus* from the South Orkney Trench (Sánchez *et al.* 2024) and *D. angustus* s. str. from the type locality in Greenland (Higgins & Kristensen 1988).

| Character | | *Echinoderes* **aff.** *angustus* | | | | | *Echinoderes angustus* | | |
| | | Antarctic Peninsula | | | South Orkney Trench | | Greenland | | |
	n	Range	Mean	SD	Range	*n*	Range	Mean	SD
TL	3	310–347	327	18.77	316	22	320–475	376	36.4
TL (CUM)	3	433–454	443	10.60	465	–	–	–	–
MSW-6	3	53–56	54	1.53	55	22	62–77	68	3.2
MSW-6/TL	3	15.6–18.1%	16.7%	1.27%	17%	22	15.1–21.2%	18.2%	1.5%
SW-10	3	41–44	43	1.53	46	22	48–60	53	3.0
SW-10/TL	3	12.7–13.9%	13.1%	0.68%	–	22	12.2–21.2%	14%	1.5%
–									
S1	3	32–33	32	0.58	36	22	33–44	38	2.6
S2	3	30–32	31	1.15	33	22	32–40	36	2.5
S3	3	33–34	33	0.58	38	22	34–42	39	2.2
S4	3	36–37	36	0.58	40	22	35–50	42	3.2
S5	3	41–42	41	0.58	43	22	37–52	45	3.9
S6	3	42–45	44	1.53	46	22	40–58	49	3.7
S7	3	44–47	46	1.73	51	22	48–64	51	5.6
S8	3	48–51	49	1.73	54	22	50–70	56	4.1
S9	3	48–51	49	1.73	51	22	50–60	55	2.4
S10	3	48–51	49	1.73	45	22	44–58	51	3.7
S11	3	30–32	31	1.15	28	22	24–34	29	2.5
–									
MD4 (ac)	3	48–52	50	2.08	52	21	38–58	49	5.7
MD5 (ac)	3	57–68	63	5.57	63	22	42–72	61	8.3
MD6 (ac)	3	67–73	70	3.06	68	21	56–89	71	8.8
MD7 (ac)	3	71–77	74	3.06	77	20	62–94	80	8.3
MD8 (ac)	3	84–88	86	2.08	92	22	74–106	89	8.7
–									
LV5 (tu)	2	12–14	13	1.41	–	15	8–24	16	4.3
LV6 (ac)	3	40–43	42	1.53	38	21	40–50	44	3.7
LV7 (ac)	3	44–51	46	4.04	39	20	41–60	50	4.2
LV8 (ac)	3	48–50	49	1.15	42	21	44–60	53	4.7
LV9 (ac)	3	42–50	46	4.04	36	22	36–56	46	6.2
–									
LTS (♂)	3	197–214	207	8.89	–	11	140–198	174	18.8
LTS (♀)	0	–	–	–	223	11	140–180	172	11.6
LTS/TL	3	60.5–66.3%	63.4%	2.87%	71%	22	29.4–54.6%	46.4%	6.5%
LTAS	0	–	–	–	51	10	48–88	71	10.5

SEGMENT 8. With spines in middorsal and lateroventral positions. Glandular cell outlets type 2 are present in sublateral positions. Sensory spots present in paradorsal positions only, and glandular cell outlets type 1 in paradorsal and ventromedial positions. Cuticular hairs as on preceding segment, but the midlateral hairless areas have moved to more laterodorsal positions, and middorsal to paradorsal positions are also devoid of hairs. Posterior segment margin and pectinate fringe as on preceding segment (Figs 25G–J, M–N, 26G–I).

Table 20. Summary of nature and location of sensory spots, glandular cell outlets, tubes, and spines arranged by series in Antarctic *Echinoderes* aff. *angustus* Higgins & Kristensen, 1988 and Arctic *E. angustus* s. str. Note that the presence of midlateral tubes on segment 11 is only confirmed from the Antarctic *Echinoderes* aff. *angustus*.

Segment	Position									
	MD	PD	SD	LD	ML	SL	LA	LV	VL	VM
1	gco1	–	ss	ss	–	–	–	gco1	–	ss
2	gco1,ss	–	gco2	gco2,ss	ss	gco2	–	–	gco2	gco1,ss
3	gco1	–	ss	–	–	ss	–	–	–	gco1
4	ac	gco1	gco2	–	–	–	–	–	–	gco1
5	ac	gco1	ss	–	gco2	–	–	tu	–	gco1,ss
6	ac	gco1,ss	ss	–	ss	–	–	ac	–	gco1,ss
7	ac	gco1,ss	–	–	ss	–	–	ac	–	gco1,ss
8	ac	gco1,ss	–	–	–	gco2	–	ac	–	gco1
9	–	gco1,ss	ss	–	ss	si	–	ac	ss	gco1
10	gco1,gco1	–	ss	gco2	–	–	–	–	ss	gco1
11	pr	ss	–	–	tu(♂),pex3(♂)	–	ltas(♀)	lts	–	–

SEGMENT 9. With spines in lateroventral positions. Sensory spots present in paradorsal, subdorsal, midlateral, and ventrolateral positions. Glandular cell outlets type 1 present in paradorsal and ventromedial positions. Small rounded sieve plates located in sublateral positions. Cuticular hairs, posterior segment margin, and pectinate fringe as on preceding segment (Figs 25O–P, R–S, 26H–J).

SEGMENT 10. With glandular cell outlets type 2 in laterodorsal positions near posterior segment margin. Sensory spots present in subdorsal and ventrolateral positions. Glandular cell outlets type 1 present as two longitudinally arranged outlets in middorsal position and in ventromedial positions. Cuticular hair covering reduced to a few (4 to 6) hairs in subdorsal positions and otherwise only hairs in laterodorsal to ventromedial areas. The posterior segment margin of the tergal plate is straight, with minute fringe tips. Sternal plate margins oblique, with longer fringe tips in ventromedial and paraventral areas (Figs 25O, Q, R–S, U, 26J–M).

SEGMENT 11. With lateral terminal spines and a middorsal protuberance emerging from the intersegmental zone between segments 10 and 11. The segment appears to consist of two tergal and two sternal plates. The visualisation of the middorsal fissure between the tergal plates easily gets obscured by the overlaying protuberance, but the presence of the fissure was nevertheless confirmed in both Antarctic (Fig. 25T) and Arctic (Fig. 25U) specimens. Females with lateral terminal accessory spines; males with thin, tubular dorsal and ventral penile spines; medial pair of penile spines cone-shaped and well-developed. Males in addition with short tubes inserted near bases of dorsal and medial penile spines; the tubes resemble an extra set of penile spines, but are much shorter, roughly 5 µm estimated from SEM; due to their minute size and the numerous other structures in this area, the tubes are difficult to visualise with LM. The presence of these tubes is only confirmed for the Antarctic specimens. Sensory spots present in paradorsal positions only. The segment is devoid of cuticular hairs, but has scattered hair-like extensions over the tergal extensions. Tergal extensions are elongate triangular, with pointed tips. Sternal extensions short, broadly triangular, and not extending beyond tergal extensions (Figs 25R–U, 26K–M).

Distribution

Antarctic Peninsula: Gerlache Strait and Andvord Bay MBA and IBB, 502 to 701 m b.s.l. See Fig. 1 for geographic overview of stations and Table 1 for station and specimen information. Possibly also South Orkney Trench, 5251 m b.s.l. (see Sánchez *et al.* 2024).
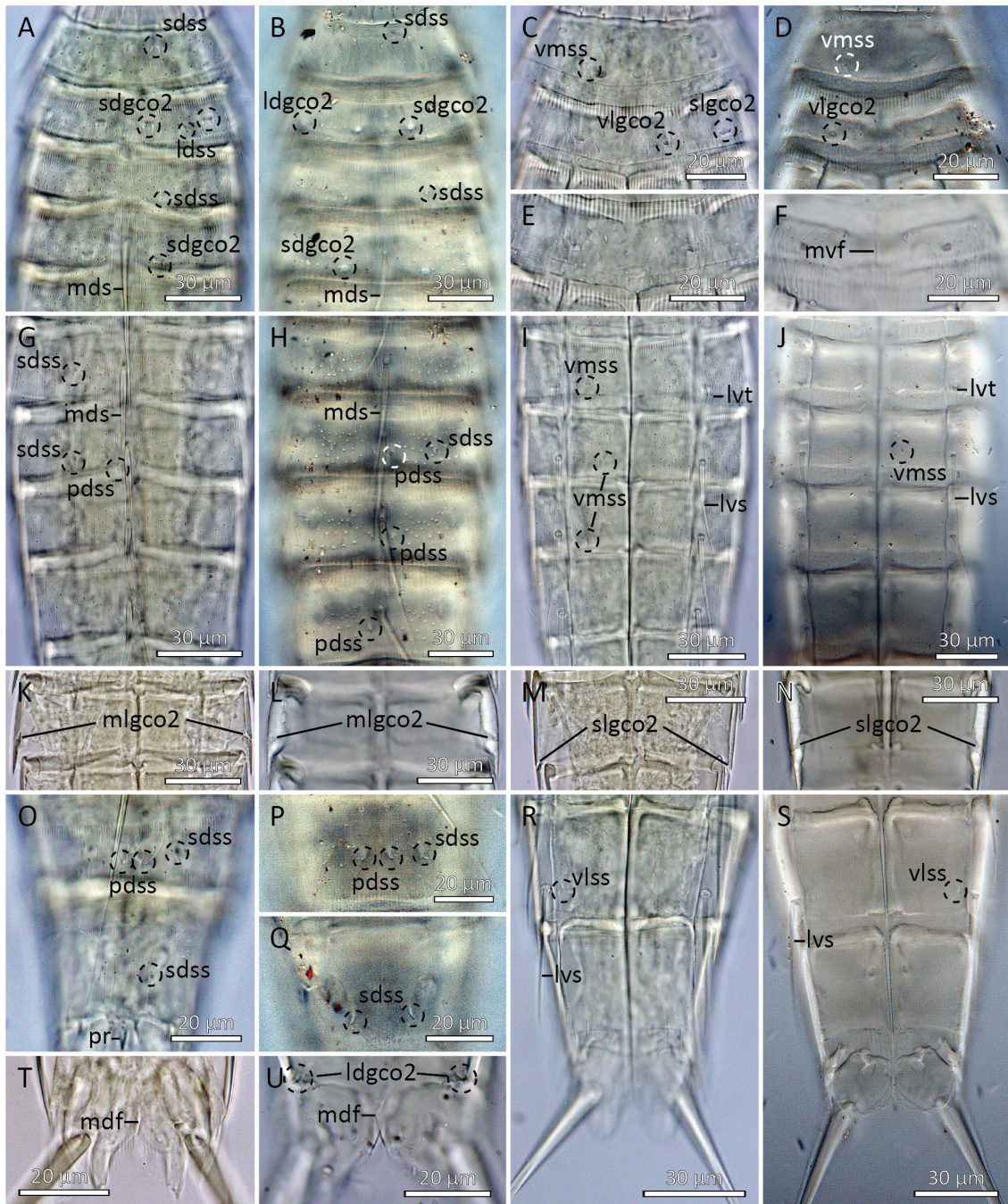
Fig. 25. Comparative light micrographs showing details of *Echinoderes* aff. *angustus* Higgins & Kristensen, 1988 from the Antarctic Peninsula (first and third column from the left) and holo- and paratypes of *E. angustus* (second and fourth column from the left). **A, C, E, G, I, K, M, O, R, T**. Male *Echinoderes* aff. *angustus* (NHMD 1790692). **B, D, H, J, P–Q, S**. Female, holotype of *E. angustus* (USNM 233200). **F, L, N**. Female, paratype of *E. angustus* (NHMD 99369). **U**. Male, paratype of *E. angustus* (NHMD 99368). **A–B**. Segments 1 to 4, dorsal view. **C–D**. Segments 1 to 2, ventral view. **E–F**. Segment 2, ventral view, focused at intracuticular level. **G–H**. Segments 5 to 8, dorsal view. **I–J**. Segments 5 to 8, ventral view. **K–L**. Segment 5, focused at midlateral level. **M–N**. Segment 8, focused at sublateral level. **O**. Segments 9 to 10, dorsal view. **P**. Segment 9, dorsal view. **Q**. Segment 10, dorsal view. **R–S**. Segments 9 to 11, ventral view. **T–U**. Segment 11, focused at midtergal fissure. Scale bars: A–B, G–N, R–S = 30 µm; C–F, O–Q, T–U = 20 µm.
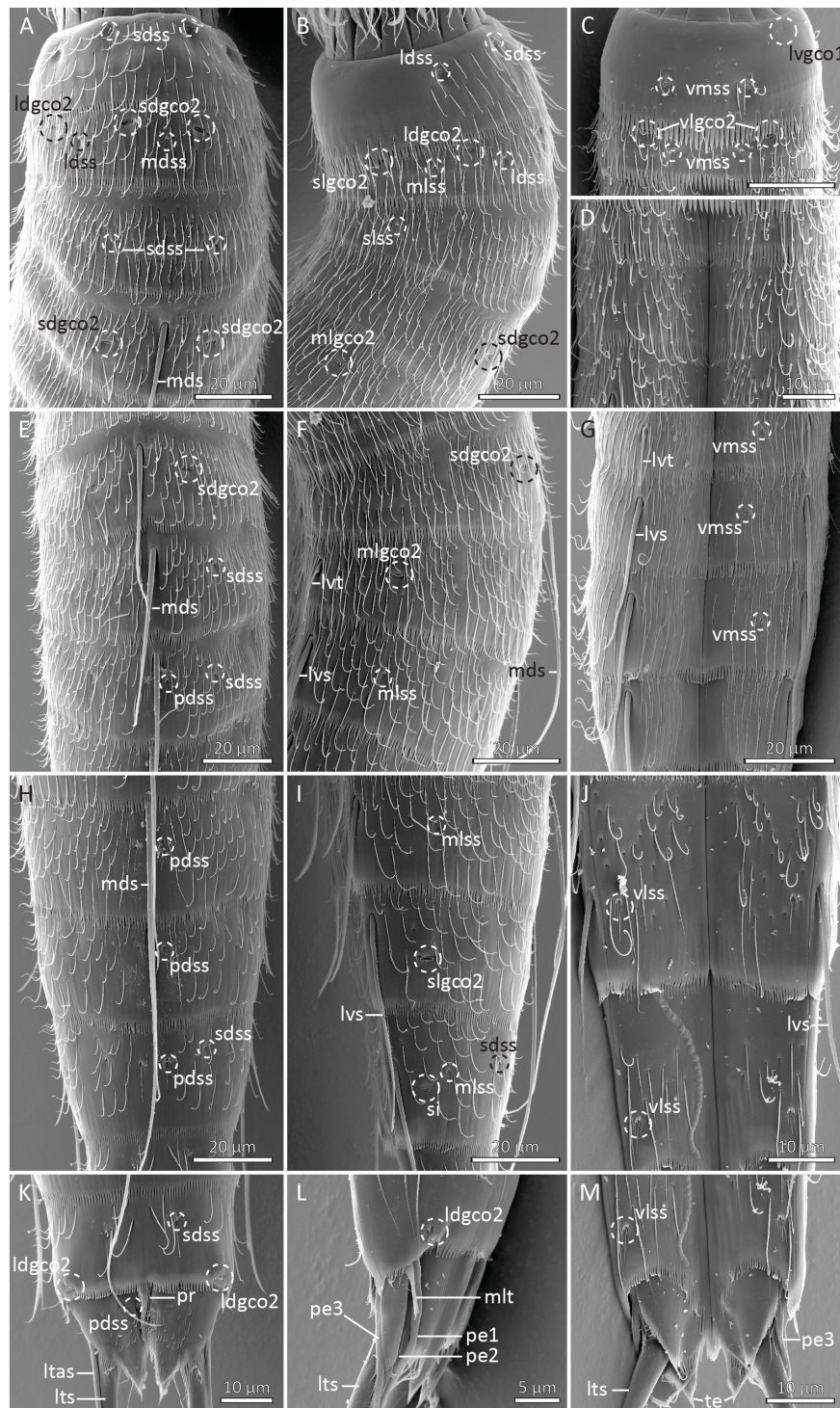
Fig. 26. Scanning electron micrographs showing overviews and details of *Echinoderes* aff. *angustus* Higgins & Kristensen, 1988. **A**. Segments 1 to 4, dorsal view. **B**. Segments 1 to 4, left lateral view. **C**. Segments 1 to 2, ventral view. **D**. Segments 3 to 4, ventral view. **E**. Segments 4 to 6, dorsal view. **F**. Segments 4 to 6, left lateral view. **G**. Segments 5 to 8, ventral view. **H**. Segments 7 to 9, ventral view. **I**. Segments 7 to 9, left lateral view. **J**. Segments 9 to 10, ventral view. **K**. Segments 10 to 11, dorsal view, showing female sexual dimorphism. **L**. Segments 10 (posterior part) to 11, left lateral view, showing male sexual dimorphism. **M**. Segments 10 to 11, ventral view, showing male sexual dimorphism. Scale bars: A–C, E–I = 20 µm; D, J–K, M = 10 µm; L = 5 µm.

Diagnostic remarks

Echinoderes angustus was described from Disko Island in West Greenland (Higgins & Kristensen 1988). It has subsequently been the subject of redescriptions and additional important notes have been added to the diagnosis of the species. Grzelak & Sørensen (2018) documented the presence of glandular cell outlets type 2 in subdorsal, laterodorsal, sublateral, and ventrolateral positions on segment 2, in subdorsal positions on segment 4, in midlateral positions on segment 5, and (very likely) in laterodorsal positions on segment 10. Shortly after, Herranz *et al.* (2018) reported the presence of a partial midventral fissure in segment 2 and noted that *E. angustus* is most easily distinguished from the highly similar species *E. pennaki* by its longer (about 20%) middorsal and laterodorsal spines. Re-examinations of type material and fresh material collected close to the type locality was carried out during the present study. They confirm these observations, add a complete mapping of sensory spots (Table 20) in *E. angustus*, and confirm the presence of laterodorsal type 2 outlets on segment 10. In addition, the examinations revealed that the species has a middorsal protuberance projecting from the intersegmental zone between segments 10 and 11, and that the tergal plate of the terminal segment is split into two halves by a middorsal fissure. Visualisation of this middorsal fissure is often obscured by the overlaying protuberance.

Since its discovery, *E. angustus* has also been recorded from the Barents Sea and the fjords of Svalbard, where it is one of the most frequently observed species (Grzelak & Sørensen 2019a, 2019b). This suggests that the species' distributional range at least covers the Arctic extension of the Atlantic Ocean. In a recent study of kinorhynchs in the Subantarctic South Orkney Trench, not too distant from the Antarctic Peninsula, Sánchez *et al.* (2024) surprisingly found a specimen that almost matched the morphology of *E. angustus*. Its distribution of spines and glandular cell outlets type 2 matched the emended diagnoses provided by Grzelak & Sørensen (2018) and Herranz *et al.* (2018), and the sensory spot distribution largely followed the pattern reported in the present study. The only two notable differences regarded its longer lateral terminal spines and the absence of a partial midventral fissure on segment 2. Based on the great level of similarity, but also taking the minor differences and the considerable geographic distance into account, Sánchez *et al.* (2024) reluctantly reported the species as *Echinoderes* cf. *angustus*.

Echinoderes aff. *angustus*, recorded in the present study, fits the Subantarctic specimen reported by Sánchez *et al.* (2024): its morphology is highly similar to that of *E. angustus*, but its lateral terminal spines are slightly longer, and there is no indication of a midventral fissure on segment 2. The difference in spine lengths is less pronounced though. Whereas the lateral terminal spines of the Subantarctic female specimen of Sánchez *et al.* (2024) measured 223 μm, unlike the only 140–180 μm in the female *E. angustus* types (Higgins & Kristensen 1988), the lengths of these spines in the Antarctic specimen are only an extension of the size range in the male types (140–198 μm in male types vs 197–214 μm in male Antarctic specimens). The Antarctic specimens are certainly conspecific with the South Orkney Trench specimen reported by Sánchez *et al.* (2024); this is supported by morphology, morphometrics and geography. The open question is obviously whether these specimens can be considered as conspecific with *E. angustus*. The lateral terminal spine lengths can hardly be used as an argument to separate the Antarctic specimens from *E. angustus*, and even though the missing midventral fissure on segment 2 could indicate that they represent a distinct species, it is hard to accept this difference as the sole diagnostic character. The only other potential differential character is the short set of midlateral tubes found in male specimens on their terminal segment. Since these tubes are only visible with SEM, the type material of *E. angustus* is not useful to confirm or reject the presence of such tubes in *E. angustus*. However, a single male *E. angustus* specimen from Svalbard did not seem to have such tubes; thus, their presence in the Antarctic specimens could support that this is a different species.

The geographic distance between the Arctic and (Sub-)Antarctic populations obviously also speaks in favour of considering them as two different species, but we have recently seen indications of other species with a potential bipolar distribution. For instance, the high Arctic, north Atlantic, and Mediterranean

species *Echinoderes pterus* has also been reported from the Atacama Trench, off Chile (Yamasaki *et al.* 2018a; Grzelak *et al.* 2021), and Grzelak & Sørensen (2022) reported specimens from New Zealand showing a close resemblance to *Echinoderes beringiensis*, which, as the name indicates, was described from the Bering Strait (Adrianov & Maiorova, 2022) (see also the following section for an additional discussion of this species). With these indications of potential bipolar kinorhynch distributions taken into account, we cannot rule out that *E. angustus* could also be present in both the Arctic and Antarctic. Thus, the only fair conclusion at this stage seems to be that it would require comparison of molecular barcodes to solve the question. It is intriguing, though, to experience how we keep observing extremely wide distributions of conspecific populations, or at least very closely related species.

Echinoderes aff. *beringiensis/romanoi/xalkutaat*
Figs 27–28, Tables 21–22

Material examined

ANTARCTICA – **Antarctic Peninsula** • 1 ♀ (mounted for LM in Fluoromount G on HS slide); CRS 1793; 64°39.53′ S, 62°55.03′ W; 701 m b.s.l.; 11 Apr. 2016; FjordEco2; soft sediment; NHMD 1790694 • 1 ♂ (mounted for SEM); CRS 1793; 64°39.53′ S, 62°55.03′ W; 701 m b.s.l.; 11 Apr. 2016; FjordEco2; soft sediment; MVS • 1 ♂, 3 ♀♀ (mounted for LM in Fluoromount G on HS slide.); CRS 1809; 64°39.59′ S, 62°55.09′ W; 694 m b.s.l.; 15 Apr. 2016; FjordEco2; soft sediment; NHMD 1790695 to 1790698 • 2 ♂♂, 3 ♀♀ (mounted for SEM); CRS 1809; 64°39.59′ S, 62°55.09′ W; 694 m b.s.l.; 15 Apr. 2016; FjordEco2; soft sediment; MVS • 2 ♀♀ (mounted for SEM); CRS 1832; 64°39.30′ S, 62°55.98′ W; 631 m b.s.l.; 21 Apr. 2016; FjordEco2; soft sediment; MVS.

Concise description

General. An overview (Fig. 27A) of measurements and dimensions is given in Table 21. Distributions of cuticular structures, i.e., sensory spots, glandular cell outlets, spines and tubes, are summarized in Table 22.

Segment 1. Consists of a complete cuticular ring. Sensory spots are present in subdorsal, laterodorsal, and ventromedial positions; sensory spots are minute, and consist of relatively few, very short micropapillae arranged around two pores. Glandular cell outlets type 1 are present in middorsal and lateroventral positions. Cuticular hairs are arranged in four to five rows: anterior rows are present only on dorsal side, between midlateral positions, whereas the posteriormost row extends around the entire segment; an additional short row is present between the ventromedial sensory spots. The posterior segment margin is straight and terminates in a pectinate fringe with broad and well-developed fringe tips; fringe tips on ventral side are slightly longer than those on the lateral and dorsal sides (Figs 27B–C, 28A–C).

Segment 2. Consists of a complete cuticular ring, without any indication of a midventral fissure. Glandular cell outlets type 2 are present in subdorsal, laterodorsal, sublateral, and ventrolateral positions. Sensory spots are present in middorsal, laterodorsal, midlateral, and ventromedial positions; the micropapillary areas around the sensory spots on this, and all following segments, are small and rounded, and point in a posterior direction; one or two long and rigid hairs (extremely extended micropapillae?) project from the micropapillary area. Glandular cell outlets type 1 are present in middorsal and ventromedial positions. Fairly long bracteate cuticular hairs are arranged in four to five transverse rows around the segment. The posterior segment margin is straight, terminating in uniform, well-developed fringe tips (Figs 27B–C, 28A–C).

Segment 3. As following seven segments, consisting of one tergal and two sternal plates. Sensory spots are present in subdorsal (not present in all specimens) and sublateral positions, and glandular cell outlets

Table 21. Measurements from light microscopy of *Echinoderes* aff. *beringiensis/romanoi/xalkutaat* (in μm) from the Antarctic Peninsula, including number of measured specimens (*n*) and standard deviation (SD), and comparative measurements of types of *E. beringiensis* Adrianov & Maiorova, 2022, *E. romanoi* Landers & Sørensen, 2016, and *E. xalkutaat* Cepeda *et al.*, 2019.

Character	*E. aff. ber./rom./xal.*				*E. beringiensis*				*E. romanoi*				*E. xalkutaat*			
	n	Range	Mean	SD	*n*	Range	Mean	SD	*n*	Range	Mean	SD	*n*	Range	Mean	SD
TL	5	271–313	300	16.73	6	269–390	337	49.79	5	201–245	233	18.23	3	282–304	290	11.6
TL (CUM)	5	396–422	408	10.35	5	371–480	441	43.40	5	293–323	306	11.30	0	–	–	–
MSW-7	5	47–56	51	1.51	6	48–68	59	7.12	5	37–40	38	1.14	2	48–49	49	0.4
MSW-7/TL	5	16.2–17.9%	17.1%	0.60%	6	15.2–20.4%	17.5%	1.85%	5	15.1–18.9%	16.5%	1.44%	2	17.1–17.2%	17.1%	0.0%
SW-10	5	40–45	42	2.07	6	40–47	44	2.48	5	32–35	34	1.10	2	40	40	0.1
SW-10/TL	5	13.6–14.8%	14.1%	0.48%	6	11.7–16.1%	13.3%	1.80%	5	13.1–16.9%	14.6%	1.42%	2	13.9–14.1%	14.0%	0.1%
S1	5	29–32	31	1.52	6	31–40	36	3.87	5	21–22	22	0.45	3	26–30	28	1.7
S2	5	29–30	30	0.45	6	27–35	31	3.22	5	23–26	24	1.30	3	26–33	30	3.2
S3	5	30–33	31	1.30	5	27–38	33	4.53	5	23–27	25	1.64	3	30–34	33	1.5
S4	5	31–35	32	1.67	5	33–40	37	3.29	5	24–26	25	0.89	3	29–33	32	2.1
S5	5	34–40	37	2.59	6	36–53	45	6.80	5	26–30	27	1.67	3	31–37	35	2.9
S6	5	38–41	40	1.41	6	32–52	45	7.43	5	27–30	29	1.14	3	35–41	38	3.0
S7	5	41–45	43	1.79	6	37–54	48	6.59	5	29–33	31	1.64	3	40–42	41	1.3
S8	5	44–48	46	1.48	6	40–56	50	6.02	5	31–33	32	0.89	3	45–47	45	1.3
S9	5	41–46	44	2.05	6	36–52	47	5.98	5	31–33	32	0.84	3	41–45	43	2.1
S10	5	40–48	43	3.27	6	35–46	42	4.68	5	30–33	32	1.52	3	35–37	35	1.2
S11	5	28–33	31	1.87	6	29–41	36	4.81	5	25–31	27	2.28	3	24–32	29	4.2
MD4 (ac)	5	40–57	47	7.06	5	40–56	46	6.38	5	28–33	30	1.92	2	42–44	43	1.7
MD5 (ac)	5	52–65	57	6.30	5	45–56	53	4.53	4	39–44	43	2.28	1	56	N/A	N/A
MD6 (ac)	5	60–77	66	7.33	6	58–71	66	4.49	5	45–55	49	4.16	3	65–75	69	5.1
MD7 (ac)	5	62–83	70	8.85	5	45–81	68	13.81	4	52–58	55	2.94	3	70–72	71	0.6
MD8 (ac)	4	80–91	84	4.79	6	62–86	81	9.33	5	56–70	63	5.22	3	77–84	80	3.8
LV/LA5 (tu)	3	12–14	13	1.15	2	16–20	18	2.83	–	–	–	–	3	8–10	9	1.2
LV6 (ac)	5	36–44	39	3.32	6	37–50	41	4.76	5	20–23	22	1.14	3	28–38	34	5.2
LV7 (ac)	5	41–48	43	2.79	6	34–46	42	4.50	5	22–28	25	2.19	2	42–43	43	0.8
LV8 (ac)	5	45–50	48	2.12	5	45–53	48	3.63	5	25–29	27	1.48	3	45–47	47	1.1
LV9 (ac)	5	40–49	44	3.91	4	35–47	39	5.32	4	24–32	27	3.70	3	32–39	35	3.7
LTS	5	177–205	190	10.18	6	123–168	150	18.36	5	138–161	145	9.53	3	171–178	176	4.0
LTS/TL	5	57.3–70.8%	63.6%	5.03%	6	36.4–62.5%	45.3%	9.09%	5	57.5–69.7%	62.5%	5.50%	3	58.9–63.0%	60.6%	2.1%
LTAS	4	42–119	75	37.97	3	70–85	80	8.39	4	51–77	65	12.52	3	50–56	53	3.0

Table 22. Summary of nature and location of sensory spots, glandular cell outlets, tubes, and spines arranged by series in *Echinoderes* aff. *beringiensis/romanoi/xalkutaat*. * marks unpaired structures in otherwise paired positions.

Segment	Position									
	MD	PD	SD	LD	ML	SL	LA	LV	VL	VM
1	gco1	–	ss	ss	–	–	–	gco1	–	ss
2	gco1,ss	–	gco2	gco2,ss	ss	gco2	–	–	gco2	gco1,ss
3	gco1	–	ss*	–	–	ss	–	–	–	gco1
4	ac	gco1	–	–	–	–	–	–	–	gco1
5	ac	gco1	ss	–	gco2	–	–	tu	–	gco1,ss
6	ac	gco1,ss	ss	–	ss	–	–	ac	–	gco1,ss
7	ac	gco1,ss	–	–	ss	–	–	ac	–	gco1,ss
8	ac	gco1,ss	–	–	–	gco2	–	ac	–	gco1
9	–	gco1,ss	ss	–	ss	si	–	ac	ss	gco1
10	gco1,gco1	–	ss	gco2	–	–	–	–	ss	gco1
11	pr	ss	–	–	tu(♂),pex3(♂)	–	ltas(♀)	lts	–	–

type 1 in middorsal and ventromedial positions. Cuticular hairs present in four to five rows on the tergal and lateral halves of the sternal plates, except in hair-less midlateral areas; paraventral areas completely devoid of hairs or hair-like extensions. Posterior segment margin straight and pectinate fringe as on preceding segment (Figs 27B–C, 28D–F).

Segment 4. With spine in middorsal position. Sensory spots are not present. Glandular cell outlets type 1 are present in paradorsal and ventromedial positions. Cuticular hairs as on preceding segment, but now arranged in five to six rows. Posterior segment margin and pectinate fringe as on preceding segment (Figs 27B–C, 28D–F).

Segment 5. With spine in middorsal position and tubes in lateroventral positions. Glandular cell outlets type 2 are present in midlateral positions. Sensory spots present in subdorsal and ventromedial positions, and glandular cell outlets type 1 in paradorsal and ventromedial positions. Cuticular hairs, posterior segment margin, and pectinate fringe as on preceding segment (Figs 27B–D, 28F–I).

Segment 6. With spines in middorsal and lateroventral positions. Sensory spots present in paradorsal, subdorsal, midlateral, and ventromedial positions; ventromedial sensory spots situated closer to midventral articulation than those on preceding segment. Glandular cell outlets type 1 present in paradorsal and ventromedial positions. Cuticular hairs, posterior segment margin, and pectinate fringe as on preceding segment (Figs 27B–F, 28G–I).

Segment 7. With spines in middorsal and lateroventral positions. Sensory spots present in paradorsal, midlateral, and ventromedial positions; ventromedial sensory spots situated more laterally than those on preceding segment and aligned with those on segment 5. Glandular cell outlets type 1 present in paradorsal and ventromedial positions. Cuticular hairs as on preceding segment, except for middorsal to paradorsal positions which are also devoid of hairs. Posterior segment margin and pectinate fringe as on preceding segment (Figs 27D–F, 28I–L).

Segment 8. With spines in middorsal and lateroventral positions. Glandular cell outlets type 2 are present in sublateral positions. Sensory spots present in paradorsal positions only, and glandular cell outlets type 1 in paradorsal and ventromedial positions. Cuticular hairs as on preceding segment, but the midlateral hairless areas have moved to more laterodorsal positions. Posterior segment margin and pectinate fringe as on preceding segment (Figs 27D–F, 28L–N).
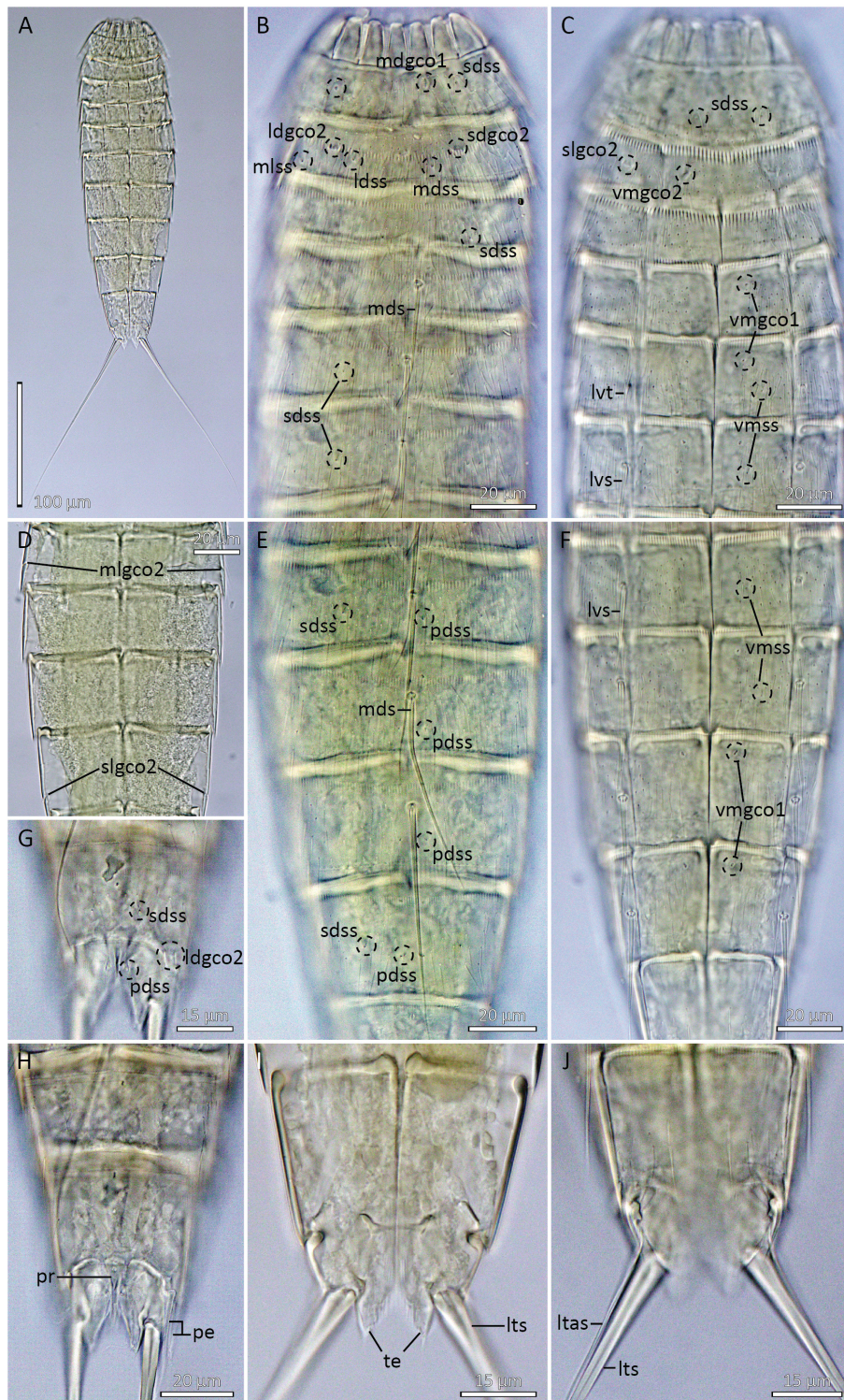
Fig. 27. Light micrographs showing overviews and details of *Echinoderes* aff. *beringiensis/romanoi/ xalkutaat*. **A–F, I–J**. Female (NHMD 1790694). **G–H**. Male (NHMD 1790696). **A**. Ventral overview. **B**. Segments 1 to 6, dorsal view. **C**. Segments 1 to 6, ventral view. **D**. Segments 5 to 8, focused mid- to sublaterally. **E**. Segments 6 to 9, dorsal view. **F**. Segments 6 to 9, ventral view. **G**. Segments 10 to 11, dorsal view. **H**. Segments 9 to 11, focused slightly deeper than G, showing male sexual dimorphism. **I**. Segments 10 to 11, focused at tergal extensions. **J**. Segments 10 to 11, ventral view, showing female sexual dimorphism. Scale bars: A = 100 µm; B–F, H = 20 µm; G, I–J = 15 µm.
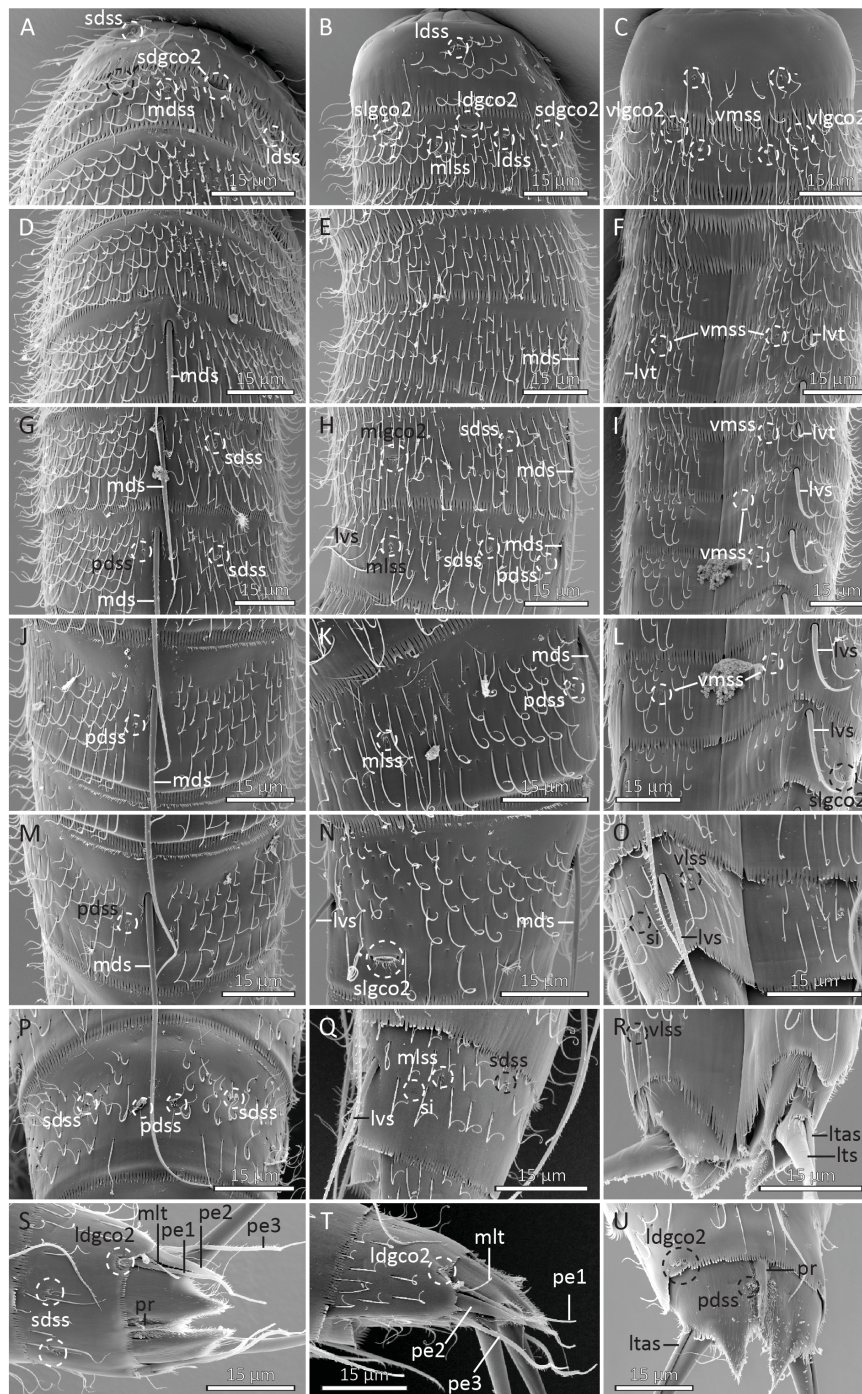
Fig. 28. Scanning electron micrographs showing overviews and details of *Echinoderes* aff. *beringiensis/romanoi/xalkutaat*. **A**. Segments 1 to 2, dorsal view. **B**. Segments 1 to 2, left lateral view. **C**. Segments 1 to 2, ventral view. **D**. Segments 3 to 4, dorsal view. **E**. Segments 3 to 4, left lateral view. **F**. Segments 3 to 5, ventral view. **G**. Segments 5 to 6, dorsal view. **H**. Segments 5 to 6, left lateral view. **I**. Segments 5 to 7, ventral view. **J**. Segment 7, dorsal view. **K**. Segment 7, left lateral view. **L**. Segments 7 to 8, ventral view. **M**. Segment 8, dorsal view. **N**. Segment 8, left lateral view. **O**. Segment 9, ventral view. **P**. Segment 9, dorsal view. **Q**. Segment 9, left lateral view. **R**. Segments 10 (posterior part) to 11, ventral view, showing female sexual dimorphism. **S**. Segments 10 to 11, dorsal view, showing male sexual dimorphism. **T**. Segments 10 to 11, left lateral view, showing male sexual dimorphism. **U**. Segments 10 (posterior part) to 11, dorsal view, showing female sexual dimorphism. All scale bars = 15 µm.

SEGMENT 9. With spines in lateroventral positions. Sensory spots present in paradorsal, subdorsal, midlateral, and ventrolateral positions. Glandular cell outlets type 1 present in paradorsal and ventromedial positions. Small rounded sieve plates located in sublateral positions. Cuticular hairs, posterior segment margin, and pectinate fringe as on preceding segment (Figs 27E–F, H, 28O–Q).

SEGMENT 10. With glandular cell outlets type 2 in laterodorsal positions near posterior segment margin. Sensory spots present in subdorsal and ventrolateral positions. Glandular cell outlets type 1 present as two longitudinally arranged outlets in middorsal position, and in ventromedial positions. Cuticular hair covering reduced to a small patch between subdorsal sensory spots, and otherwise only hairs in laterodorsal to ventromedial areas. The posterior segment margin of the tergal plate is straight, with minute fringe tips. Sternal plate margins oblique, with longer fringe tips in ventromedial and paraventral areas (Figs 27G–J, 28R–U).

SEGMENT 11. With lateral terminal spines and a middorsal protuberance emerging from the intersegmental zone between segments 10 and 11. The segment consists of two tergal and two sternal plates, but visualisation of the middorsal fissure between the tergal plates is obscured by the overlaying protuberance. Females with lateral terminal accessory spines; males with thin, tubular dorsal and ventral penile spines; medial pair of penile spines cone-shaped and well-developed. Males in addition with thin tube, attaching between dorsal and medial penile spines; the tube diameter is > 50% of the dorsal penile spine diameter and > 20% of the penile spine length. Sensory spots present in paradorsal positions only. The segment is devoid of cuticular hairs, but has scattered hair-like extensions along the inferior margins of the tergal plates. Tergal extensions are triangular, with pointed tips. Sternal extensions short, broadly triangular, and not extending beyond tergal extensions (Figs 27G–J, 28R–U).

Distribution

Antarctic Peninsula: Gerlache Strait, 631 to 701 m b.s.l. See Fig. 1 for geographic overview of stations and Table 1 for station and specimen information.

Diagnostic remarks

Identification of these specimens turned out to be difficult, since they show a very close resemblance with no less than three congeners, i.e., *E. beringiensis*, *E. romanoi*, and *E. xalkutaat*. This high level of similarity not only hampers identification of the Antarctic specimens, but also indicates that the three species in question potentially could be synonymous. In the following, comparison of the Antarctic specimens with each of the three species will be carried out in separate sections. In addition, a comparison with *E. angustus*, *E.* aff. *angustus* (addressed above) and *E.* aff. *beringiensis/galadrielae* sensu Grzelak & Sørensen (2022) will be included, since these species also share so many similarities that it could indicate the existence of a new species group. Observed differences between the species are summarised in Table 23.

Comparison with *E. beringiensis*

The distribution of spines and sensory spots on segments 1 to 9 is nearly identical in *E. beringiensis* and the Antarctic *Echinoderes* aff. *beringiensis/romanoi/xalkutaat* (Adrianov & Maiorova 2022; Table 22 in present contribution). The only detectable difference regards the tubes on segment 5, which are displaced to a lateral accessory position in *E. beringiensis* (see Adrianov & Maiorova 2022: figs 5a, 6a). The two species also share the same segment compositions, including the midtergal division of segment 11. Morphometric ranges for trunk and spine lengths are also overlapping in nearly all cases, except regarding the lateral terminal spines, which are longer in the Antarctic species, 177–205 µm vs 123–168 µm (Table 21). The potential main differences between the two species might be found in their distribution of glandular cell outlets type 2. They have outlets in identical positions on segments 2 and 8.

Table 23. Comparative table showing potential differential character traits between highly similar species, including *Echinoderes* aff. *beringiensis/ galadrielae* from New Zealand (Grzelak & Sørensen 2022), as well as *E.* aff. *beringiensis/romanoi/xalkutaat* and *E.* aff. *angustus* Higgins & Kristensen, 1988 from Antarctica (present study). Potential differential character traits are in boldface.

Character	*E.* aff. *beringiensis/ romanoi/xalkutaat*	*E. beringiensis*	*E.* aff. *beringiensis/ galadrielae*	*E. romanoi*	*E. xalkutaat*	*E.* aff. *angustus*
S1 VM sensory spot	present	present	**absent**	present	VL	present
S4 SD GCO2	absent	absent	absent	absent	absent	**present**
S5 tubes	LV	LA	LA	LV	LV	LV
S8 lateral GCO2	SL GCO2	**ML**(♀)+SLGCO2	SL GCO2	SL GCO2	SL GCO2	SL GCO2
S10 LD GCO2	present	present	present	present	present	present
S11 MD protuberance	present	present	**absent**	**absent**	?	present
S11 midtergal fissure	present	present	present	present	?	present
TL range	271–313 µm	269–390 µm	**196–211 µm**	**196–247 µm**	282–304 µm	310–347 µm
LTS range	177–205 µm	123–168 µm	181–254 µm	127–232 µm	171–178 µm	197–214 µm

However, adult female specimens of *E. beringiensis* appear to have two pairs of outlets on segment 8, in midlateral and sublateral positions, as opposed to only a single pair in sublateral positions in the Antarctic specimens. Having a double set of large glandular cell outlets 2 type on segment 8 is truly a unique trait among species of *Echinoderes*, but the diagnostic value of the character gets challenged by the fact that it has only been observed in five (?) adult females (and documented in one), whereas males and younger females only have the much more common sublateral pair (Adrianov & Maiorova 2022). It would be desirable to obtain a better understanding of this trait and, eventually through observation of a larger sample size, decide whether this is truly a consistent character or if the double outlet pairs are abnormalities.

Another potential difference might be found in the laterodorsal positions of the posterior segment margin of segment 10, where *E. beringiensis* is reported to have sensory spots (Adrianov & Maiorova 2022), unlike the Antarctic specimens which have glandular cell outlets type 2 in these positions. However, these structures are quite well documented in the description of *E. beringiensis*, and fig. 8e in Adrianov & Maiorova (2022) clearly shows that the structures are glandular cell outlets type 2 rather than sensory spots.

Otherwise, there are no conspicuous differences between *E. beringiensis* and the Antarctic *Echinoderes* aff. *beringiensis/romanoi/xalkutaat*, and potential differences narrow down to the lengths of their lateral terminal spines, and the somehow questionable double pair of glandular cell outlets type 2 on segment 8.

Comparison with *Echinoderes* aff. *beringiensis/galadrielae* sensu Grzelak & Sørensen (2022)

Following their description of *E. galadrielae* from New Zealand, Grzelak & Sørensen (2022) reported the co-occurring species *Echinoderes* aff. *beringiensis/galadrielae*, which appeared to "represent an intermediate between *E. galadrielae* sp. nov. and *E. beringiensis*" (Grzelak & Sørensen 2022: 82). The distribution of cuticular structures generally followed the pattern of *E. galadrielae*, whereas the tergal extensions were similar with those in *E. beringiensis* and thus differing considerably from the long and slender extensions in *E. galadrielae*.

Comparison with *Echinoderes* aff. *beringiensis/romanoi/xalkutaat* reveals that the Antarctic specimens are nearly identical with *Echinoderes* aff. *beringiensis/galadrielae*. The spine/tube pattern of the two species differs only in the position of tubes on segment 5 (lateral accessory vs lateroventral), and even the spine length ranges overlap. The only conspicuous morphometric difference between the two species regards the considerable difference in trunk length, i.e., 271–313 µm in the Antarctic species vs 210–235 µm in the New Zealand species. There are, however, more considerable differences in the sensory spot distribution, as the New Zealand species apparently lacks ventromedial sensory spots on segments 1, 5, and 7, and subdorsal sensory spots on segment 6, which are all present in the Antarctic species. The absence of subdorsal structures on segment 6 could potentially be due to intraspecific variation, and the missing ones on segments 5 and 7 might have been hidden under dirt, but the absence of ventromedial sensory spots on segment 1 is a distinct difference that could speak against conspecificity.

Echinoderes aff. *beringiensis/galadrielae* is reported to have males with short laterodorsal tubes on segment 10, whereas the females have 'similar slit-like, fringed openings' (Grzelak & Sørensen 2022). However, a re-examination of the specimens clearly shows that these structures are glandular cell outlets type 2, which corresponds to the morphology in the Antarctic specimens.

Segment 11 is similar in composition, i.e., consisting of two tergal and two sternal plates, but it differs by the lack of a middorsal protuberance in the New Zealand species. An additional apparent difference

between the two species regards the cuticular hair covering, which generally is much denser on the Antarctic specimens.

Comparison with *E. romanoi*

The comparison of the Antarctic species with *E. romanoi* from the Gulf of Mexico prompted some re-examinations of *E. romanoi* type specimens as well as non-types mounted for SEM. Unfortunately, the latter were in a rather sad condition, but new and significant information was nevertheless obtained. Most importantly, it could be documented that *E. romanoi* has laterodorsal glandular cell outlets on segment 10, and that the tergal plate of segment 11 has a middorsal fissure (Fig. 29B, D). Furthermore, some minor details in the original description could be corrected, i.e., 1) that the reported sublateral glandular cell outlets type 1 on segment 1 are muscular attachment sites, 2) that a middorsal sensory spot and glandular cell outlet type 1 are present on segment 2, 3) that segment 3 has a single middorsal glandular cell outlet type 1, rather than a pair of paradorsal outlets, and 4) that laterodorsal sensory spots on segment 10 are missing, whereas ventrolateral ones are present. Likewise, type specimens were re-measured (Table 21), and a couple of potential pre-adults that were part of the original morphometric data provided by Landers & Sørensen (2016) were excluded.

With this new information established, the spine, sensory spot, and glandular cell outlet patterns for the Antarctic species and *E. romanoi* are the same, and differences come down to morphometrics and the absence of a middorsal protuberance on segment 11 in *E. romanoi*. Morphometrically, *E. romanoi* differ from the Antarctic species by being smaller. The trunk is shorter, 196–247 µm vs 271–313 µm, and all middorsal and laterodorsal spines are generally about 20% shorter in *E. romanoi* (see Table 21). Only the length ranges of the lateral terminal spines are overlapping in the two species.

Comparison with *E. xalkutaat*

Echinoderes xalkutaat is known from the Gulf of California, and the description was based on three specimens mounted for LM (Cepeda *et al.* 2019b). The condition of the type material could have been better, and with the lack of information from SEM, some characters in *E. xalkutaat* remain to be confirmed. However, it is clear that the distribution patterns of spines, tubes, and glandular cell outlets types 1 and 2 are identical with the patterns in the Antarctic species. Morphometrically, ranges of trunk and spine lengths are also overlapping for the two species (Table 21).

Potential differences might be found in the sensory spot distribution and characters related to the terminal segment. As for the latter, *E. xalkutaat* is described as having a terminal segment with a complete tergal plate and no middorsal protuberance. However, due to the condition of the type specimens, this information needs to be validated. It is correct that there is no evidence for the presence of a protuberance, but the dorsal view of segment 11 shown in fig. 16i by Cepeda *et al.* (2019a) actually has indications of a middorsal fissure on the segment, suggesting that the tergal plate could be split into two. Regarding sensory spots, the main difference appears to be expressed in the dorsal series, which are more laterodorsal in *E. xalkutaat*, as opposed to subdorsal in the Antarctic specimens, but again, confirmation from SEM would be desirable.

Comparison with Arctic *E. angustus* and Antarctic *E. angustus* and *E.* aff. *angustus*

The Arctic species *E. angustus* and the Antarctic *E. angustus* and *E.* aff. *angustus* clearly differ from *Echinoderes* aff. *beringiensis/romanoi/xalkutaat* and the other species discussed above by having subdorsal glandular cell outlets on segment 4. They have, however, been included in the comparison because of the striking similarities regarding all other cuticular structures. Morphometrically, *E. angustus* and the Antarctic, potentially conspecific population are in the upper range or larger than *Echinoderes* aff. *beringiensis/romanoi/xalkutaat*, both regarding trunk and lateral terminal spine lengths, but the

ranges of other spines are overlapping. When it comes to cuticular hairs, spines, tubes, and glandular cell outlets (except type 2 outlets on segment 4), the species are basically identical, which stresses the close phylogenetic relationship between the species.

In conclusion, *E. angustus* and the Antarctic *E. angustus* and *E.* aff. *angustus* are easily distinguished from the other species in question based on their presence of subdorsal glandular cell outlets type 2 on segment 4. When it comes to the remaining species, the differential characters are much more subtle, and
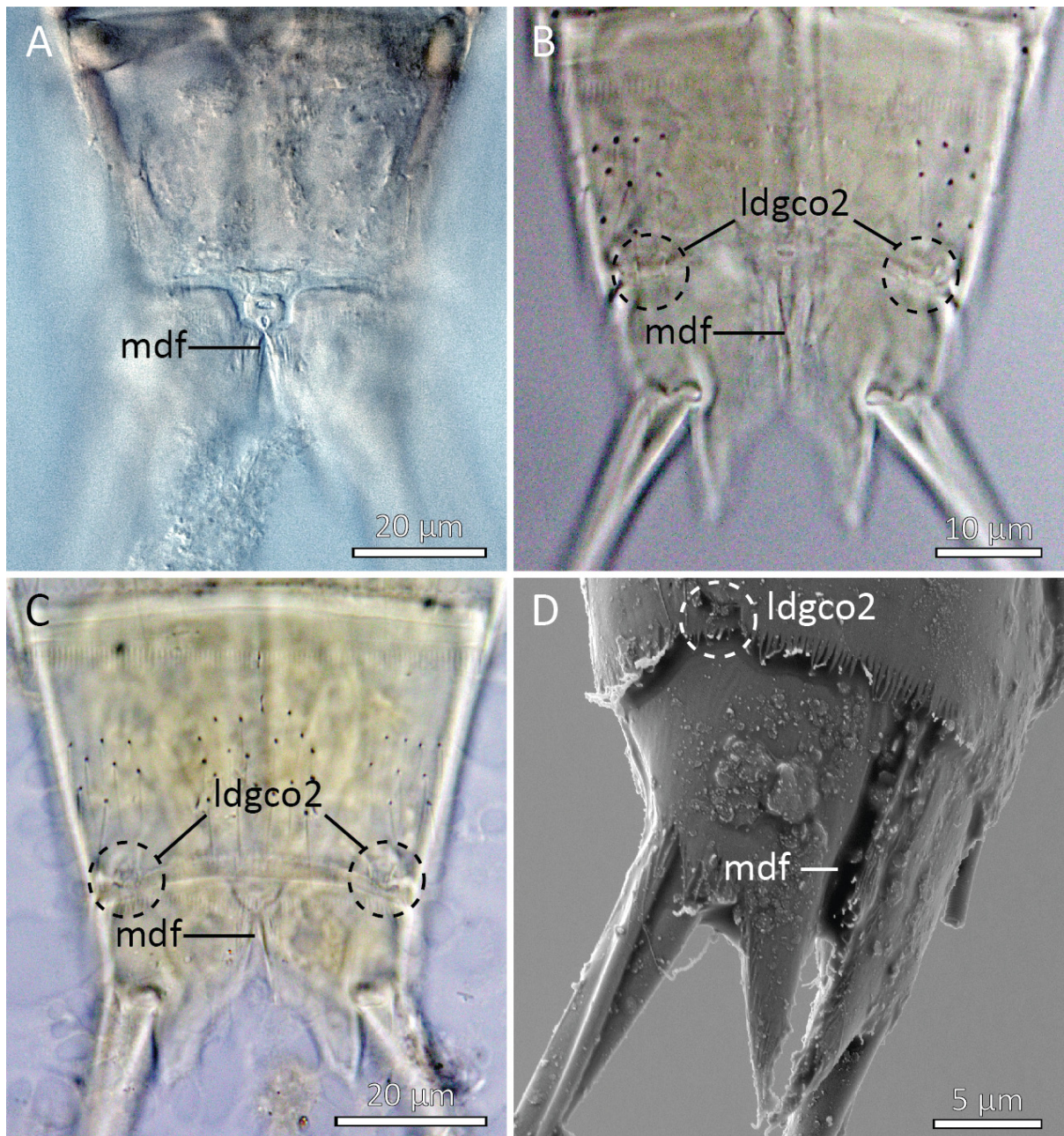
Fig. 29. Light micrographs (A–C) and scanning electron micrographs (D) showing segments 10 to 11, dorsal view, in selected *Echinoderes* spp. **A**. Female, holotype of *E. pennaki* Higgins, 1960 (USNM 29746). **B**. Male, holotype of *E. romanoi* Landers & Sørensen, 2016 (NHMD 100307). **C**. Female, paratype of *E. obtuspinosus* Sørensen *et al.*, 2012 (NHMD 99894). **D**. Female, non-type of *E. romanoi*. Scale bars: A, C = 20 μm; B = 10 μm; D = 5 μm.

clear species barriers are questionable. *Echinoderes beringiensis* might be distinguished by its double set of glandular cell outlets type 2 on segment 8 in females, but since this character does not appear consistently – not even amongst females – its taxonomic significance needs to be validated. *Echinoderes* aff. *beringiensis/galadrielae* from New Zealand is perhaps the potential species that stands out the most, by its consistent lack of ventromedial sensory spots on segment 1. At the same time, it is also smaller than the other species, and the range of its trunk length only overlaps with that of *E. romanoi*. The latter species does not really stand out in any conspicuous way. One potential differential character could be the absence of a middorsal protuberance on segment 11, but since we have very limited understanding of the variability and taxonomic significance of this character, we would be hesitant about basing the species diagnosis exclusively on this trait. *Echinoderes xalkutaat* might be recognised by its slightly different sensory spot pattern, but since the species description is based on LM observations of very few specimens in relatively poor condition, the general morphology of this species needs to be validated. Thus, to sum up, it is not possible to assign the Antarctic *Echinoderes* aff. *beringiensis/romanoi/ xalkutaat* to any known species. Instead, the three candidate species could potentially be synonymous, and morphological re-examinations, or ideally molecular barcoding, are required to solve the taxonomic nature of these species.

Discussion

Abundance and habitat preferences of polar kinorhynchs

The abundance and distribution patterns of the adult kinorhynchs show a clear preference for the Gerlache Strait and Andvord Bay, as opposed to the open continental shelf. This is expressed in both species richness as well as abundance in the three regions (Tables 3–4). The observed differences in abundance correspond well with the only other quantitative study of kinorhynch communities in the Polar Regions (Grzelak & Sørensen 2019b). That study compared kinorhynch species richness and abundance in four fjords, with open water areas east and north of Svalbard, and finds that species abundance was up to one hundredfold higher in the fjords. However, the observed species richness differs between the present study and the one from Svalbard. When fjords and open water regions are compared, Grzelak & Sørensen (2019b) find similar diversities in the compared areas, with 13 species in both the fjords and the open water areas. Four species are exclusively fjord species and 5 appear only in the open water, whereas the remaining 8 species occur in both regions. Of the 12 species recorded in the present study, 9 were restricted to the coastal strait and bay regions, whereas 2 were only found in the open continental shelf area. Only a single species, *Polacanthoderes* sp., which potentially could represent more than one species, occurred on both the open continental shelf, in the strait, and in Andvord Bay. However, the open water coverage in the study of Grzelak & Sørensen (2019b) is much more comprehensive than in the present study, where sampling was more concentrated in Andvord Bay, and it is therefore not unlikely that more species would have shown up in the open continental shelf region if it had been sampled more intensively.

Thus, while it might be premature to draw general conclusions about species richness in open water vs fjord or strait communities in polar regions, we see very clearly from both the Svalbard study and the present one that the abundance is considerably higher in fjords and straits. A third Arctic region that is well explored in terms of kinorhynch communities is Disko Island, West Greenland. Kinorhynchs have been sampled around Disko Island at several occasions, most recently during the NHMD project 'DiskoVery' in 2023 (see Zalewska *et al.* 2024). Results from complete analyses of quantitative data are still not available for Disko Island, but it was the clear impression from both the DiskoVery project (Zalewska *et al.* 2024), as well as previous sampling campaigns (M.V. Sørensen, pers. obs), that samples collected in the three western fjords of the island always produce considerably more specimens than samples collected from the open water area in Disko Bay, south of the island. Thus, based on the limited data available, it seems fair to conclude that polar kinorhynch abundances are highest in fjord and strait habitats.

Bipolar distribution of closely related species

Throughout the first 150 years of taxonomic kinorhynch research, all known species appeared to have rather restricted regional distribution ranges, which was expected considering their lack of pelagic stages for dispersal. As late as 1998, Pardos *et al.* (1998) noted that "The greatest distance between published valid/recognizable species geographic records is that between Roscoff on the north coast of France and Palma, Mallorca in the Mediterranean Sea". This picture slowly started changing over the following 20 years. Neuhaus (2004) showed how the distributional range of the Antarctic species *Campyloderes vanhoeffeni* extended into the tropical East Pacific, and a few years later Neuhaus & Sørensen (2013) could expand the distributional range even further and demonstrated that *C. vanhoeffeni* was a cosmopolitan species or complex of closely related species. In the meantime, wide distributional ranges were demonstrated for other species. For instance, the Yellow Sea species *Echinoderes tchefouensis* Lou, 1934 was recorded from as far away as Singapore (Sørensen *et al.* 2016), Borneo, and the Mariana Islands (Sørensen *et al.* 2012). The Northeast Atlantic species *Echinoderes unispinosus* Yamasaki *et al.*, 2018b was soon after its description also reported from several localities off the US west coast (Sørensen *et al.* 2018), and subsequently also from the Gulf of Mexico (Álvarez-Castillo *et al.* 2020) and the Southwest Indian Ocean, near Madagascar (Cepeda *et al.* 2020). The latter study also reported the presence of another Northeast Atlantic species, *Echinoderes apex* Yamasaki *et al.*, 2018c, and the species *E. hviidarum* Sørensen *et al.*, 2018, which was described as part of a US west coast study. Another species described from the US west coast, *E. juliae* Sørensen *et al.*, 2018, was soon after reported from the tropical East Pacific (Sánchez *et al.* 2022), the Atacama Trench (Grzelak *et al.* 2021), and New Zealand (Grzelak & Sørensen 2022).

Thus, over a short period of 25 years the narrative of kinorhynchs as a group with regionally distributed species changed to the realisation that most species could potentially be cosmopolitan, or at least be present in several World oceans. More recently, a new and intriguing trend started to be uncovered through studies on the Southern Hemisphere. Despite the newly achieved knowledge about the dispersal capacity in kinorhynch species, it was with some surprise that Grzelak *et al.* (2021) identified the species *E. pterus* from samples taken in the Atacama Trench. *Echinoderes pterus* was described from the Mediterranean Sea, but the description also included records of the species from high Arctic localities, as far north as 86° N, which makes it the northernmost kinorhynch species ever recorded. Even in light of the newly obtained knowledge, it seemed unexpected to find a North Pole species off the coast of Chile. More species with close ties to the Arctic region showed up in a subsequent study on kinorhynchs from New Zealand (Grzelak & Sørensen 2022). A species reported as *Echinoderes* aff. *balerioni* showed close resemblance to another high Arctic species, *E. balerioni* Grzelak & Sørensen, 2019a, which was described from open water areas north of Svalbard. Likewise, another species, reported as *Echinoderes* aff. *galadrielae*/*beringiensis*, showed a very close resemblance to the low Arctic species *E. beringiensis*, described from waters off northern Kamchatka, Russia (Adrianov & Maiorova 2022).

Finding conspecific, or at least highly similar and thus putatively closely related species in nearly antipodean positions is obviously unexpected. One explanation could be that the species in question are distributed throughout the world oceans, but still remain to be found. However, it allows another hypothesis, namely that certain species, or complexes of closely related species, might show bipolar distribution patterns. The latter hypothesis gains further support from the present study. No less than three of the species recorded from the Antarctic Peninsula in the present study are highly similar to Arctic species. *Echinoderes antarcticus* sp. nov. is a distinct species, but it is obviously also sister-species to the highly similar *E. peterseni*, known from Greenland and Svalbard. Likewise, *Echinoderes* aff. *angustus* is conspecific, or closely related, with *E. angustus*, also known from Greenland and Svalbard. *Echinoderes* aff. *angustus* was not only found at the Antarctic Peninsula in the present study, but has recently been reported from the South Orkney Trench (Sánchez *et al.* 2024). The third species in question, *Echinoderes* aff. *beringiensis*/*romanoi*/*xalkutaat* is more challenging to put in context, because

it shows a close resemblance to no less than three species. As discussed above, it is possible that the three species could be synonyms, which would have to be clarified through examination of fresh material and/ or molecular barcoding. However, if we assess them as three separate species, the Antarctic specimens show a close resemblance to *E. beringiensis*. The resemblance is so close that they could be considered conspecific, and this would support the hypothesis about the existence of bipolar species or sibling species. The finding of a very similar species in New Zealand (*Echinoderes* aff. *galadrielae/beringiensis* in Grzelak & Sørensen 2022) only supports this idea even further.

New species groups

Recent taxonomic studies on *Echinoderes* have attempted to point out putatively monophyletic groups within the genus, partly to cope with the overwhelming number of species in the genus, and partly to pave the way for future phylogenetic analyses of the genus by reducing the number of potential Operational Taxonomic Units (Sørensen 2014; Yamasaki & Fujimoto 2014; Landers & Sørensen 2018; Sørensen *et al.* 2018, 2020). Based on the present study, two new species groups can be proposed.

The *Echinoderes aragorni* species group is a quite obvious group, based on a single known species and a new species described in the present contribution, and the similarities between the two species are already discussed above. The group includes *E. aragorni*, a deep-sea species from New Zealand, and *E. crux* sp. nov. The group is characterised by species with middorsal spines on segments 4, 6, and 8; slit-like openings anteriorly on segment 1; and numerous (30+) minute glandular cell outlets type 2 distributed over segments 2 to 9 (Grzelak & Sørensen 2022; present contribution). Especially the slit-like openings and the numerous outlets are so characteristic that the close relationship between the two species can hardly be disputed.

The second proposed group will be referred to as the *Echinoderes remanei* species group, and it is characterised by a more complex set of characters and represents at the same time some taxonomic challenges to be addressed in future studies. The group, as suggested here, includes 11 described species and 3 with uncertain identities: *Echinoderes remanei* (Blake, 1930), *E. angustus*, *Echinoderes* aff. *angustus* (sensu Sánchez *et al.* 2024; present study), *Echinoderes* aff. *beringiensis/romanoi/xalkutaat* (present study); *Echinoderes* aff. *galadrielae/beringiensis* (sensu Grzelak & Sørensen 2022), *E. obtuspinosus*, *E. pennaki*, *E. quasae*, *E. romanoi*, and *E. xalkutaat*, as well as the four species *E. beringiensis*, *E. cernunnos*, *E. drogoni*, and *E. galadrielae* which already has been proposed as the *E. cernunnos* species group by Grzelak & Sørensen (2022). The *E. remanei* species group is characterised by the following combined traits: middorsal spines on segments 4 to 8; lateroventral spines on segments 6 to 9; and glandular cell outlets type 2 in subdorsal, laterodorsal, sublateral, and ventrolateral/ventromedial positions on segment 2, in middorsal positions on segment 5, and sublateral positions on segment 8. While the spine pattern is rather trivial, it is the combination of glandular cell outlets type 2 that identifies the species group.

Additional potential character traits for the species group include the presence of glandular cell outlets type 2 in laterodorsal positions on segment 10 and the middorsal division of the tergal plate on segment 11. Both characters are often very difficult to visualise, and they are easily overlooked. The laterodorsal outlets on segment 10 are located in a position with several layers of cuticle underneath, which makes observation with LM difficult. Thus, confirmation of their presence through SEM is usually necessary, but even with SEM the outlets might be hard to observe if they sit right at the posterior segment margin and the view is obscured by the margin's pectinate fringe.

Among the identified and formally described species, the presence of laterodorsal outlets on segment 10 has been confirmed for *E. remanei* (see Grzelak *et al.* 2023), *E. angustus*, and *E. romanoi* (see present contribution, Fig. 29B, D), *E. drogoni* (see Grzelak & Sørensen 2018), *E. quasae* (see Herranz *et al.*

2024), and *E. xalkutaat* (Cepeda *et al.* 2019a). The outlets are not mentioned in the description of *E. beringiensis*, but fig. 8e in Adrianov & Maiorova (2022) shows an SEM image of laterodorsal structures in the posterior segment margin of segment 10. The authors interpret the structures as sensory spots, but they show greater similarity with glandular cell outlets type 2. Likewise, in the description of *E. cernunnos*, fig. 6f in Sørensen *et al.* (2012) shows structures marked as 'ldt?' [= laterodorsal tubes?] in the same positions, and these structures are very clearly glandular cell outlets type 2. Also, *E. galadrielae* was described as having either "very short laterodorsal tubes in males" or "slit-like fringed openings" in females (see fig. 31i in Grzelak & Sørensen 2022), and these structures can also be interpreted as glandular cell outlets type 2 with minute projections. Neither the original description of *E. pennaki* (see Higgins 1960) nor the more recent redescription (Herranz *et al.* 2018) mention the presence of laterodorsal outlets on segment 10. However, unpublished SEM images used for the study of Herranz *et al.* (2018) confirm their presence. The outlets are even vaguely indicated in fig. 7i (Herranz *et al.* 2018) of the redescription. The possible presence of laterodorsal outlets on segment 10 in *E. obtuspinosus* was already suggested by Herranz *et al.* (2024), and novel examinations of a female paratype confirm this (Fig. 29C).

The second potential character trait for the species group is the middorsal division of the tergal plate of segment 11. Also, this character can be difficult to visualise and might have been overlooked in previous studies. Again, as was the case with the segment 10 outlets, the middorsal fissure can be hard to observe under LM because of other cuticular structures in the area, and in particular because of the midsternal junction on the ventral side that often will appear stronger and 'over-shine' a midtergal division. Thus, confirmation from SEM is desirable, but even this might be challenging. If a middorsal protuberance is present, it will cover the area of the tergal fissure and, in addition, the tergal plate(s) will often have a dense covering of short, hair-like extensions, which can also distort the view. Thus, regarding the middorsal fissure, our information is not as complete as we could wish for. For the described species, the presence of a divided tergal plate on the terminal segments is documented for *E. remanei* (see Grzelak *et al.* 2023: fig. 6k), *E. beringiensis* (see Adrianov & Maiorova 2022), *E. cernunnos* (see Sørensen *et al.* 2012), *E. drogoni* (see Grzelak & Sørensen 2018), and *E. galadrielae* (see Grzelak & Sørensen 2022). Novel examinations of type material furthermore confirm its presence in *E. angustus* (Fig. 25U), *E. pennaki* (Fig. 29A), *E. romanoi* (Fig. 29B), and *E. obtuspinosus* (Fig. 29C). Only *E. xalkutaat* is reported as having a complete tergal plate on the terminal segment (Cepeda *et al.* 2019a), but this information would need to be verified with SEM imaging.

The multiple characters provide good support for considering the *E. remanei* species group as a monophyletic entity, and we can even get hints about interrelationships within the group. Among the species, we find four which share the presence of subdorsal glandular cell outlets type 2 on segment 4, i.e., *E. angustus*, *E. remanei*, *E. obtuspinosus*, and *E. quasae*. Within this subclade, the latter two appear to be sister species, based on their conspicuously shorter lateral terminal spines. Another putative subclade within the species group is formed by *E. cernunnos* and *E. galadrielae*, which share the presence of long, pointed tergal extensions.

Patterns of glandular cell outlets type 1

In their paper on the *Echinoderes dujardinii* species group, Sørensen *et al.* (2020) addressed the distribution of dorsal glandular cell outlets type 1 (gco1) on segments 1 to 9 in echinoderids and concluded that numerous species appeared to follow one of three common distribution patterns, i.e., 1) middorsal gco1 on segments 1 to 3 and subdorsal on 4 to 9; 2) middorsal gco1 on segments 1 to 3 and paradorsal on 4 to 9; or 3) middorsal gco1 on segments 1 to 3, 5, and 7, and paradorsal on 4, 6, 8, and 9. The dorsal gco1 pattern could be mapped for all echinoderids described in the present study (information was only missing for segment 2 in *E. crux* sp. nov.), and all species fit with either the second or third pattern. Table 24 lists echinoderid species following one of the three dorsal gco1 patterns, as presented by Sørensen

et al. (2020), but with added information for species described after 2020 (plus a few additional species that were missing in the previous list). The updated list now includes 100 of the 191 currently recognised species of Echinoderidae. With more than half of the known species following one of three patterns, and with the remaining half mostly including species for which the gco1 distribution is unknown or too fragmented to be listed, it is obvious that clear, conserved patterns for dorsal gco1 do exist.

As already discussed by Sørensen *et al.* (2020), the dorsal gco1 pattern might reflect some phylogenetic signals, as putatively closely related species also share the same dorsal gco1 patterns. For instance, all species in the *Echinoderes remanei* species group (for which the dorsal gco1 pattern is known) follow the same pattern (Table 24). As another example, Sørensen *et al.* (2020) mentioned *E. horni* Higgins, 1983 and *E. parahorni* Cepeda *et al.*, 2019b, which share the same pattern and clearly belong to the same species group. Since 2020 one additional species, *E. wilberti* Anguas-Escalante *et al.*, 2023, has been added to this species group and, not surprisingly, it has the same dorsal gco1 pattern (Table 24). Among species described in the present contribution, *E. ahlfeldae* sp. nov. shows a close resemblance to *E. leduci*, whereas *E. antarcticus* sp. nov. is putatively closely related to *E. peterseni*, and in both cases we also see that the species in question share the same dorsal gco1 pattern.

Another noteworthy observation regards the three known species of *Polacanthoderes*, which all share the same dorsal gco1 pattern, i.e., middorsal gco1 on segments 1 to 3 and paradorsal on 4 to 9. Both the phylogenies of Sørensen (2008b) (morphology) and Yamasaki *et al.* (2022) (18S + 28S rRNA) suggest that *Polacanthoderes* represents the sister group to all other Echinoderidae, and if the dorsal gco1 pattern truly possesses a phylogenetic signal, this would also suggest that the pattern with paradorsal gco1 on segments 4 to 9 represents the plesiomorphic condition within the family and that other patterns are derived from it.

When attempting to correlate the dorsal gco1 distribution with other characters, such as spine patterns, there are no fully consistent relations, but still there are some distinct trends. First of all, there seems to be a clear correlation between the MD Seg. 1–3, PD 4–9 gco1 pattern and the presence of middorsal spines on segments 4 to 8. Of the 36 listed *Echinoderes* spp. with this gco1 pattern, 26 have middorsal spines on segments 4 to 8. Among the ten species deviating from this pattern, six belongs to the *E. coulli* species group, which has obviously been through a series of morphological modifications and spine reductions (Randsø *et al.* 2019). The remaining four all have middorsal spines on segments 4, 6, and 8 only, and include *E. kajiharai* Yamasaki *et al.*, 2020a, *E. riedli* Higgins, 1966, *E. samwisei* Grzelak & Sørensen, 2022, and *E. schwieringae* Yamasaki *et al.*, 2019. It is not clear why these particular four species deviate from the majority pattern, but their uncommon combined middorsal spine and gco1 patterns makes them stand out as four flagged species that should be considered in more detail in a future revision of Echinoderidae. Likewise, we see a correlation between the MD Seg. 1–3, 5, 7, PD 4, 6, 8–9 gco1 pattern and the presence of middorsal spines on segments 4, 6, and 8. Thirty-eight *Echinoderes* spp. are listed with this gco1 pattern and out of these, 25 have middorsal spines on segments 4, 6, and 8. Among the exceptions are four species with middorsal spines on segments 4 and 6 only, three non-*E. coulli* group species with only a single middorsal spine located on segment 4, and three species of the *E. horni* species group, which have lost all middorsal spines. Although the spine to gco1 correlation might appear less obvious here, we still see some interesting patterns. Whereas we have a relatively conserved MD Seg. 1–3, PD 4–9 gco1 pattern versus middorsal spines on segments 4 to 8 correlation, it appears that the modification towards the more uncommon spine patterns, with middorsal spines on two or fewer segments, all evolved within a group of species with three middorsal spines and the MD Seg. 1–3, 5, 7, PD 4, 6, 8–9 gco1 pattern. This would in turn support that the MD Seg. 1–3, PD 4–9 gco1 pattern (and middorsal spines on segments 4 to 8?) represents the plesiomorphic condition within *Echinoderes* or Echinoderidae, and that other dorsal gco1 and spine patterns are derived from this.

Table 24. Species with the three most common echinoderid dorsal patterns of glandular cell outlets type 1 on segments 1 to 9, listed together with the middorsal spine pattern (MDS) for each species. The table is updated from Sørensen *et al.* (2020), and names in boldface mark newly added species. In each column species of already recognised or newly proposed species groups are listed together, followed alphabetically by additional species that so far have not been assigned to a species group.

MD seg. 1–3 PD seg. 4–9		MD seg. 1–3 PD seg. 4–9		MD seg. 1–3, 5, 7 PD seg. 4, 6, 8–9	
MDS		MDS		MDS	
4-8	*Cephalorhyncha nybakkeni* (Higgins, 1986)		*E. coulli* species group:		*E. horni* species group:
		4	**E. cyaneafictus Cepeda et al., 2022**	–	*E. horni* Higgins, 1983
	E. coulli species group:	–	**E. inaequalis Herranz et al., 2023**	–	*E. parahorni* Cepeda et al. 2019
4	*E. blazeji* Grzelak & Sørensen, 2022 [1]	4	*E. marthae* Sørensen, 2014	–	**E. wilberti Anguas-Escalante et al., 2023**
4	**E. angelae Cepeda et al., 2022** [2]	4	*E. ohtsukai* Yamasaki & Kajihara, 2012		
		4	*E. regina* Yamasaki, 2016	4,6,8	*Echinoderes abbreviatus* Higgins, 1983
	E. dujardinii species group:	4	*E. serratulus* Yamasaki, 2016	4,6,8	**E. ahlfeldae sp. nov.**
4-8	*E. chandrasekharai* Sørensen *et al.*, 2020			4,6,8	**E. anniae Sørensen et al., 2018** [3]
4-8	*E. dujardinii* Claparède, 1863		*E. remanei* species group:	4	*E. antalyaensis* Yamasaki & Durucan, 2018
4-8	*E. gerardi* Higgins, 1978	4-8	*E. angustus* Higgins & Kristensen, 1988	4,6,8	**E. antarcticus sp. nov.**
4-8	*E. imperforatus* Higgins, 1983	4-8	**E. beringiensis Adrianov & Maiorova, 2022**	4,6,8	*E. apex* Yamasaki *et al.*, 2018
4-8	*E. kozloffi* Higgins, 1977	4-8	**E. galadrielae Grzelak & Sørensen, 2022**	4,6,8	*E. arlis* Higgins, 1966
4-8	*E. pacificus* Schmidt, 1974	4-8	**E. quasae Herranz et al., 2024**	4,6	*E. astridae* Sørensen, 2014
4-8	*E. sensibilis* Adrianov *et al.*, 2002	4-8	*E. pennaki* Higgins, 1960	4-8	*E. aureus* Adrianov *et al.*, 2002
4-8	*E. songae* Sørensen *et al.*, 2020	4-8	**E. remanei (Blake, 1930)**	4,6,8	*E. bermudensis* Higgins, 1982
4-8	*E. sublicarum* Higgins, 1977	4-8	**E. romanoi Landers & Sørensen, 2016**	4,6	*E. bispinosus* Higgins, 1982
4-8	*E. worthingi* Southern, 1914	4-8	*E. xalkutaat* Cepeda *et al.*, 2019	4,6,8	*E. brevipes* Cepeda *et al.*, 2019
4-8	*Echinoderes* sp. Andaman Isl.			4	*E. capitatus* Zelinka, 1928
		4-8	*Cephalorhyncha polunga* Sánchez *et al.*, 2019	4,6,8	**E. crux sp. nov.** [2]
		4-8	***Echinoderes abeli* Anguas-Escalante *et al.*, 2023**	4,6	**E. dalzottoi Grzelak & Sørensen, 2022**
		4-8	***Echinoderes adrianovi* Herranz *et al.*, 2014**	4,6	**E. goku Rucci et al., 2022**
		4-8	*E. aquilonius* Higgins & Kristensen, 1988	4,6,8	*E. hakaiensis* Herranz *et al.*, 2018
		4-8	*E. augustae* Sørensen & Landers, 2015	4,6,8	*E. hamiltonorum* Sørensen *et al.*, 2018
		4-8	**E. australis Sánchez et al., 2024** **	4,6,8	*E. higginsi* Huys & Coomans, 1989
		4-8	*E. barbadensis* Cepeda *et al.*, 2019	4,6,8	**E. intermedius Sørensen, 2006**
		4-8	*E. bookhouti* Higgins, 1964	4,6,8	**E. kathleenhannae sp. nov.**
		4-8	**E. dubiosus Sørensen et al., 2018** [2,3],**	4,6,8	**E. leduci Grzelak & Sørensen, 2022**
		4-8	*E. ferrugineus* Zelinka, 1928	4,6,8	**E. legolasi Grzelak & Sørensen, 2022**
		4-8	*E. gama* Yamasaki *et al.*, 2020	4,6,8	*E. multiporus* Yamasaki *et al.* 2018
		4-8	*E. juliae* Sørensen *et al.*, 2018	4,6,8	**E. nataliae sp. nov.**
		4-8	*E. kaempfae* Yamasaki *et al.*, 2019	4-8	**E. okiensis Yamasaki et al. 2024**
		4,6,8	*E. kajiharai* Yamasaki *et al.*, 2020	4,6,8	*E. peterseni* Higgins & Kristensen, 1988
		4-8	*E. kanni* Thormar & Sørensen, 2010	4,6,8	*E. riceae* Herranz *et al.*, 2014
		4-8	*E. levanderi* Karling, 1954	4-8	**E. sanctorum Sanchez et al., 2022**
		4-8	***E. mamaqucha* Grzelak *et al.*, 2021** **	4,6,8	**E. shahmaranae Sørensen et al., 2021**
		4-8	*E. muricatus* Pardos *et al.*, 2016	4,6,8	**E. skipperae Sørensen & Landers, 2014**
		4,6,8	*E. riedli* Higgins, 1966	4	*E. unispinosus* Yamasaki *et al.*, 2018
		4,6,8	**E. samwisei Grzelak & Sørensen, 2022**	4,6	*E. uozumii* Yamasaki *et al.*, 2020
		4,6,8	*E. schwieringae* Yamasaki *et al.*, 2019	4,6,8	*E. wallaceae* Higgins, 1983
		4-8	*E. tchefouensis* Lou, 1934	4,6,8	**E. xiphophorus Adrianov & Maiorova, 2021**
		4-8	**E. zeppilliae Sanchez et al. 2022**	4-6,8	*Fissuroderes sorenseni* Herranz & Pardos, 2013
		4-8	*Fissuroderes higginsi* Neuhaus & Blasche, 2006	4,6,8	*Meristoderes boylei* Herranz & Pardos, 2013
		4-8	*F. novaezealandia* Neuhaus & Blasche, 2006	4	*M. galatheae* Herranz *et al.*, 2012
		4-8	*Meristoderes taro* Sánchez *et al.*, 2019	4,6,8	*M. herranzae* Sørensen *et al.*, 2013
		4-8	***Polacanthoderes grzelakae* sp. nov.**	4,6,8	*M. macracanthus* Herranz *et al.*, 2012
		4-8	*P. martinezi* Sørensen, 2008		
		4-8	**P. shiraseae Yamasaki et al. 2022**		

[1–3] Indicates the segment(s) from which information is missing, although other outlets fit the pattern.
** The species has two middorsal outlets on segment 1.

Conclusions

The present study reveals that the Antarctic Peninsula hosts a rich, and so far mostly unknown, kinorhynch fauna. Seven new species were described, including a new species of *Polacanthoderes*, a genus which is so far endemic to Antarctica, a new species of *Condyloderes*, only the second species of the genus known from the Southern Hemisphere, and five new species of *Echinoderes*. Interestingly, the otherwise abundant and diverse family Pycnophyidae was only represented by a single, juvenile specimen. The sampling was concentrated on an open continental shelf area, a strait, and a bay, and the results indicate clearly that the highest kinorhynch abundance was reached in the strait, followed by the bay. Species richness did not differ between the strait and bay regions, but was considerably higher than in the open continental shelf area.

Besides the new species, the samples also yielded two species that could not be identified with certainty, because their morphology was too close to those of existing species. This prompted a closer comparison with several known species, which conclusively led to proposing a new species group, the *Echinoderes remanei* species group, including *E. remanei*, *E. angustus*, *E. cernunnos*, *E. drogoni*, *E. galadrielae*, *E. obtuspinosus*, *E. galadrielae*, *E. quasae*, *E. pennaki*, *E. beringiensis*, *E. romanoi*, and *E. xalkutaat*. The comparison furthermore indicated that the diagnostic differences separating the latter three species are unclear and suggested that they potentially could represent synonyms of one species.

This study, which in terms of recovered diversity represents the most comprehensive kinorhynch study from the Antarctic continent so far, also indicates the existence of species, or complexes of closely related species, with a bipolar distribution. Testing this hypothesis could lead to a new understanding of kinorhynch distribution patterns.

Acknowledgements

References

Adrianov A.V. & Maiorova A.S. 2021. *Echinoderes xiphophorus* sp. nov. – the first deep-water representative of Echinoderidae in the Sea of Japan (Kinorhyncha: Cyclorhagida). *European Journal of Taxonomy* 773: 169–186. https://doi.org/10.5852/ejt.2021.773.1523

Adrianov A.V. & Maiorova A.S. 2022. *Echinoderes beringiensis* sp. nov. – the first representative of the Kinorhyncha from the deep-sea methane seepages in the North Pacific (Kinorhyncha: Cyclorhagida). *Deep-Sea Research Part II* 204: e105154. https://doi.org/10.1016/j.dsr2.2022.105154

Adrianov A.V. & Malakhov V.V. 1999. *Cephalorhyncha of the World Ocean*. KMK Scientific Press, Moscow.

Álvarez-Castillo L., Cepeda D., Pardos F., Rivas G. & Rocha-Olivares A. 2020. *Echinoderes unispinosus* (Kinorhyncha: Cyclorhagida), a new record from deep-sea sediments in the Gulf of Mexico. *Zootaxa* 4821 (1): 196–200. https://doi.org/10.11646/zootaxa.4821.1.13

Anguas-Escalante A., Herranz M., Martínez-Arce A., De Jesús-Navarrete A. & Sørensen M.V. 2023. New *Echinoderes* (Kinorhyncha: Cyclorhagida) from Mexico: molecular barcoding demonstrate species delimitation between highly similar morphospecies. *Zoologischer Anzeiger* 302: 146–165. https://doi.org/10.1016/j.jcz.2022.12.001

Blake C.H. 1930. Three new species of worms belonging to the order Echinodera. *Biological Survey of the Mount Desert Region* 4: 3–10.

Brown R. 1985. *Developmental and Taxonomic Studies of Sydney Harbour Kinorhyncha*. PhD Thesis. Macquarie University, Australia.

Brown R. & Higgins R.P. 1983. A new species of *Kinorhynchus* (Homalorhagida, Pycnophyidae) from Australia with a redescription and range extension of other Kinorhyncha from the South Pacific. *Zoologica Scripta* 12: 161–169. https://doi.org/10.1111/j.1463-6409.1983.tb00561.x

Carus J.V. 1885. *Prodromus Faunae Mediterraneae sive Descriptio Animalium maris Mediterranei Incolarum quam Comparata Silva Rerum Quatenus Innotiut Adiectis et Nominibus Vulgaribus eorumque Auctoribus in Commodum Zoologorum. Vol. I. Coelenterata, Echinodermata, Vermes, Arthropoda*. E. Schweizerbart'sche Verlagsbuchhandlung E. Koch, Stuttgart. https://doi.org/10.5962/bhl.title.11523

Cepeda D., Álvarez-Castillo L., Hermoso-Salazar M., Sánchez N., Gómez S. & Pardos F. 2019a. Four new species of Kinorhyncha from the Gulf of California, eastern Pacific Ocean. *Zoologischer Anzeiger* 282: 140–160. https://doi.org/10.1016/j.jcz.2019.05.011

Cepeda D., Sánchez N. & Pardos F. 2019b. First extensive account of the phylum Kinorhyncha from Haiti and the Dominican Republic (Caribbean Sea), with the description of four new species. *Marine Biodiversity* 49: 2281–2309. https://doi.org/10.1007/s12526-019-00963-x

Cepeda D., Pardos F., Zeppilli D. & Sánchez N. 2020. Dragons of the deep sea: Kinorhyncha communities in a pockmark field at Mozambique Channel, with the description of three new species. *Frontiers in Marine Science* 7: e665. https://doi.org/10.3389/fmars.2020.00665

Cepeda D., Gayet N., Spedicato A., Michaud E. & Zeppilli D. 2022a. Two new species of the *Echinoderes coulli*-group (Kinorhyncha: Cyclorhagida: Echinoderidae) from a low human-impacted mangrove swamp in French Guiana (western Atlantic Ocean). *Zoologischer Anzeiger* 301: 179–185. https://doi.org/10.1016/j.jcz.2022.10.008

Cepeda D., González-Casarrubios A., Sánchez N., Spedicato A., Michaud E. & Zeppilli D. 2022b. Two new species of mud dragons (Scalidophora: Kinorhyncha) inhabiting a human-impacted mangrove from Mayotte (Southwestern Indian Ocean). *Zoologischer Anzeiger* 301: 23–41. https://doi.org/10.1016/j.jcz.2022.09.001

Cepeda D., Sánchez N., Olu K. & Zeppilli D. 2022c. *Ryuguderes casarrubiosi* sp. nov., a new deep-sea representative of the enigmatic genus *Ryuguderes* (Kinorhyncha: Cyclorhagida: Campyloderidae) from the Indian Ocean. *Zoologischer Anzeiger* 300: 92–101. https://doi.org/10.1016/j.jcz.2022.08.001

Claparède A.R.E. 1863. *Zur Kenntnis der Gattung* Echinoderes *Duj. Beobachtungen über Anatomie und Entwicklungsgeschichte wirbelloser Thiere an der Küste von Normandie angestellt.* Verlag von Wilhelm Engelmann, Leipzig. https://doi.org/10.5962/bhl.title.10030

Dal Zotto M., Di Domenico M., Garraffoni A. & Sørensen M.V. 2013. *Franciscideres* gen. nov. – a new, highly aberrant kinorhynch genus from Brazil, with an analysis of its phylogenetic position. *Systematics and Biodiversity* 11: 303–321. https://doi.org/10.1080/14772000.2013.819045

Dal Zotto M., Neuhaus N., Yamasaki Y. & Todaro M.A. 2019. The genus *Condyloderes* (Kinorhyncha: Cyclorhagida) in the Mediterranean Sea, including the description of two new species with novel characters. *Zoologischer Anzeiger* 282: 206–231. https://doi.org/10.1016/j.jcz.2019.05.006

Garraffoni A., Sørensen M.V., Worsaae K., Di Domenico M., Sales L.P., Santos J. & Lourenço A. 2021. Geographical sampling bias on the assessment of endemism areas for marine meiobenthic fauna. *Cladistics* 37: 571–585. https://doi.org/10.1111/cla.12453

Gerlach S.A. 1956. Über einen aberranten Vertreter der Kinorhynchen aus dem Küstengrundwasser. *Kieler Meeresforschung* 12: 120–124.

Grzelak K. & Sørensen M.V. 2018. New species of *Echinoderes* (Kinorhyncha: Cyclorhagida) from Spitsbergen, with additional information about known Arctic species. *Marine Biology Research* 14: 113–147. https://doi.org/10.1080/17451000.2017.1367096

Grzelak K. & Sørensen M.V. 2019a. Diversity and distribution of Arctic *Echinoderes* species (Kinorhyncha: Cyclorhagida), with the description of one new species and a redescription of *E. arlis* Higgins, 1966. *Marine Biodiversity* 49: 1131–1150. https://doi.org/10.1007/s12526-018-0889-2

Grzelak K. & Sørensen M.V. 2019b. Diversity and community structure of kinorhynchs around Svalbard: first insights into spatial patterns and environmental drivers. *Zoologischer Anzeiger* 282: 31–43. https://doi.org/10.1016/j.jcz.2019.05.009

Grzelak K. & Sørensen M.V. 2022. *Echinoderes* (Kinorhyncha: Cyclorhagida) from the Hikurangi Margin, New Zealand. *European Journal of Taxonomy* 844: 1–108. https://doi.org/10.5852/ejt.2022.844.1949

Grzelak K. & Sørensen M.V. 2024. Kingdom Animalia, phylum Kinorhyncha (mud dragons). *In:* Kelly M., Mills S., Terezow M., Sim-Smith C. & Nelson W. (eds) *The Marine Biota of Aotearoa New Zealand. NIWA Biodiversity Memoir* 136: 455–462. NIWA, New Zealand.

Grzelak K., Zeppilli D., Shimabukuro M. & Sørensen M.V. 2021. Hadal mud dragons: first insight into the diversity of Kinorhyncha from the Atacama Trench. *Frontiers in Marine Science* 8: e670735. https://doi.org/10.3389/fmars.2021.670735

Grzelak K., Yamasaki H., Mincks S., Phillips A.J. & Sørensen M.V. 2023. Revision of an Arctic kinorhynch species: *Echinoderes svetlanae* and *E. tubilak* are junior synonyms of *E. remanei*. *Zoologischer Anzeiger* 302: 75–89. https://doi.org/10.1016/j.jcz.2022.11.001

Herranz M., Yangel E. & Leander B. 2018. *Echinoderes hakaiensis* sp. nov.: a new mud dragon (Kinorhyncha, Echinoderidae) from the northeastern Pacific Ocean with the redescription of *Echinoderes pennaki* Higgins, 1960. *Marine Biodiversity* 48: 303–325 https://doi.org/10.1007/s12526-017-0726-z

Herranz M., Stiller J., Worsaae K. & Sørensen M.V. 2022. Phylogenomic analyses of mud dragons (Kinorhyncha). *Molecular Phylogenetics and Evolution* 168: e107375. https://doi.org/10.1016/j.ympev.2021.107375

Herranz M., Leander B.S. & Grzelak K. 2024. First evidence of cryptic speciation in mud dragons (Kinorhyncha) and description of *Echinoderes quasae* sp. nov. from the northeastern Pacific coast. *Zoologischer Anzeiger* 313: 241–254. https://doi.org/10.1016/j.jcz.2024.10.010

Higgins R.P. 1960. A new species of *Echinoderes* (Kinorhyncha) from Puget Sound. *Transactions of the American Microscopical Society* 79: 85–91. https://doi.org/10.2307/3223976

Higgins R.P. 1966. Faunistic studies in the Red Sea (in winter, 1961–1962). *Zoologische Jahrbücher, Abteilung für Systematik, Ökologie und Geographie der Tiere* 93: 118–126.

Higgins R.P. 1967. The Kinorhyncha of New-Caledonia. *Expédition française sur les Recifs coralliens de la Nouvelle-Calédonie 2*. Fondation Singer-Polignac, Paris.

Higgins R.P. 1968. Taxonomy and postembryonic development of the Cryptorhagae, a new suborder for the mesopsammic kinorhynch genus *Cateria*. *Transactions of the American Microscopical Society* 87: 21–39. https://doi.org/10.2307/3224334

Higgins R.P. 1969a. Indian Ocean Kinorhyncha 2. Neocentrophyidae, a new homalorhagid family. *Proceedings of the Biological Society of Washington* 82: 113–128.

Higgins R.P. 1969b. Indian Ocean Kinorhyncha: 1, *Condyloderes* and *Sphenoderes*, new cyclorhagid genera. *Smithsonian Contributions to Zoology* 14: 1–13. https://doi.org/10.5479/si.00810282.14

Higgins R.P. 1983. The Atlantic barrier reef ecosystem at Carrie Bow Cay, Belize, II: Kinorhyncha. *Smithsonian Contributions to Marine Science* 18: 1–131. https://doi.org/10.5479/si.01960768.18.1

Higgins R.P. & Kristensen R.M. 1988. Kinorhyncha from Disko Island, West Greenland. *Smithsonian Contributions to Zoology* 458: 1–56. https://doi.org/10.5479/si.00810282.458

Kirsteuer E. 1964. Zur Kenntnis der Kinorhynchen Venezuelas. *Zoologischer Anzeiger* 173: 388–393.

Lang K. 1949. Echinoderida. *In*: Odhner N.H. (ed.) *Further Zoological Results of the Swedish Antarctic Expedition, 1901–1903* Vol. 4: 1–22.

Lang K. 1953. Reports of the Lund University Chile Expedition 1948–49. *Kungliga fysiografiska Sällskapets Handlingar* 64: 1–8.

Landers S.C. & Sørensen M.V. 2016. Two new species of *Echinoderes* (Kinorhyncha, Cyclorhagida), *E. romanoi* sp. n. and *E. joyceae* sp. n., from the Gulf of Mexico. *ZooKeys* 594: 51–71. https://doi.org/10.3897/zookeys.594.8623

Landers S.C. & Sørensen M.V. 2018. *Echinoderes sylviae* n. sp. (Kinorhyncha, Cyclorhagida), from the Gulf of Mexico, with comparative notes on a similar species *Echinoderes spinifurca*. *Bulletin of Marine Science* 94: 1499–1514. https://doi.org/10.5343/bms.2017.1167

Lemburg C. 2002. A new kinorhynch *Pycnophyes australensis* sp. n. (Kinorhyncha: Homalorhagida: Pycnophyidae) from Magnetic Island, Australia. *Zoologischer Anzeiger* 241: 173–189. https://doi.org/10.1078/S0044-5231(04)70072-8

Lou T.-H. 1934. Sur la présence d'un nouveau kinorhynque à Tchefou: *Echinoderes tchefouensis* sp. nov. *Contributions from the Institute of Zoology, National Academy of Peiping* 1: 1–9. [In Chinese with French translation.]

Lundesgaard O., Winsor P., Truffer M., Merrifield M., Powell B., Statscewich H., Eidam E. & Smith C.R. 2020. Hydrography and energetics of a cold fjord: Andvord Bay, western Antarctic Peninsula. *Progress in Oceanography* 181: e102224. https://doi.org/10.1016/j.pocean.2019.102224

Martorelli S. & Higgins R.P. 2004. Kinorhyncha from the stomach of the shrimp *Pleoticus muelleri* (Bate, 1888) from Comodoro Rivadavia, Argentina. *Zoologischer Anzeiger* 243: 85–98. https://doi.org/10.1016/j.jcz.2004.07.003

Neuhaus B. 2004. Description of *Campyloderes* cf. *vanhoeffeni* (Kinorhyncha, Cyclorhagida) from the Central American East Pacific Deep Sea with a review of the genus. *Meiofauna Marina* 13: 3–20.

Neuhaus B. 2013. Kinorhyncha (= Echinodera). *In:* Schmidt-Rhaesa A. (ed.) *Handbook of Zoology. Gastrotricha, Cycloneuralia and Gnathifera. Volume 1: Nematomorpha, Priapulida, Kinorhyncha, Loricifera*: 181–348. De Gruyter, Berlin/Boston. https://doi.org/10.1515/9783110272536.181

Neuhaus B. & Blasche T. 2006. *Fissuroderes*, a new genus of Kinorhyncha (Cyclorhagida) from the deep sea and continental shelf of New Zealand and from the continental shelf of Costa Rica. *Zoologischer Anzeiger* 245: 19–52. https://doi.org/10.1016/j.ode.2007.11.003

Neuhaus B. & Sørensen M.V. 2013. Populations of *Campyloderes* sp. (Kinorhyncha, Cyclorhagida): one global species with significant morphological variation? *Zoologischer Anzeiger* 252: 48–75. https://doi.org/10.1016/j.jcz.2012.03.002

Neuhaus B., Dal Zotto M., Yamasaki H. & Higgins R.P. 2019. Revision of *Condyloderes* (Kinorhyncha, Cyclorhagida) including description of *Condyloderes shirleyi* sp. nov. *Zootaxa* 4561 (1): 1–91. https://doi.org/10.11646/zootaxa.4561.1.1

Omer-Cooper J. 1957. Deux nouvelles espèces de Kinorhyncha en provenance de l'Afrique du Sud. *Bulletin mensuel de la Société linnéenne de Lyon* 26: 213–216. https://doi.org/10.3406/linly.1957.7920

Ostmann A., Nordhaus I. & Sørensen M.V. 2012. First recording of kinorhynchs from Java, with the description of a new brackish water species from a mangrove-fringed lagoon. *Marine Biodiversity* 42: 79–91. https://doi.org/10.1007/s12526-011-0094-z

Pardos F., Higgins R.P. & Benito J. 1998. Two new *Echinoderes* (Kinorhyncha, Cyclorhagida) including a reevaluation of kinorhynch taxonomic characters. *Zoologischer Anzeiger* 237: 195–208.

Pardos F., Herranz M. & Sánchez N. 2016a. Two sides of a coin: the phylum Kinorhyncha in Panama. I) Caribbean Panama. *Zoologischer Anzeiger* 265: 3–25. https://doi.org/10.1016/j.jcz.2016.06.005

Pardos F., Herranz M. & Sánchez N. 2016b. Two sides of a coin: the phylum Kinorhyncha in Panama. II) Pacific Panama. *Zoologischer Anzeiger* 265: 26–47. https://doi.org/10.1016/j.jcz.2016.06.006

Randsø P.V., Yamasaki H., Bownes S.J., Herranz M., Di Domenico M., Qii G.B. & Sørensen M.V. 2019. Phylogeny of the *Echinoderes coulli*-group (Kinorhyncha: Cyclorhagida: Echinoderidae) – a cosmopolitan species group trapped in the intertidal. *Invertebrate Systematics* 33: 501–517. https://doi.org/10.1071/IS18069

Rucci K.A., Neuhaus B. & Bulnes V.N. 2022. A new species of *Echinoderes* (Kinorhyncha: Cyclorhagida: Echinoderidae) from the Argentinean continental shelf with notes on its postembryonic development and on subcuticular morphological characters unreported for Kinorhyncha. *Zootaxa* 5099 (1): 65–90. https://doi.org/10.11646/zootaxa.5099.1.3

Sánchez N., González-Casarrubios A., Cepeda D., Khodami S., Pardos F., Vink A. & Martínez Arbizu P. 2022. Diversity and distribution of Kinorhyncha in abyssal polymetallic nodule areas of the Clarion-Clipperton Fracture Zone and the Peru Basin, East Pacific Ocean, with the description of three new species and notes on their intraspecific variation. *Marine Biodiversity* 52: e52. https://doi.org/10.1007/s12526-022-01279-z

Sánchez N., García-Cobo M., Shimabukuro M., Zeppilli D., Nomaki H. & González-Casarrubios A. 2024. Discovery of a new Kinorhyncha species from the uncharted South Orkney Trench (Southern Ocean). *Zoologischer Anzeiger* 313: 315–331. https://doi.org/10.1016/j.jcz.2024.10.016

Schmidt P. 1974. Interstitielle Fauna von Galapagos. 10. Kinorhyncha. *Microfauna des Meeresbodens* 43: 1–15.

Somerfield P.J. & Warwick R.M. 1996. *Meiofauna in Marine Pollution Monitoring Programmes: a Laboratory Manual*. Ministry of Agriculture, Fisheries and Food, Lowestoft, UK.

Sørensen M.V. 2006. New kinorhynchs from Panama, with a discussion of some phylogenetically significant cuticular structures. *Meiofauna Marina* 15: 51–77.

Sørensen M.V. 2008a. A new kinorhynch genus from the Antarctic deep-sea and a new species of *Cephalorhyncha* from Hawaii (Kinorhyncha: Cyclorhagida: Echinoderidae). *Organisms Diversity and Evolution* 8: 230.e1–230.e18. https://doi.org/10.1016/j.ode.2007.11.003

Sørensen M.V. 2008b. Phylogenetic analysis of the Echinoderidae (Kinorhyncha: Cyclorhagida). *Organisms Diversity and Evolution* 8: 233–246. https://doi.org/10.1016/j.ode.2007.11.002

Sørensen M.V. 2014. First account of echinoderid kinorhynchs from Brazil, with the description of three new species. *Marine Biodiversity* 44: 251–274. https://doi.org/10.1007/s12526-013-0181-4

Sørensen M.V. 2023. New data on the *Echinoderes coulli*-group (Kinorhyncha: Cyclorhagida: Echinoderidae): a new species from New Caledonia mangroves, and a redescription of *E. bengalensis* (Timm, 1958). *Zoologischer Anzeiger* 302: 90–101. https://doi.org/10.1016/j.jcz.2022.11.009

Sørensen M.V. & Grzelak K. 2024. A new deep-sea *Cristaphyes* (Kinorhyncha: Allomalorhagida: Pycnophyidae) from the continental rise of South Island, New Zealand. *New Zealand Journal of Zoology*. https://doi.org/10.1080/03014223.2024.2308020

Sørensen M.V. & Kristensen R.M. 2000. Marine Rotifera from Ikka Fjord, SW Greenland. *Meddelelser om Grønland, Bioscience* 51: 1–46. https://doi.org/10.7146/mogbiosci.v51.142614

Sørensen M.V. & Thormar J. 2010. *Wollunquaderes majkenae* gen. et sp. nov. – a new cyclorhagid kinorhynch genus and species from the Coral Sea, Australia. *Marine Biodiversity* 40: 261–275. https://doi.org/10.1007/s12526-010-0048-x

Sørensen M.V. & Yamasaki H. 2024. An interactive identification key to species of the kinorhynch orders Kentrorhagata, Xenosomata, and Anomoirhaga. *Zoologischer Anzeiger* 311: 45–47. https://doi.org/10.1016/j.jcz.2024.06.003

Sørensen M.V., Jørgensen A. & Boesgaard T.M. 2000. A new *Echinoderes* (Kinorhyncha: Cyclorhagida) from a submarine cave in New South Wales, Australia. *Cahiers de Biologie marine* 41: 167–179. https://doi.org/10.21411/CBM.A.F11FEF78

Sørensen M.V., Rho H.S., Min W., Kim D. & Chang C.Y. 2012. An exploration of *Echinoderes* (Kinorhyncha: Cyclorhagida) in Korean and neighboring waters, with the description of four new species and a redescription of *E. tchefouensis* Lou, 1934. *Zootaxa* 3368 (1): 161–196. https://doi.org/10.11646/zootaxa.3368.1.8

Sørensen M.V., Dal Zotto M., Rho H.S., Herranz M., Sánchez N., Pardos F. & Yamasaki H. 2015. Phylogeny of Kinorhyncha based on morphology and two molecular loci. *PLoS One* 10: e0133440. https://doi.org/10.1371/journal.pone.0133440

Sørensen M.V., Gąsiorowski L., Randsø P.V. Sánchez N. & Neves R.C. 2016. First report of kinorhynchs from Singapore, with the description of three new species. *Raffles Bulletin of Zoology* 64: 3–27.

Sørensen M.V., Rohal M. & Thistle D. 2018. Deep-sea Echinoderidae (Kinorhyncha: Cyclorhagida) from the Northwest Pacific. *European Journal of Taxonomy* 456: 1–75. https://doi.org/10.5852/ejt.2018.456

Sørensen M.V., Thistle D. & Landers S.C. 2019. North American *Condyloderes* (Kinorhyncha: Cyclorhagida: Kentrorhagata): female dimorphism suggests moulting among adult *Condyloderes*. *Zoologischer Anzeiger* 282: 232–251. https://doi.org/10.1016/j.jcz.2019.05.015

Sørensen M.V., Goetz F.E., Herranz M., Chang C.Y., Chatterjee T., Durucan F., Neves R.C., Yildiz N.Ö, Norenburg J. & Yamasaki H. 2020. Description, redescription and revision of sixteen putatively closely related species of *Echinoderes* (Kinorhyncha: Cyclorhagida), with the proposition of a new species group – the *Echinoderes dujardinii* group. *European Journal of Taxonomy* 730: 1–101. https://doi.org/10.5852/ejt.2020.730.1197

Yamasaki H. & Dal Zotto M. 2019. Investigation of echinoderid kinorhynchs described 90 years ago: redescription of *Echinoderes capitatus* (Zelinka, 1928) and *Echinoderes ferrugineus* Zelinka, 1928. *Zoologischer Anzeiger* 282: 189–205. https://doi.org/10.1016/j.jcz.2019.05.013

Yamasaki H. & Fujimoto S. 2014. Two new species in the *Echinoderes coulli* group (Echinoderidae, Cyclorhagida, Kinorhyncha) from the Ryukyu Islands, Japan. *ZooKeys* 382: 27–52. https://doi.org/10.3897/zookeys.382.6761

Yamasaki H., Grzelak K., Sørensen M.V., Neuhaus B. & George K.H. 2018a. *Echinoderes pterus* sp. n. showing a geographically and bathymetrically wide distribution pattern on seamounts and on the deep-sea floor in the Arctic Ocean, Atlantic Ocean, and the Mediterranean Sea (Kinorhyncha, Cyclorhagida). *ZooKeys* 771: 15–40. https://doi.org/10.3897/zookeys.771.25534

Yamasaki H., Neuhaus B. & George K.H. 2018b. New species of *Echinoderes* (Kinorhyncha: Cyclorhagida) from Mediterranean seamounts and from the deep-sea floor in the Northeast Atlantic Ocean, including notes on two undescribed species. *Zootaxa* 4387 (3): 541–566. https://doi.org/10.11646/zootaxa.4387.3.8

Yamasaki H., Neuhaus B. & George K.H. 2018c. Three new species of Echinoderidae (Kinorhyncha: Cyclorhagida) from two seamounts and the adjacent deep-sea floor in the Northeast Atlantic Ocean. *Cahiers de Biologie marine* 59: 79–106. https://doi.org/10.21411/CBM.A.124081A9

Yamasaki H., Neuhaus B. & George K.H. 2019. Echinoderid mud dragons (Cyclorhagida: Kinorhyncha) from Senghor Seamount (NE Atlantic Ocean) including general discussion of faunistic characters and distribution patterns of seamount kinorhynchs. *Zoologischer Anzeiger* 282: 64–87. https://doi.org/10.1016/j.jcz.2019.05.018

Yamasaki H., Fujimoto S. & Tanaka H. 2020a. Three new meiobenthic species from a submarine cave in Japan: *Echinoderes gama*, *E. kajiharai*, and *E. uozumii* (Cyclorhagida: Kinorhyncha). *Journal of the Marine Biological Association of the United Kingdom* 100: 537–558. https://doi.org/10.1017/S0025315420000429

Yamasaki H., Herranz M. & Sørensen M.V. 2020b. An interactive identification key to species of Echinoderidae (Kinorhyncha). *Zoologischer Anzeiger* 287: 14–16. https://doi.org/10.1016/j.jcz.2020.05.002

Yamasaki H., Fujimoto S., Tanaka H., Shimada D., Ito M., Tokuda Y. & Tsujimoto M. 2022. Taxonomy, genetic diversity, and phylogeny of the Antarctic mud dragon, *Polacanthoderes* (Kinorhyncha: Echinorhagata: Echinoderidae). *Zoologischer Anzeiger* 301: 42–58. https://doi.org/10.1016/j.jcz.2022.09.003

Zalewska A., Herranz M., Lubosny M., Sørensen M.V. & Grzelak K. 2024. To be, or not tu-be? Population structure and connectivity in three Arctic kinorhynch species: *Echinoderes aquilonius*, *Echinoderes eximus* and *Echinoderes remanei*. *Zoologischer Anzeiger* 313: 289–297. https://doi.org/10.1016/j.jcz.2024.10.013

Zelinka C. 1913. *Der Echinoderen der Deutschen Südpolar-Expedition, 1901–1903*. Vol. 14. Reimer, Berlin.

Zelinka K. 1896. Demonstration von Tafeln der *Echinoderes*-Monographie. *Verhandlungen der deutschen Zoologischen Gesellschaft* 6: 197–199.